

제11 호 2004년  
[특집]  
Hemodialysis Vascular Access

# 인터벤션 영상의학회지

Journal of Korean  
Interventional Radiology

대한인터벤션 영상의학회  
대한영상의학회

*intervention*®

Korean Society of  
Interventional Radiology



제11 호 2004년  
[특집]  
Hemodialysis Vascular Access

# 인터벤션 영상의학회지

Journal of Korean  
Interventional Radiology


대한인터벤션 영상의학회  
대한영상의학회

*intervention*®

Korean Society of  
Interventional Radiology



|   |                 |   |
|---|-----------------|---|
|   | Vascular Access |   |
| 5   | <               | > |
| 16  | <               | > |
| Endovascular Management of Failing Native Hemodialysis Fistulas |                 |   |
| 22  | <               | > |
| 27  | <               | > |
| /   |                 |   |
| 35  | <               | > |



### 1. Non-Vascular intervention

|         |   |    |
|---------|---|----|
| Case 1. | Congenital Tracheal Stenosis: Treatment with Balloon Posterior Tracheal Splitting and Temporary Placement of a Covered Retrievable Metallic Stent | 42 |
| Case 2. | Deep Tracheal Laceration with Pneumomediastinum after Tracheobronchial Balloon Dilation   | 47 |
| Case 3. |   | 52 |
| Case 4. | covered metallic stent  | 54 |
| Case 5. | 가 Double - J  | 57 |
| Case 6. | - stent - graft   | 61 |

### 2. Vascular intervention

|          |                                   |                 |    |
|----------|-----------------------------------|-----------------|----|
| Case 7.  | Type B                            | 가               | 64 |
| Case 8.  | penetrating atherosclerotic ulcer | 가 stent - graft | 67 |
| Case 9.  | Type II endoleak                  |                 | 69 |
| Case 10. | graft - stent                     |                 | 72 |
| Case 11. |                                   |                 | 74 |
| Case 12. |                                   |                 | 77 |
| Case 13. |                                   |                 | 80 |



|   |     |
|---|-----|
| Case 14.                                    | 82  |
| Case 15.                                    | 84  |
| Case 16.                                    | 86  |
| Case 17. ;                                  | 88  |
| Case 18. Coil :                             | 91  |
| Case 19. : 2                                | 93  |
| Case 20.                                    | 96  |
| Case 21.                                    | 99  |
| Case 22.                                    | 102 |
| Case 23.                                    | 105 |
| Case 24.                                    | 107 |
| Case 25. Dieulafoy                          | 109 |
| Case 26.                                    | 111 |
| Case 27.                                    | 114 |
| Case 28.                                    | 116 |
| Case 29. 가                                  | 118 |
| Case 30. 가                                  | 120 |
| Case 31.                                    | 123 |
| Case 32.                                    | 125 |
| Case 33.                                    | 128 |
| Case 34.                                    | 131 |
| Case 35.                                    | 134 |
| Case 36.                                    | 136 |
| Case 37. -                                  | 139 |
| Case 38.                                    | 142 |
| Case 39. (isolated iliac artery aneurysm) - | 145 |
| Case 40. Covered stent                      | 148 |
| Case 41.                                    | 151 |
| Case 42. 가                                  | 154 |
| Case 43. Budd - Chiari : TIPS               | 157 |
| Case 44. Budd - Chiari syndrome             | 160 |
| Case 45. TrapEase                           | 164 |
| Case 46.                                    | 168 |
| Case 47.                                    | 170 |
|   | 173 |





# Vascular Access

가

DOQI(Dialysis Outcome Quality Initiative)

300,000 가 3,100  
 1985  
 220 , 1,200  
 가 30 가 2002  
 가 6,600 , 가 26,000  
 가 가  
 가 350ml/min  
 가  
 가  
 가

(3).  
 가  
 가  
 (polytetrafluoroethylene, PTFE)  
 가 1  
 가  
 가  
 (vascular access team)

1966 Brescia  
 - (radiocephalic fistula)  
 가  
 (1).  
 (side - to - side)  
 (end - to - side)  
 가 43  
 가 75 가  
 가  
 30 (chronic glo-  
 merulonephritis)  
 2002  
 45%가 67  
 90%가  
 가,  
 가  
 (2).

## A Multidisciplinary Approach to Vascular Access Care

Vascular access coordinator,  
 가  
 vascular access program 가  
 (4).

Vascular Access Work Group  
 11,000  
 (evidence - based)  
 , 2001

## Patient History and Physical Examination Prior to Permanent Access Selection

가  
 가  
 가  
 (DOQI guideline 1)  
 (Table 1).



Table 1. Patient Evaluation Prior to Access Placemen

| Consideration   | Relevance  |
|---|--|
| <b>Patient History</b>  |  |
| History of previous central venous catheter   | Previous placement of a central venous catheter is associated with central venous stenosis.  |
| Dominant arm  | To minimize negative impact on quality of life, use of the nondominant arm is preferred.   |
| History of pacemaker use  | There is a correlation between pacemaker use and central venous stenosis.  |
| History of severe congestive heart failure  | Accesses may alter hemodynamics and cardiac output.  |
| History of arterial or venous peripheral catheter   | Previous placement of an arterial or venous catheter may have damaged target vasculature.  |
| History of diabetes mellitus  | DM is associated with damage to vasculature for internal accesses.   |
| History of anticoagulant Tx or any coagulation disorder   | Abnormal coagulation may cause clotting or problems with hemostasis of accesses.   |
| Presence of comorbid conditions, such as malignancy or coronary artery ds. that limit patient's life expectancy | Morbidity associated with placement and maintenance of certain accesses may not justify their use in patients.   |
| History of vascular access  | Previously failed vascular accesses will limit available sites for accesses; the cause of a previous failure influence planned access if the cause is still present. |
| History of heart valve disease or prosthesis  | Rate of infection associated with specific access should be considered.  |
| History of previous arm, neck, or chest surgery/trauma  | Vascular damage associated with previous surgery trauma may limit viable access sites.   |
| Anticipated renal transplant from living donor  | Temporary access may be sufficient.  |
| <b>Physical Examination</b>   |  |
| Physical Examination of Arterial System   |  |
| Character of peripheral pulses, supplemented by hand-held Doppler evaluation when indicated                     | An adequate arterial system is needed for access; quality of the arterial system will influence the access site.   |
| Results of Allen test   | Abnormal arterial flow pattern to the hand contraindicate the creation of a radial-cephalic fistula.   |
| Bilateral upper extremity blood pressures   | Pressures determine suitability of arterial access in upper extremities.   |
| Physical Examination of Venous System   |  |
| Evaluation for edema  | Edema indicates venous outflow problems that may limit usefulness of the associated potential access site extremity for access placement.                            |
| Assessment of arm size comparability  | Differential arm size may indicate inadequate veins or venous obstruction which should influence choice of   |



|   |  |
|---|--|
|   | access site.   |
| Examination for collateral veins  | Collateral veins are indicative of venous obstruction.   |
| Tourniquet venous palpation with vein mapping                                     | Palpation and mapping allow selection of ideal veins for access.   |
| Examination for evidence of previous central or peripheral venous catheterization | Use of central venous catheters is associated with central venous stenosis; previous placement of venous catheters may have damaged target vasculature necessary access. |
| Examination for evidence of arm, chest, or neck surgery/trauma                    | Vascular damage associated with previous surgery trauma may limit access sites.  |
| Cardiovascular Evaluation   |  |
| Examination for evidence of heart failure   | Accesses may alter cardiac output.   |

## Diagnostic Evaluation Prior to Permanent Access Selection

|                    |  |
|--------------------|--|
|                    | Duplex                                     |
|                    | 가  |
|                    | 가  |
| 100 mmHg           | Allen test                                 |
| 1.5 - 2.0 mm       | 가  |
|                    | Ankle-brachial index(ABI)가 0.8             |
| 가                  | (7).                                       |
| (Venography) 가     |  |
| (DOQI guideline 2) |  |
| 1.                 |  |
| 2.                 | Selection of Permanent Vascular Access and |
| (Collateral vein)  | Order of Preference for Placement of AV    |
| 3.                 | Fistulae                                   |
| 가                  |  |
| 4.                 | (DOQI                                      |
|                    | guideline 3)                               |
| 5.                 | 1. ( , radio-cephalic) 가                   |
| 6.                 | 2. ( , brachio-cephalic)                   |
|                    | 가  |
| 7.                 | 가 가  |
|                    | 3.   |
|                    | 4. -                                       |
| Duplex             | (transposed brachial basilic vein          |
| Duplex             | fistula)                                   |
|                    |  |
| (5,6).             |  |

가 (patency), , , (vascular steal phenomenon) , 가 (Fig. 1). 4가 8-12mm 가 , 가 ( - ) , (eversion) 가 , 1-4 , 가 (7).

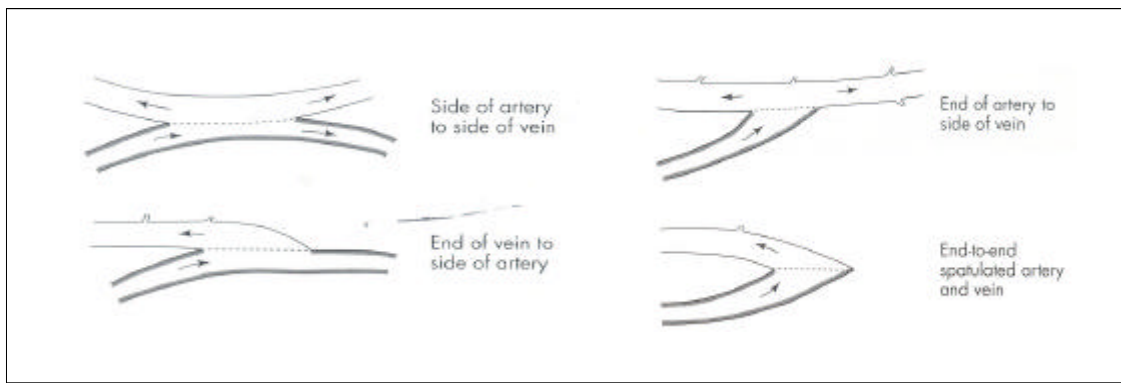


Fig. 1. Four different anastomoses commonly constructed between radial artery and cephalic vein

DOQI guideline 29

40% 가 , 가 30% 가 가 multi-disciplinary 44% 74.6% 가 50% 가 (4). (transposed brachial-basilic fistula) (Fig. 2). ( - , brachial - cephalic fistula)가 2 가 .

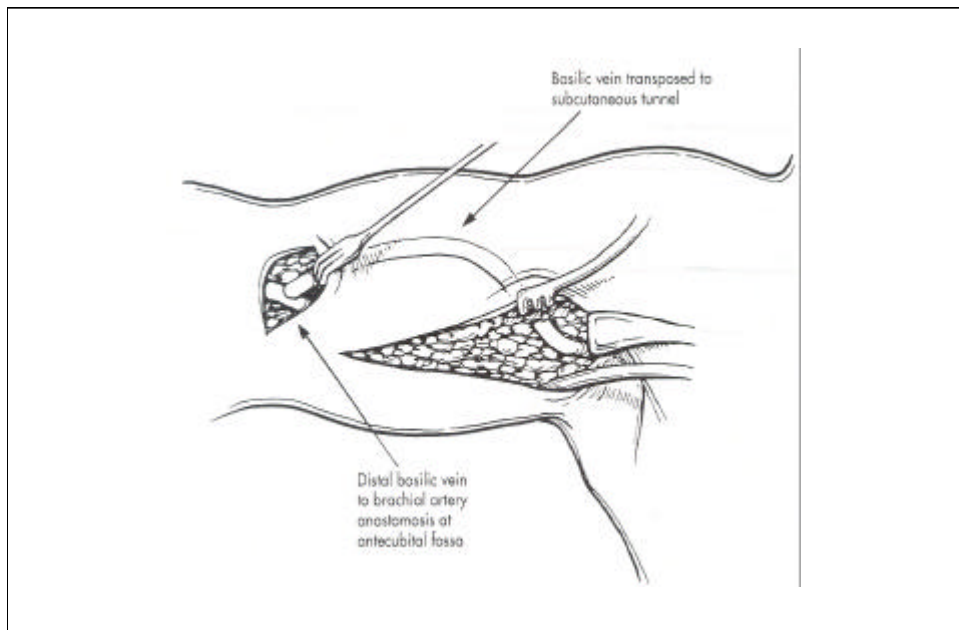


Fig. 2. Placement of the incisions and the subcutaneous tunnel, to which the basilic vein is transposed.

|   |               |  |
|---|---------------|--|
| 가   | 10-15%        | 1. 가 가   |
|   |               | 2. 가   |
| 3 78%   | 3 92%         | 3. 2   |
|   | , 1, 2        | 4. 가 가   |
| 75%, 70%  |               | 5.   |
| DOQI guideline 36                                 | 1             | 6.   |
| , 2, 3  | 70%, 60%, 50% |  |
| Type and Location of Dialysis AV Graft Placement  |               |  |
| 가   | 가             | (antecubital loop graft)                         |
|   |               | (upper arm curved graft) 가                       |
| 가   | 가             |  |
| polytetrafluoro-                                  |               |  |
| ethylene(PTFE) tube가 가                            |               | 8mm  |
| , ta-   | PTFE          | 가 700mL/min                                      |
| pered/ uniform, externally supported/unsupported, |               |  |
| thick - /thin - walled elastic/ nonelastic        |               | 6mm PTFE   |
| (straight), (looped), (curved)                    |               |  |
| 가   |               |  |
| 가   |               |  |
| (DOQI guideline 4)                                |               | Monitoring, Surveillance, and Diagnostic Testing |

가 가

31%

(DOQI guideline 10)

1. (Monitoring); ,

(thrill) 가 >450 mL/min

(pulse)

(bruit)

2. (Surveillance); 가

(Intra - access flow); 1

가 600mL/min

1000mL/min 4 가 25%

(fistulogram)

(Static venous dialysis pressure);

가 0.5 ( ) )

(Dynamic venous pressure);

가 200mL/min

가

Access recirculation using urea concentration

Recirculation using dilution techniques(nonurea - based)

Unexplained decreases in the measured amount of hemodialysis delivered

;

가 increased

negative arterial pre - pump pressure

(Doppler ultrasound);

가

3. (Diagnostic testing);

## Complications of Vascular Access Procedure: Stenosis, Thrombosis etc

1990

가

가

85 - 90%

가

가

가

가

20%

가

## Potential Biologic Determinants and Role of Intimal Hyperplasia

가

가

가

0.1%

heparin heparin sul -

fate가

(8).

( ' Response to Injury')

platelet - derived growth factor (PDGF)

가

(Fig. 3) (9).

shear stress가

(10).

PDGF 2 polypeptide glycoprotein

가

가

(G0) G1



DNA

90%

가

가

heparin

sulfate 가

, PDGF,

가

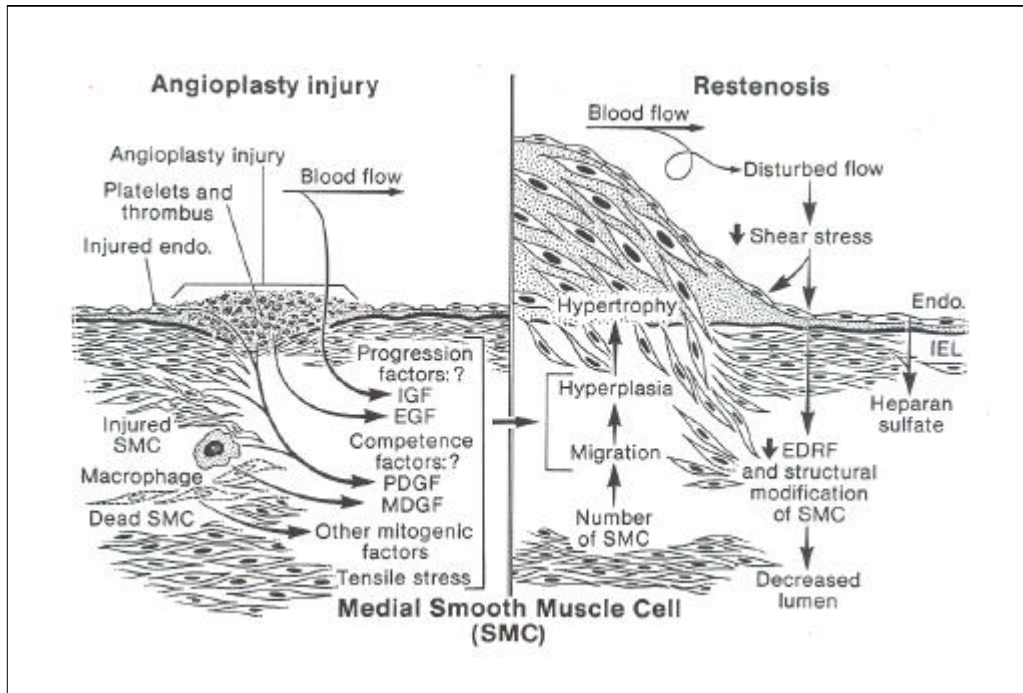


Fig. 3. Illustration of postulated mechanism of intimal hyperplasia

Thrombosis

가 50%

thrombosis), 1  
bosis)

1

(early  
(late throm -

Urea

가

angioplasty, PTA)  
(DOQI guideline 19)

(Percutaneous transluminal

2-3mm

가

(antecubital fossa)

PTA

6

unassisted patency가

20-30ml

50%

30%

1

unassisted patency가 50%

3

가

가

PTA가

가

stent

Treatment of Stenosis Without Thrombosis in  
Dialysis AV Grafts and Primary AV Fistula

## Treatment of Thrombosis and Associated Stenosis in Dialysis AV Grafts

21)

3 (unassisted patency) 40%  
 6, 1 (unassisted  
 patency) 50%, 40%  
 85%

access

catheter)

(Balloon embolectomy

fistulogram

85%

가  
 (adherent clot catheter) (Fig. 4, 5)

(Graft thrombec-

tomy catheter) (Fig. 6. 7)

. (DOQI guideline

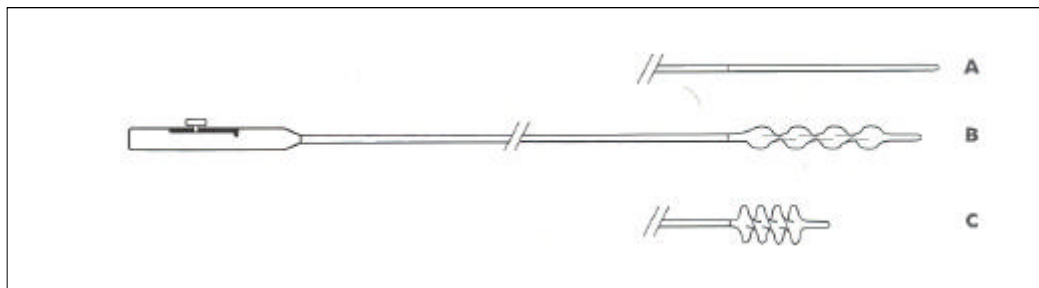


Fig. 4. Adherent clot catheter. A, Collapsed position. B, Partially expanded. C, Fully expanded.

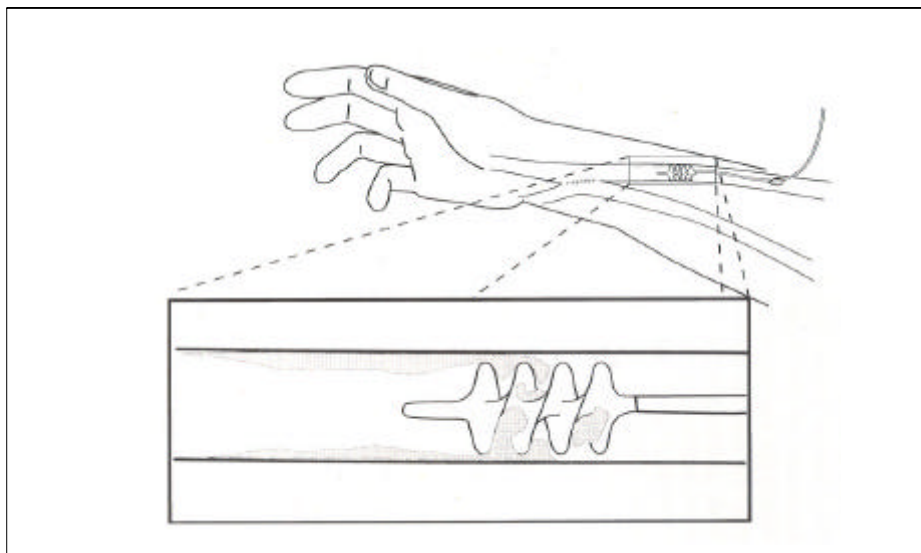
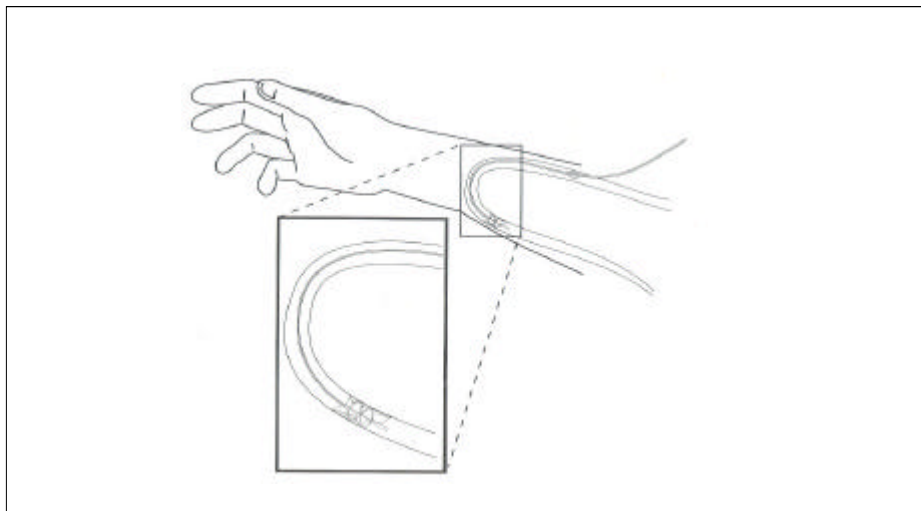
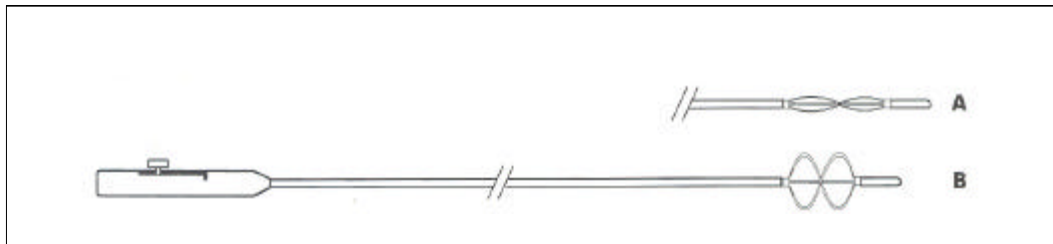


Fig. 5. Adherent clot catheter expanded within autogenous fistula



## Treatment of Thrombosis in Primary AV Fistula

가

가

가 . (DOQI guideline 22)

## Treatment of Infection of Primary AV Fistula & AV Graft

가

2 - 3%

11 - 35%

DOQI guideline 32

가

1%

10%

80%  
(S. aureus)

가

90

가

가

가 가

(subacute bacterial endocarditis)

6

. (DOQI guideline 25)

가 가

(Fig. 8),

가

1

. (DOQI guideline 24)

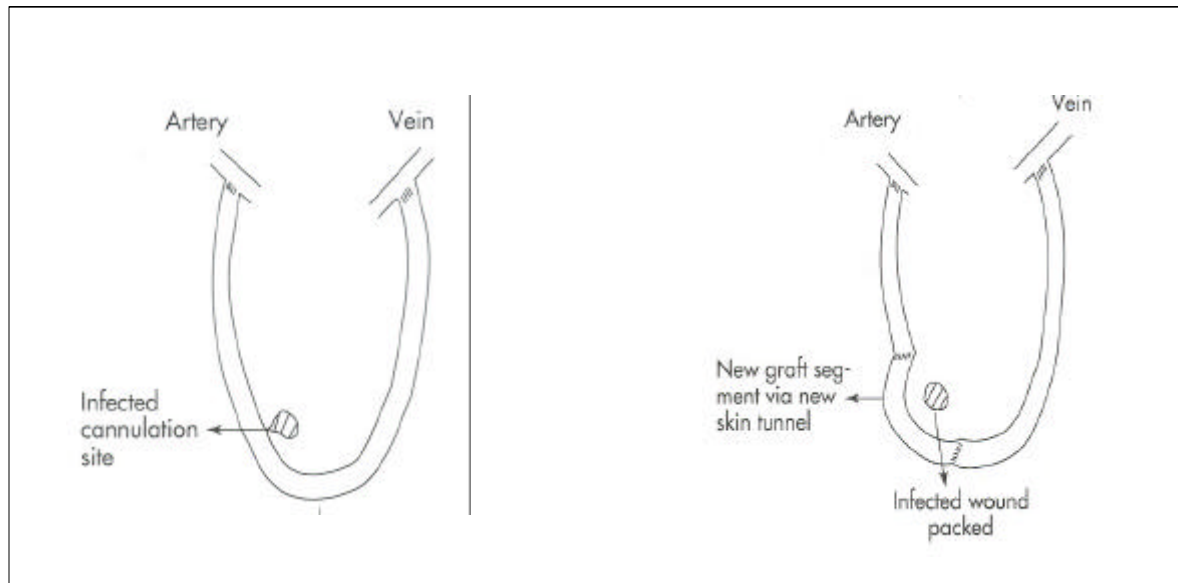


Fig. 8. Technique of local graft revision

## Treatment of Pseudoaneurysm of Dialysis AV Graft

가 (true aneurysm)가 , 가 . 가 (DOQI guideline 28)

가 2가 가 . 가 (bite)

가 /

가 (coordinator)가 multidisciplinary 가 , DOQI guideline

가 가 . 가 2 , 가 가 가 . (DOQI guideline 27)

## Treatment of Aneurysm of Primary AV Fistula

1. Brescia MJ, Cimino JE, Appel K. Chronic hemodialysis using venipuncture and surgically created arteriovenous fistula. N Engl J Med 1966;275:1089-1092
2. U.S. Renal Data system: USRDS 2002 Annual Data Report. Bethesda, MD: National institutes of



Health, National Institute of Diabetes and Digestive and Kidney Diseases, 2002

3. NKF-K/DOQI Clinical Practice Guidelines for Vascular Access: update 2000. *Am J Kidney Dis* 2001;37(1 Suppl 1):S137-S181

4. Charmaine EL, Matthew JO. Overcoming barriers to arteriovenous fistula creation and use. *Semin Dial* 2003;16:189-196

5. Marko Malovrh. The role of sonography in the planning of arteriovenous fistulas for hemodialysis. *Semin Dial* 2003;16:299-303

6. Earl S, Blayne AS, John WR, et al. Achieving vascular access success in the quality outcomes era. *Am J Surg* 2004;187:585-589

7. Samuel EW. Vascular access Principles and Practice. 3rd ed. Mosby. 1996

8. Clowes AW, Rosenberg RD, Clowes MM. Regulation of arterial smooth muscle cell proliferation by heparin in vivo. *Surg Forum* 1983;34:357-360

9. Ming WL, Gary SR, Spencer BK III. Restenosis after coronary angioplasty potential biologic determinants and role of intimal hyperplasia. *Circulation* 1989;79:1374-1384

10. Willis AI, Pierre-Paul D, Sumpio BE, Gahtan V. Vascular smooth muscle cell migration: current research and clinical implications. *Vasc Endovascular Surg* 2004 ;38:11-23



## Monitoring and Surveillance of Vascular Access

(7).

가 , 2000

37

5  
190

(1).

2.

. AVG  
(47%),  
1 cm  
(6%),  
(8).  
(peripheral basilic) (19%),  
(11%), (6%),  
(4%), midgraft (2%)  
(9): 1 ; 2  
(static venous pressure); 3)  
(dynamic venous pressure); 4)  
; 5)  
6) 7) 8)  
9) Doppler

1.

가 (autologous  
arteriovenous fistula, AVF)  
(arteriovenous graft, AVG)  
( , , )가 AVF  
AVG 3-4  
AVF  
가, 가,  
가, 가,  
가 (3, 4).  
AVF 가  
(5, 6). doppler (venous mapping)  
가  
2 mm  
3 mm  
AVF 가 450-600 ml/min  
AVG 600-800 ml/min  
가 (11-13).  
가 25%  
1

(14). , (22).

(indicator) (15) , 1998 (22).

Krivitsky (16) (ultrasound velocity dilution technique) (Transonic System Inc., Ithaca, NY, USA) AVF AVG .

'gold standard' 가 (23, 24).

가 2 AVF AVG (14).

가 (3) (urea recirculation ratio)

(2) 가 가 (25).

two needle method 10% .

(collateral circulation) 가 AVF 가 AVF AVF 가

가 가 가 AVF 가 (dialysis adequacy) Kt/Vurea

가 AVF AVG 가 urea reduction ratio (URR)

(normalization) (19, 20). 가 (26).

50% 50% (5)

(19). 50%

(venous pressure) (thrill) (bruit)

1 0 ml/min (static venous pressure) 가 가

transducer 가 (21).

Access Alert (Medisystems) (6)

(hydrophobic) luer connector, (aneroid manometer) (fistulogram)

(7)

Smits (28) static pressure  
Transonic  
가  
(dynamic venous pressure) static pressure  
50%

가  
가  
AVG  
AVF

3.

(1)

50 - 70%  
(transluminal angioplasty)  
, 6 가  
, AVG  
50% 3  
metallic stent  
, stent PDGF  
stent  
(30). 가 90%

urokinase (UK), UK +  
3가

(2)

(A)

(B)

AVG 가 di-  
pyridamole fish oil 가  
Dipyridamole aspirin 가  
, 1994 Sreedhara (31) AVG  
가 aspirin  
expanded polytetrafluoroethylene (ePTFE)  
graft  
graft  
dipyridamole aspirin 18  
dipyridamole 219%, dipyridamole aspirin  
2511%, 4213%, as -  
pirin 8012%, , dipyridamole  
가 0.35 aspirin  
1.99 2

, aspirin dipyridamole  
, PDGF  
가 (32) dipyridamole (33)  
, Warfarin AVG  
가 (34), adenosine  
diphosphate clopidogrel AVG 가  
가 (35).  
, fish oil - 3 fatty acids가

가 . Schmitz (36) 24  
AVG fish oil 12 12  
12 1  
fish oil 75.6%  
14.9% fish oil

AVG AVF  
. Grontoft (37) AVF 42  
ticlopidine 4



ticlopidine AVF . AVF .  
 NIH Dialysis Access Consortium (D)  
 clopidogrel AVF ,  
 가 .  
 (C) 가 (41).  
 4.  
 keloid  
 (fibrovascular proliferation)  
 가 (38). 가 AVF . , 1 1  
 가 가  
 (39),  
 (40).

1.

|  |
|--|
| Color Doppler ultrasound (quantitative color velocity imaging) |
| Ultrasound flow dilution (Transonics)                          |
| Crit-Line III (In-Line Diagnostics)                            |
| Crit-Line III TQA (In-Line Diagnostics)                        |
| Variable flow (VF) Doppler (Specs USA)                         |
| InGraft Velocitymetry (InGraft Technology)                     |
| Blood Velocity Meter (EchoCath, Inc.)                          |

2.

static pressure

| Degree of stenosis | Graft arterial segment | Graft venous segment | Native arterial segment  |                 |
|--------------------|------------------------|----------------------|--------------------------|-----------------|
| < 50% D            | 0.35-0.74              | 0.15-0.49            | 0.13-0.43                |                 |
| > 50% D            |                        |                      |                          |                 |
| V. Outlet          | >0.75 or > 0.5         |                      | > 0.43 or > 0.35         |                 |
| Intra-Access       | >0.65 and < 0.5        |                      | > 0.43 and < 0.35        |                 |
| A. Infl            | < 0.3                  | Clinical findin      | < 0.13 + Clinical findin | Clinical findin |

1. United States Renal Data System: USRDS 2002 Annual Data Report, Bethesda, MD, The National Institutes of Health, National Institute of Diabetes and Digestive and Kidney Diseases, 2002
2. Health Care Financing Administration: Annual Report, End-Stage Renal Disease Clinical Performance Measures Project. Baltimore, Department of Health and Human Services, Health Care Financing Administration, Office of Clinical Standards and Quality, 2000
3. Hirth RA, Turenne MN, Woods JD, Young EW, Port FK, Pauly MV, Held PJ: Predictors of type of vascular access in hemodialysis patients. *JAMA* 1996;276:1303-1308.
4. Kaufmann JL: The decline of the autogenous hemodialysis access site. *Semin Dial* 1995;8:59-61.
5. Lemson MS, Leunissen KML, Tordoir JGM: Does preoperative duplex examination improve patency rates of Brescia-Cimino fistulas? *Nephrol Dial Transplant* 1998;13:1360-1361.
6. Sedlacek M, Teodorescu V, Falk A, Vassolotti JA, Uribarri J: Hemodialysis access placement with pre-operative noninvasive vascular mapping: Comparison between patients with and without diabetes. *Am J Kidney Dis* 2001;38:560-564.
7. Besarab A, Escobar FS III: A Glimmer of hope: Increasing the construction and maturation of autologous arteriovenous fistulas. *Am J Kidney Dis* 1999;33:977-979.
8. Kanterman RY, Vesely TM, Pilgram TK, Guy BW, Windus DW, Picus D: Dialysis access grafts: anatomic location of venous stenosis and results of angioplasty. *Radiology* 1995;195:135-139.
9. Ascher E, Hingorani A: The Dialysis Outcome and Quality Initiative (DOQI) recommendations. *Semin Vasc Surg* 2004;17:3-9.
10. Sherman R, Besarab A, Schwab SJ, Beathard GA: Recognition of the failing vascular access: A current perspective. *Semin Dial* 1997;10:1-5.
11. Bosman PJ, Boereboorn FTJ, Eikelboom BC, Koomans HA, Blankestijn PJ: Graft flow as a predictor of thrombosis in hemodialysis grafts. *Kidney Int* 1998;54:1726-1730.
12. May RE, Himmelfarb J, Yenicesu M, Knights S, Ikizler TA, Schulman G, Hernanz-Schulman M, Shyr Y, Hakim RM: Predictive measures of vascular access thrombosis - A prospective study. *Kidney Int* 1997;52:1656-1662.
13. Neyra NR, Ikizler TA, May RE, Himmelfarb J, Schulman G, Shyr Y, Hakim RM: Changes in access blood flow over time predicts vascular access thrombosis. *Kidney Int* 1998;54:1714-1719.
14. Besarab A: Preventing Vascular Access Dysfunction: Which Policy to Follow. *Blood Purif* 2002;20:26-35.
15. Lindsay R, Leypoldt J: Monitoring vascular access flow. *Adv Renal Replace Ther* 1999;30:273-277.
16. Krivitsky NM, MacGibbon D, Gleed RD, Dobson A: Accuracy of dilution technique for access flow measurement during hemodialysis. *Am J Kidney Dis* 1998;31:502-508.
17. Weitzel WF, Rubin JM, Swartz RD, Wolman DJ, Messaana JM: Variable flow Doppler of hemodialysis access evaluation. Theory and clinical feasibility. *ASAIO J* 2000;46:65-69.
18. Steuer RR, Miller DR, Zhang S, Bell DA, Leypoldt JK: Noninvasive transcutaneous determination of access blood flow rate. *Kidney Int* 2001;60:284-291.
19. Besarab A, Sullivan KL, Ross R, Moritz M: The utility of intra-access monitoring in detecting and correcting venous outlet stenoses prior to thrombosis. *Kidney Int* 1995;47:1364-1373.
20. Besarab A, Lubkowski T, Vu A, Aslam M, Frinak S: Determinants of vascular access flow. *ASAIO J* 2001;47:501-506.
21. Besarab A, Frinak S, Sherman RA, Goldman J, Dumler F, DeVita MV, Kapoian T, Al-Saghir F, Lubkowski T: Simplified measurement of intra-access pressure. *J Am Soc Nephrol* 1998;9:284-289.
22. Besarab A, Lubkowski T, Frinak S: A simpler method for measuring intra-access pressure (abstract). *J Am Soc Nephrol* 1999;11:202A.
23. Besarab A, Lubkowski T, Frinak S, Ramanathan S, Escobar F: Detection of strictures and vascular outlet stenoses in vascular accesses: Which test is best? *ASAIO J* 1997;43:M543-M547.
24. Besarab A, Lubkowski T, Frinak S, Ramanathan S, Escobar F: Detecting vascular access dysfunction. *ASAIO J* 1997;43:M539-M543.
25. , , , , :

1998;54:729-736.

26. Besarab A, Samarapungavan D: Measuring the adequacy of hemodialysis access. *Curr Opin Nephrol Hypertens* 1996;5:527-531.

27. Beathard GA: Physical examination of AV grafts. *Semin Dial* 1996;5:74.

28. Smits JHM, Van der Linden J, Hagen EC, Modderkolk-Cammwraat EC, Feith GW, Koomans HA, van den Dorpel MA, Blankestijn PJ: Graft surveillance: Venous pressure, access flow, or the combination? *Kidney Int* 2001;59:1551-1558.

29. Beathard GA: Percutaneous angioplasty for the treatment of venous stenosis: A nephrologists view. *Semin Dial* 1995;8:166-170.

30. Burger H, Zijlstra JJ, Kluchert SA, Scholten AP, Kootstra G: Percutaneous transluminal angioplasty improves longevity in fistulae and shunts for hemodialysis. *Nephrol Dial Transplant* 1990;5:608-611.

31. Sreedhara R, Himmelfarb J, Lazarus JM, Hakim RM: Antiplatelet therapy in graft thrombosis: results of a prospective, randomized double-blind study. *Kidney Int* 1994;45:1477-1483.

32. Harvey R, Bredenberg CE, Couper L, Himmelfarb J: Aspirin enhances platelet-derived growth factor-induced vascular smooth muscle cell proliferation. *J Vasc Surg* 1997;25:689-695.

33. Himmelfarb J, Couper L: Dipyridamole inhibits PDGF- and bFGF-induced vascular smooth muscle cell proliferation. *Kidney Int* 1997;52:1671-1677.

34. Crowther MA, Clase CM, Margetts PJ, et

al: Low-intensity warfarin is ineffective for the prevention of PTFE Graft failure in patients on hemodialysis: a randomized controlled trial. *J Am Soc Nephrol* 2002;13:2331-2337.

35. Kaufman J, O'Connor T, Cronin R, et al: Combination aspirin plus clopidogrel in the prevention of hemodialysis access graft thrombosis [abstract]. *J Am Soc Nephrol* 2001;12:291A.

36. Schmitz PG, McCloud LK, Reikes ST, et al: Prophylaxis of hemodialysis graft thrombosis with fish oil: double-blind, randomized, prospective trial. *J Am Soc Nephrol* 2002;13:184-190.

37. Grontoft KC, Mulec H, Gutierrez A, Olander R: Thromboprophylactic effect of ticlopidine in arteriovenous fistulas for haemodialysis. *Scand J Urol Nephrol* 1985;19:55-57.

38. Lindsey WH, Davis PT: Facial keloid: a 15 year experience. *Arch Otolaryngol Head Neck Surg* 1998;123:397-400.

39. Teirstein PS, Massullo V, Jani S, Popma JJ, Mitnz GS, Russo RJ, et al: Catheter-based radiotherapy to inhibit restenosis after coronary stenting. *New Engl J Med* 1997;1997:1697-1703.

40. Wong FK, Kwok PC, Ngan RK, Wong RK, Wong K, Chan S, Chau K, Li C: Prevention of restenosis of central venous stricture after percutaneous transluminal angioplasty and endovascular stenting by brachytherapy. *Kidney Int* 1999;55:742-743.

41. Sukhatme V: Vascular access stenosis: prospects for prevention and therapy. *Kidney Int* 1996;49:1161-1174.



# Endovascular Management of Failing Native Hemodialysis Fistulas

/

(vascular access)  
 . 1966 Brescia  
 (radial artery) (cephalic vein)  
 (autogenous arteriovenous fistula, AVF )  
 . Dialysis Outcomes Quality Initiative  
 (DOQI) , polytetrafluoroethylene (PTFE)  
 AVF  
 . AVF (forearm)  
 radiocephalic (Brescia-Cimino)  
 fistula가 가 (upper  
 arm) (brachial artery) brachioce-  
 phalic, brachio basilic, brachial artery - to - median cubi-  
 tal vein AVF  
 가  
 . AVF  
 (hemodialysis access  
 failure)  
 가  
 , 10-20% AVF가 3 , 2  
 60-70% AVF 가  
 AVF  
 가

## Arteriovenous Fistula Stenosis

### A. Etiology and Definitions

AVF  
 (intimal hyperplasia)  
 . AVF

1)  
 2cm juxtaanastomotic stenosis (Fig 1), 2)  
 2cm  
 proximal stenosis (Fig 2), 3)  
 central stenosis 3가  
 juxtaanas-  
 tomotic stenosis가 가  
 2-5%  
 50%  
 50%  
 . AVF 1/3  
 2  
 AVF  
 3  
 (early failure) , 3  
 (late failure) 2가  
 juxtaanastomotic stenosis accessory vein  
 Accessory vein AVF (outflow vein)  
 . Accessory vein  
 siphoning  
 가 AVF 가  
 . Accessory vein  
 . Accessory vein  
 (pulse) (thrill) 가  
 accessory vein . Accessory vein  
 1/3

### B. Fistulography

AVF  
 (inflow artery)  
 ,  
 ,  
 ,  
 AVF



micropuncture set  
5Fr dilator  
sheath  
가

60-70% , 6 81-100%, 12  
80-100%  
2-6%  
2%  
4-5  
urokinase

### C. Angioplasty

6-7 Fr sheath 5,000 U Heparin  
. 0.035 inch (Terumo)  
가 , elastic recoil  
(high-pressure) , 16  
20-30%  
4mm, brachial artery  
6mm, juxtaanastomosis, proximal  
stenosis 6-8mm  
(inflation time) 1  
, 2-3 10mL  
10  
5mL  
20  
, 0.05mg fentanyl citrate 1mg mid-  
azolam , 0.25mg  
nitroglycerin  
sheath side arm  
가  
가  
30%  
가  
AVF (thrill) , (pulse)  
AVF 가 20% 가  
, 3 2

### D. Stenting

AVF  
. AVF  
1)elastic recoil  
, 2)  
3)  
(Fig 3).  
가 , Brescia-Cimino AVF  
6 , 1 47% 20%  
가 가  
covered stent

### Arteriovenous Fistula Thrombosis

AVF 3  
가 ,  
85%  
plug . AVF 1)  
taanastomotic , 3) , 2) jux -  
3가 ,  
. 1) 가 , 2)  
. 3)  
가  
(percutaneous declotting)

### Percutaneous declotting

(primary patency) , AVF  
(secondary patency) . AVF  
6 71-81%, 12

(pharmacomechanical method) ,





Figure 1. Left brachial arteriogram injection shows diffuse and severe juxtaanastomotic stenosis (arrows) in the left radiocephalic fistula.

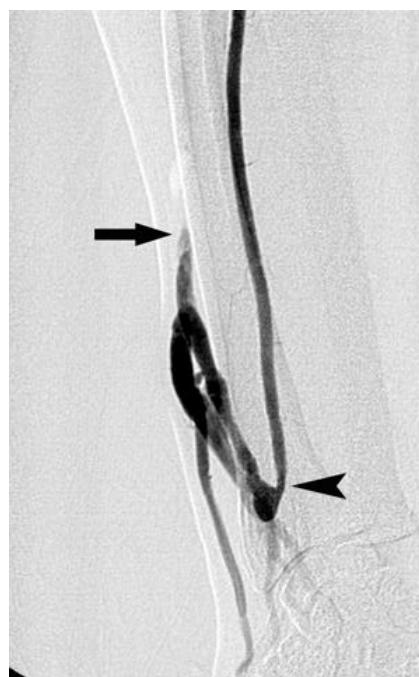


Figure 3. Angioplasty and stenting for the treatment of AVF occlusion. (a, b,c)

Fig. 3a. Right brachial artery injection shows complete occlusion of distal outflow vein (arrow) and stenosis in the anastomotic site (arrowhead). Both stenoses were dilated with a 6-mm balloon catheter.



Figure 2. Right brachial arteriogram shows severe proximal venous stenosis (arrow) and anastomotic site stenosis (arrowhead).

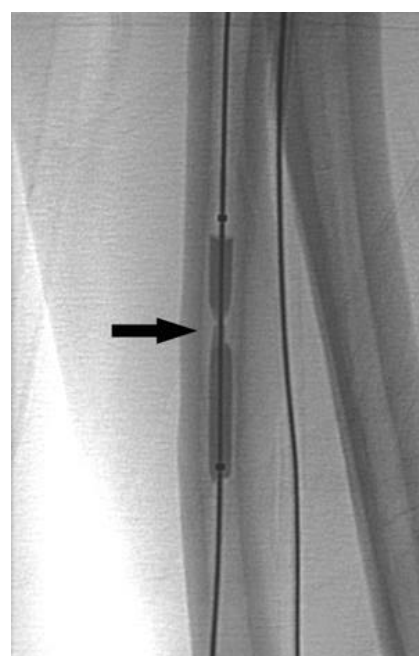


Fig. 3b. Plain radiograph obtained during balloon inflation shows tight stenosis (arrow) in the distal portion of outflow vein.



Fig. 3c. Angiogram obtained after angioplasty shows intraluminal thrombosis, elastic recoil, and a focus of contrast extravasation.



Fig. 3d. Angiogram obtained after placement of a stent with 6mm in diameter shows patent lumen and good flow through AVF.

Fig. 4. Pharmacomechanical declotting for the treatment of AVF thrombosis. (a, b, c, d)

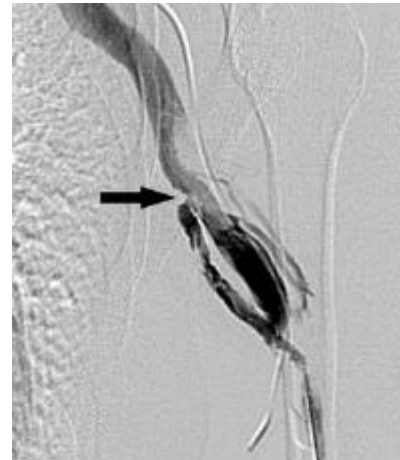


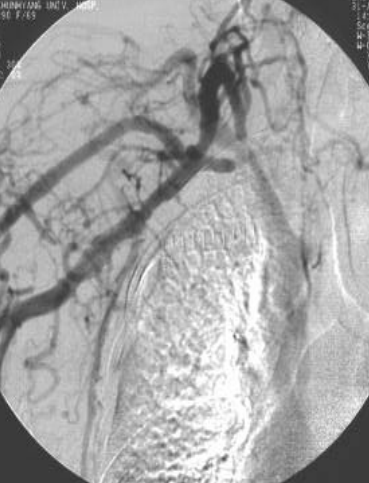
Fig.4a. Fistulogram obtained after puncture of AVF shows large amounts of thrombi filling the entire outflow vein and underlying venous stenosis (arrow).



Fig. 4b. Fistulogram obtained after thrombolysis with "lyse and wait" technique followed by subsequent angioplasty shows restoration of shunt flow but remained stenosis due to elastic recoil.



Fig. 4c. Fistulogram obtained after stenting (arrow) followed by aspiration thrombectomy shows good result.



## Interventional Treatment for Hemodialysis Arteriovenous Graft

가

가

(1).

59%

(8).

fistula)

(arteriovenous graft)

가 가

(arteriovenous

가

가

, 가  
가 ,

가

가

(2).

(bovine vein),  
(PTFE)

(Dacron),

PTFE

(3). PTFE

1

5 F

60 - 80%

(4, 5).

50 %

(6, 7)

(9).

1.

DOQI

가

(vascular

(thrill)

(pulse)

가

sheath)

(Fig. 1).

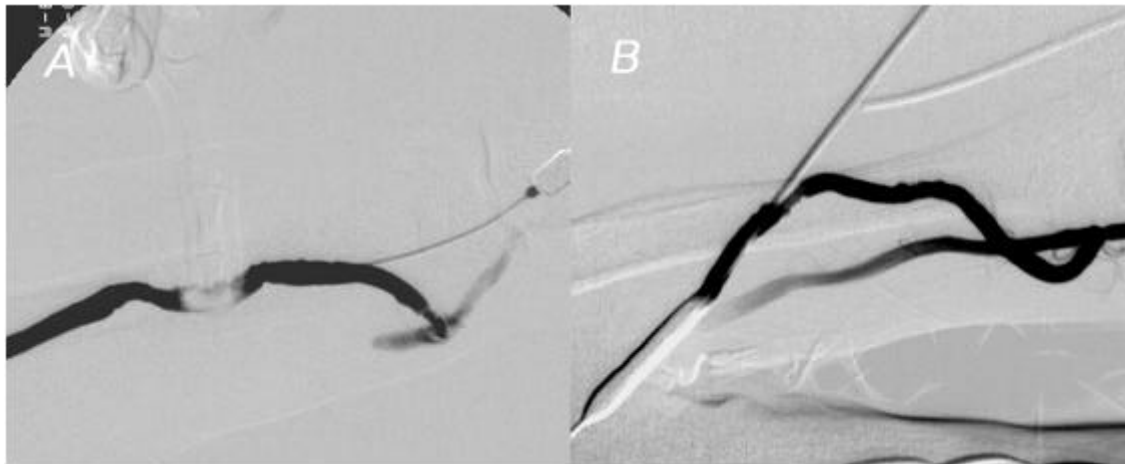


Fig. 1. The arterial anastomosis can be evaluated by manual compression of graft (A) or inflation of balloon catheter (B) during injection of contrast media.

nique) (10), (apex puncture tech- (Fig. 2).  
1~2cm

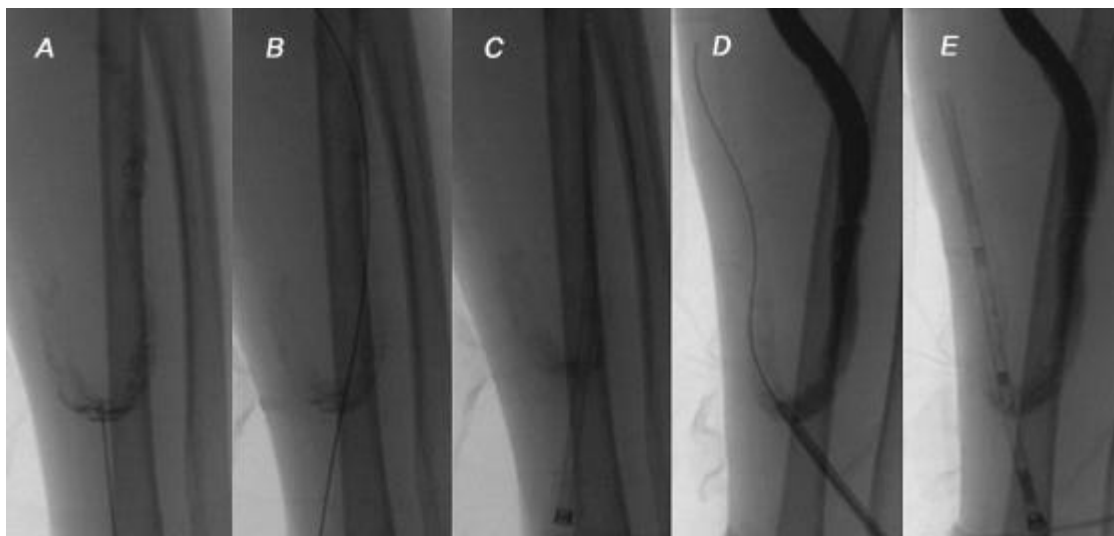


Fig. 2. Apex puncture technique. A & B. The apex of the U-configured graft was punctured with a 21 G needle and 0.019 inch air wire was then inserted toward venous anastomosis. C. A vascular sheath was inserted for angioplasty. D & E. After balloon angioplasty was performed at the venous anastomosis, the vascular sheath was placed into the arterial limb over the guide wire.

가  
가 가  
가

2.

1) 7 mm 8 mm 1~2mm PTFE 가 (Fig. 3). 10~14 mm (11).

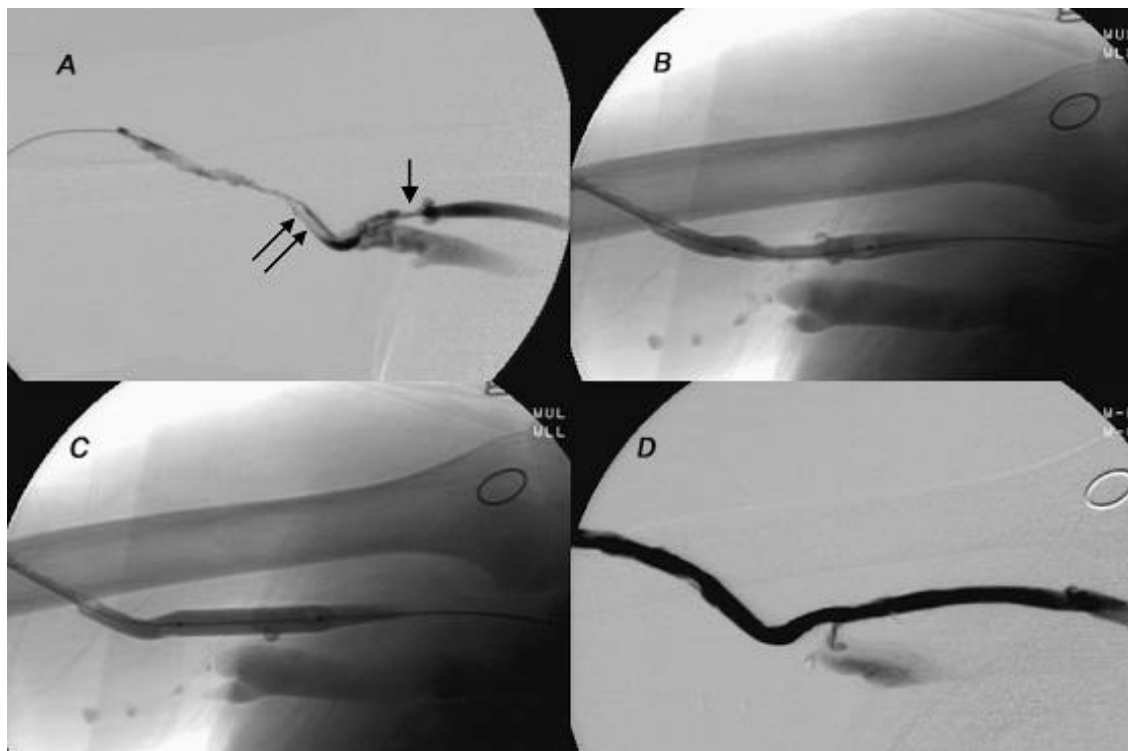


Fig. 3. A. Fistulogram of right brachioaxillary graft shows severe stenosis which involves venous anastomosis site (long arrow) with intraluminal thrombi (arrows). B & C. The stenosis site is dilated with balloon catheter. D. After the intragraft thrombi have been removed, follow-up fistulography shows no residual stenosis or thrombi.

(elastic recoil) 20~30 가 . 30% 가 (11).

(cutting) (Fig. 4).  
(Fig. 5) (12).



Fig. 4. A. Fistulogram shows severe stenosis which involves venous anastomosis site (long arrow). B. The stenosis site is dilated with a 6mm-4cm balloon catheter. C. Residual stenosis is seen on follow-up fistulogram. D. The stenosis site is again dilated with an 8mm-4cm balloon catheter. E. No residual stenosis is noted at venous anastomosis site.

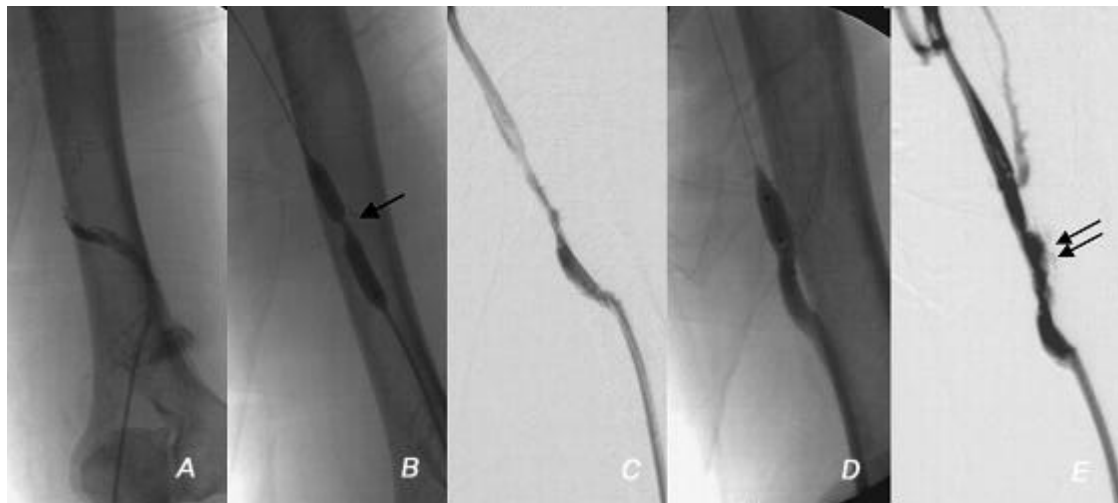


Fig. 5. A. Fistulogram shows severe stenosis which involves venous anastomosis of brachio-basilic graft. B. Although the stenosis site is dilated using a 6mm-4cm balloon catheter with 20 atm, the waist of the balloon remains (arrow). C. Residual stenosis persists on follow-up fistulogram. D. The stenosis site is again dilated with a 6mm-4cm cutting balloon catheter. E. No residual stenosis site is observed, but evidence of minimal rupture is seen (arrows).

가 10 mmHg , DOQI  
33% , 3  
가  
(13). 가  
가  
(Fig. 6) (14, 15).



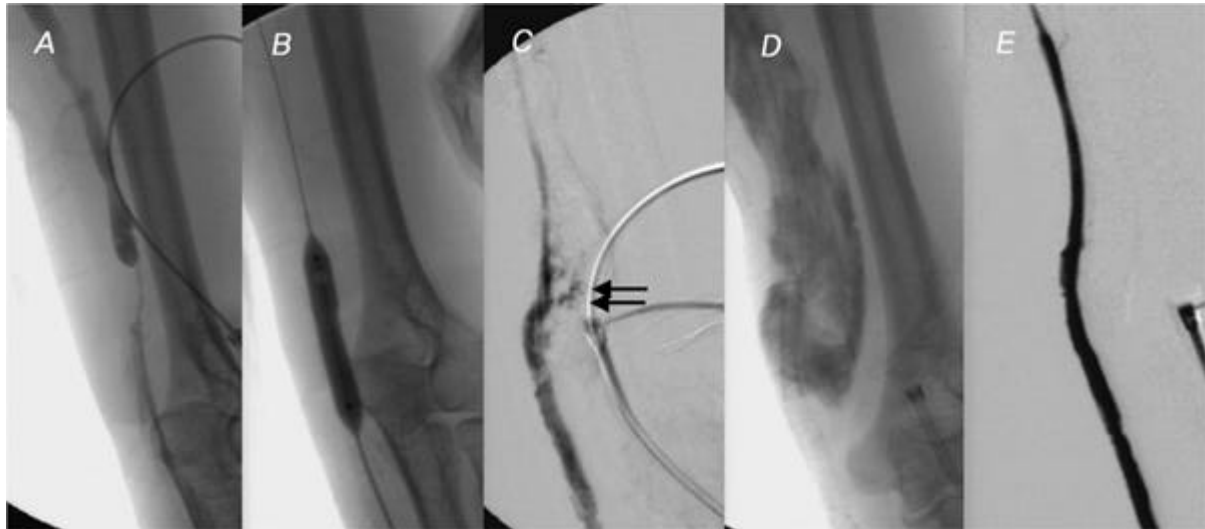


Fig. 6. A. Fistulogram shows severe stenosis at venous anastomosis of brachio basilic graft. B. The stenosis site is dilated using an 8mm-4cm balloon catheter C. The stenotic site shows extravasation of contrast media (arrows) and residual narrowing due to hematoma. D. A self-expandable, uncovered intravascular stent (8X38 mm, Easywall; Boston Scientific) is deployed at the rupture site. E. Follow-up fistulogram shows no more residual narrowing or extravasation.

3. 가 (17). (pulse-spray technique) , 50 5,000 0.2~0.4 mL 30 jump revision 가 (16), 가 "Lyse and wait" 가 1) (Thrombolysis) 가 1-2 "lyse and wait" 25 2,000~5,000 (18). 가 30-90 (Fig. 7).

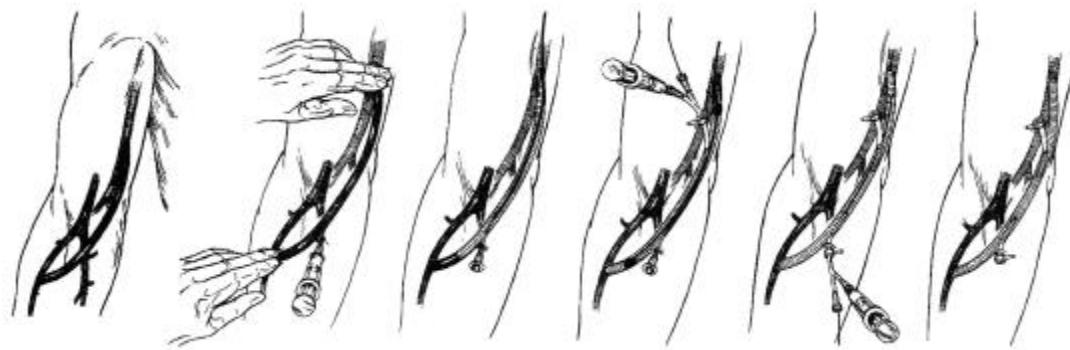


Fig. 7. "Lyse and wait" technique.

2) (Thrombectomy)

(Fig. 8).

3

35~45%

4 cm3

(balloon thrombectomy)

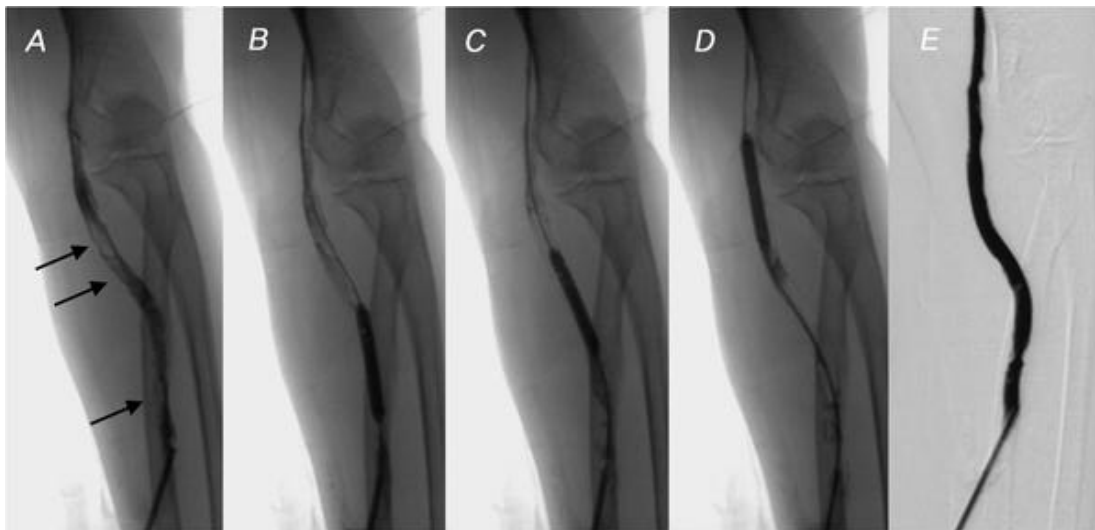


Fig. 8. Balloon thrombectomy. A. Thrombi are seen as filling defects within venous limb of brachiocephalic graft (arrows). B-D. After the thrombi are macerated by inflated balloon catheter, they are swept into pulmonary circulation by the inflated balloon catheter. E. Follow-up fistulogram shows no residual thrombi.

(thromboaspiration)

가

(BAT; balloon assisted

thromboaspiration)

(19). BAT 7~8 F

4

3)

(Mechanical

Thrombectomy Devices)

(Fig. 9) (20 - 22).

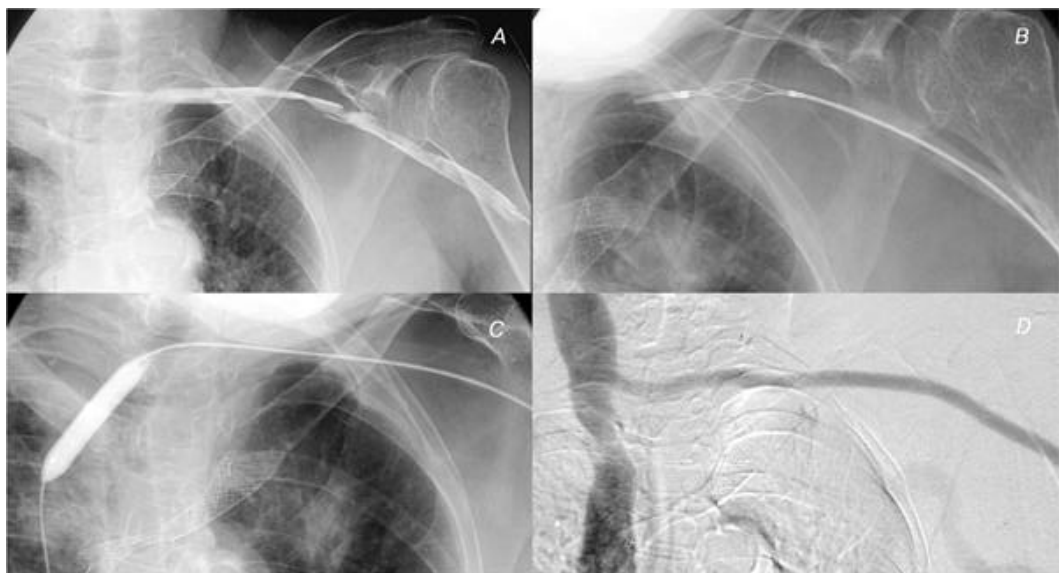


Fig. 9. Trerotola-PTD. A. Thrombi are seen as filling defects within left axillojugular graft. B. The thrombi are fragmented using Trerotola-PTD device. C. Residual thrombi are swept into pulmonary circulation by balloon catheter. D. Follow-up fistulogram shows no residual thrombi within graft.

가

,

,

가

.

3

EndoVac (Neurovascular Technologies, Brooklyn, NY) Trerotola-PTD가

.

가 가 (23).

Trerotola-PTD가

.

가

가

가

,

.

가

.

가

,

,

,?

,

?

.

가

?

- 2002-22(S2): S353-368
- Gaylord GM, Taber TE. Long-term hemodialysis access salvage: problems and challenges for nephrologists and interventional radiologists. *Vasc Interv Radiol* 1993;4:103-7
- Butler HG 3rd, Baker LD Jr, Johnson JM. Vascular access for chronic hemodialysis: polytetrafluoroethylene (PTFE) versus bovine heterograft. *Am J Surg* 1977;134:791-3
- Munda R, First MR, Alexander JW, Linnemann CC Jr, Fidler JP, Kittur D. Polytetrafluoroethylene graft survival in hemodialysis. *JAMA* 1983;249:219-22
- Palder SB, Kirkman RL, Whittemore AD, Hakim RM, Lazarus JM, Tilney NL. Vascular access for hemodialysis. Patency rates and results of revision. *Ann Surg* 1985;202:235-9
- Sullivan KL, Besarab A. Hemodynamic screening and early percutaneous intervention reduce hemodialysis access thrombosis and increase graft longevity. *J Vasc Interv Radiol* 1997;8(2):163-70
- Schwab SJ, Oliver MJ, Suhocki P, McCann R. Hemodialysis arteriovenous access: detection of stenosis and response to treatment by vascular access blood flow. *Kidney Int* 2001;59(1):358-62
- Trerotola SO, Scheel PJ Jr, Powe NR, Prescott C, Feeley N, He J, Watson A. Screening for dialysis access graft malfunction: comparison of physical examination with US. *J Vasc Interv Radiol* 1996;7(1):15-20
- Eknoyan G, Levin NW, Eschbach JW, et al. Continuous quality improvement: DOQI becomes K/DOQI and is updated. National Kidney Foundations Dialysis Outcomes Quality Initiative. *Am J Kidney Dis* 2001;37:179-194
- Hathaway PB, Vesely TM. The apex-puncture technique for mechanical thrombolysis of loop hemodialysis grafts. *J Vasc Interv Radiol* 1999;10(6):775-9
- Weintraub JL, Rundback JH. Endovascular intervention: fistulography, angioplasty, and stents. In Gray RJ, Sands JJ. *Dialysis Access: a multidisciplinary approach*. Philadelphia: Lippincott Williams & Wilkins 2002:161-169
- Vorwerk D, Gunther RW, Schurmann K, Sieberth HG. Use of a cutting balloon for dilatation of a resistant venous stenosis of a hemodialysis fistula. *Cardiovasc Intervent Radiol*. 1995;18:62-4
- Sullivan KL, Besarab A. Strategies for maintaining dialysis access patency. In: Cope C, ed. *Current techniques in interventional radiology*, 2nd ed. Philadelphia: Current Medicine, 1995:125-131
- Funaki B, Szymiski GX, Leef JA, Rosenblum JD, Burke R, Hackworth CA. Wallstent deployment to salvage dialysis graft thrombolysis complicated by venous rupture: early and intermediate results. *AJR* 1997;169(5):1435-7
- Rundback JH, Leonardo RF, Poplausky MR, Rozenblit G. Venous rupture complicating hemodialysis access angioplasty: percutaneous treatment and outcomes in seven patients. *AJR* 1998;171(4):1081-4
- Bitar G, Yang S, Badosa F. Balloon versus patch angioplasty as an adjuvant treatment to surgical thrombectomy of hemodialysis grafts. *Am J Surg* 1997;174(2):140-2
- Valji K, Bookstein JJ, Roberts AC, Oglevie SB, Pittman C, O'Neill MP. Pulse-spray pharmacomechanical thrombolysis of thrombosed hemodialysis access grafts: long-term experience and comparison of original and current techniques. *AJR* 1995;164(6):1495-500
- Cynamon J, Lakritz PS, Wahl SI, Bakal CW, Sprayregen S. Hemodialysis graft declotting: description of the "lyse and wait" technique. *J Vasc Interv Radiol* 1997 ;8(5):825-9
- Sharafuddin MJ, Kadir S, Joshi SJ, Parr D. Percutaneous balloon-assisted aspiration thrombectomy of clotted hemodialysis access grafts. *J Vasc Interv Radiol* 1996;7(2):177-83
- Sharafuddin MJ, Hicks ME. Current status of percutaneous mechanical thrombectomy. Part I. General principles. *J Vasc Interv Radiol* 1997;8(6):911-21
- Sharafuddin MJ, Hicks ME. Current status of percutaneous mechanical thrombectomy. Part II. Devices and mechanisms of action. *J Vasc Interv Radiol* 1998;9:15-31
- Sharafuddin MJ, Hicks ME. Current status of percutaneous mechanical thrombectomy. Part III. Present and future applications. *J Vasc Interv Radiol* 1998;9(2):209-24
- Puckett JW, Lindsay SF. Midgraft curettage as a routine adjunct to salvage operations for thrombosed polytetrafluoroethylene hemodialysis access grafts. *Am J Surg* 1988;156(2):139-43



/

2002 33,993 ( 가 가 .  
20,010 , 5,712 , 8,271 )  
40.7%, 16%,  
14% 가  
(1).

(Fig 1)(6). Itkin  
44% ,  
(elastic recoil)가 stent  
가 .

가 ,  
(2).

가 .

가 (3).  
40-50% , 0-10%  
(4).

1)  
가

가

1-2mm  
12mm  
10mm

high flow, turbulence-induced intimal shear injury, release of platelet-derived growth factors  
(2). 가

14-18mm  
가 1

가  
가  
가

(Fig 1, 2).  
(Fig 3).  
Pinch-Off

가 (5).  
Doppler wave  
가  
MRI가

가 (Fig 1).

가 가  
가

Glanz (2) 1 35%  
Beathard 29%(6 ), 0%(1 )  
가 3  
100%  
(7).

가  
(8).  
24  
coagulation  
anti-  
high flow가  
low-dose warfarin aspirin

## 2) Stent

stent  
가 Glanz 5-10 mmHg  
(9). DOQI guideline 20 stent  
3 2  
가  
stent  
가 (Fig 4). 가  
Wallstent 6 42-56%  
stent  
가  
stent  
stent  
가 highly flexible stent가  
balloon ex -  
pandable stent Wallstent self expandable  
stent Wallstent  
가  
가 Stent  
stent가  
가  
stent  
stent  
3  
fistulogram  
stent  
(10). Wallstent  
96-100%, 6, 12 42-56%, 20-31%  
(11-13). Stent stent  
(Fig 5). stent  
stent  
rigid stent  
stent (8).  
Stent  
atherectomy stent  
Kwok(14)  
stent brachytherapy

stent graft  
stent  
가  
stent  
Quinn (15) stent

## 3) Sharp Recanalization

가  
가 stent  
Murphy(16) 가 가  
11-24% 가  
Rosch-Uchida Transjugular Liver Access  
set(COOK, Bloomington, IN)  
가  
2-3cm 가  
occlusion balloon  
Rosch-Uchida needle  
occlusion balloon 가  
Rosch-Uchida needle  
needle occlusion balloon  
stent 가  
가  
stent 가  
occlusion balloon  
Rosch-Uchida needle  
(lateral view)  
needle  
needle  
(abduction) (17). 가  
needle  
(Fig 6).

## 4) Complications of central vein PTA

가 stent  
7.7%

가 (Fig 7)(18).  
 가  
 Stent , stent 2.5%  
 (19). Stent stent  
 stent . Stent  
 1 - 2mm  
 가 . stent  
 stent 가 . Palmaz stent  
 stent . snare . snare  
 stent . Wallstent 가 Goose neck  
 snare  
 snare intravascular forcep  
 (19). snare stent  
 stent  
 가 가 (Fig 8).

## 5) Intervention or Surgery

surgery(Fig 9) direct repair가 graft bypass  
 acotomy가 thor-  
 (20).  
 가 DOQI guide-  
 line  
 Bhatia(21)  
 stent  
 가  
 El-Sabrou(22) 9  
 - 10-16mm graft bypass  
 1.5-52( 15.4)  
 가

1. 2002.  
 2003;22(s2):S353-368
2. Glanz S, Bashist B, Gordon DH, Butt K, Adamsons

R: Axillary and subclavian vein stenosis: Percutaneous angioplasty. Radiology 1988;168:371-373

3. Trerotola SO: Interventional radiology in central venous stenosis and occlusion. Semin Intervent Radiol 1994;11:291-304

4. Cimochowski GE, Worley E, Rutherford WE et al. Superiority of the internal jugular over the subclavian access for temporary hemodialysis. Nephron. 1990;54:154-161

5. Middleton WD, Picus DD, Marx MV, Melson GL. Color doppler sonography of hemodialysis vascular access: Comparison with angiography. AJR 1989;152: 633-639

6. Itkin M, Kraus MJ, Trerotola SO. Extrinsic compression of the left innominate vein in hemodialysis patients. JVIR. 2004;15:51-56

7. Glanz S, Gordon D, Butt KMH, et al. Dialysis access fistulas: treatment of stenoses by transluminal angioplasty. Radiology. 1984;152:637-642

8. Dondelinger RF, Goffette P, Kurdziel JC, et al. Expandable metal stents for stenoses of the venae cavae and large veins. Semin Intervent Radiol. 1991;8:252-263

9. Glanz S, Gordon DH, Butt KMH, et al. The role of percutaneous angioplasty in the management of chronic hemodialysis fistula. Ann Surg. 1987;206:777-781

10. Vesely TM, Hovsepian DM, Pilgram TK, Coyne DW, Shenoy S. Upper extremity central venous obstruction in hemodialysis patients: treatment with Wallstents Radiology 1997;204:343-348

11. Gray RJ, Horton KM, Dolmatch BL, et al. Use of Wallstents for hemodialysis access-related venous stenoses and occlusions untreatable with balloon angioplasty. Radiology. 1995;195:479-484

12. Vorwerk D, Guenther RW, Mann H, et al. Venous stenosis and occlusion in hemodialysis shunts: follow-up results of stent placement in 65 patients. Radiology. 1995;195:140-146

13. Vesely TM, Hovsepian DM, Pilgram TK, Coyne DW, et al. Upper extremity central venous obstruction in hemodialysis patients: treatment with Wallstents. Radiology. 1997;204:343-348.

14. Kwok PC, Wong KM, Ngan RK, Chan SC, Wong WK, Wong KY, Wong AK, Chau KF, Li CS. Prevention of recurrent central venous stenosis using endovascular irradiation following stent placement in hemo-

dialysis patients. *Cardiovasc Intervent Radiol*. 2001;24:400-406

15. Quinn SF, Shuman ES, Hall E, et al. Venous stenosis in patients who undergo hemodialysis; treatment with self-expandable endovascular stents. *Radiology*. 1992;183:499-504

16. Murphy TP, Webb MS. Percutaneous venous bypass for refractory dialysis-related subclavian vein occlusion. *JVIR*. 1999;9:935-939

17. . . . .  
: 1 .  
2000;42:469-471

18. . . . .  
:  
2002;46:221-227

19. Slonim SM, Dake MD, Razavi MK, Kee ST, Samuels SL, Rhee JS, Semba CP. Management of Misplaced or Migrated Endovascular Stents. *JVIR* 1999;10:851-859

20. Wisselink W, Money SR, Becker MO, et al. Comparison of operative reconstruction and percutaneous balloon dilatation for central venous obstruction. *Am J Surg*. 1993;166:200-205

21. Bhatia DS, Money SR, Ochsner JL, Crockett DE, et al. Comparison of surgical bypass and percutaneous balloon dilation with primary stent placement in the treatment of central venous obstruction in the dialysis patient: one-year follow-up. *Ann Vasc Surg* 1996;10:452-45

22. El-Sabrout RA, Duncan JM. Right atrial bypass grafting for central venous obstruction associated with dialysis access: another treatment option. *J Vasc Surg*. 1999;30:582-584

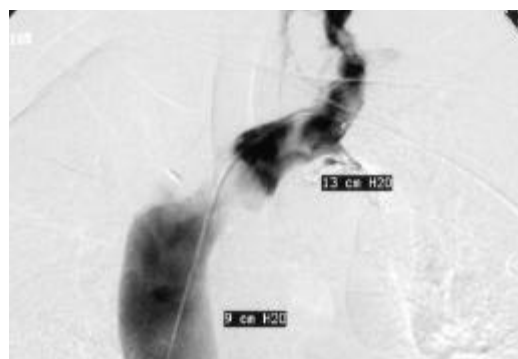


Fig 1a. Post-balloon angioplasty fistulogram shows marked residual stenosis of the innominate vein due to extrinsic compression



Fig 1b. CT venogram shows the left innominate vein is compressed between sternum and right innominate artery.

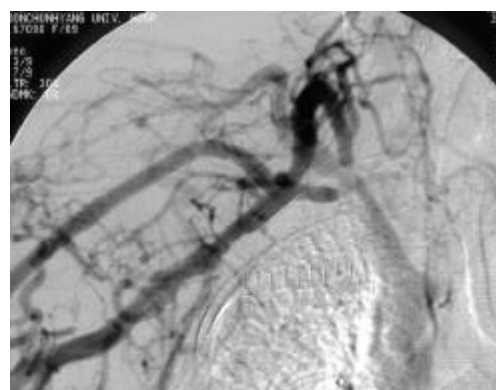


Fig 2. Fistulogram demonstrates short segmental obstruction of the right subclavian vein with multiple collaterals about the right neck.



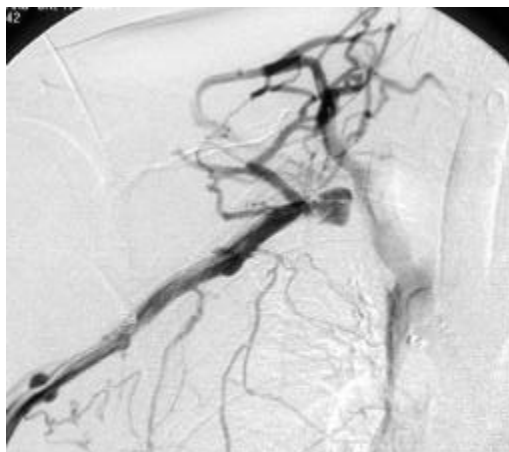


Fig 3a. Fistulogram in a patient with a right arm swelling reveals total occlusion of the right subclavian vein with marked collateralization.



Fig 4b. After a 12mm balloon angioplasty, there is some improvement in flow but persistent collateralization and pressure gradient due to elastic recoil.

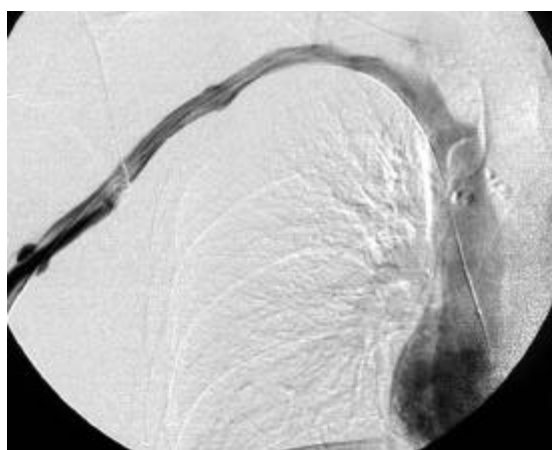


Fig 3b. Post-balloon angioplasty fistulogram reveals complete recanalization of the subclavian vein.

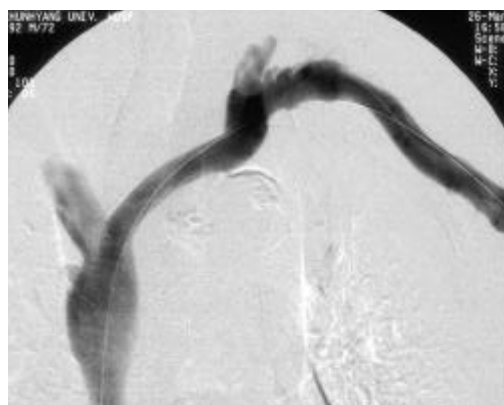


Fig 4c. After a 12mm stent placement, there is an excellent fistulographic result with complete resolution of the pressure gradient and all the collaterals.

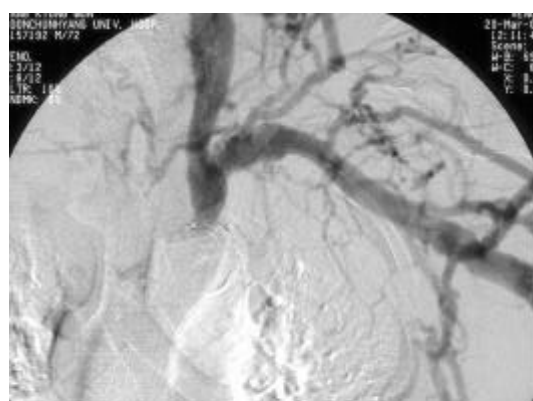


Fig 4a. Fistulogram in a patient with a left arm swelling shows complete obstruction of the left innominate vein.

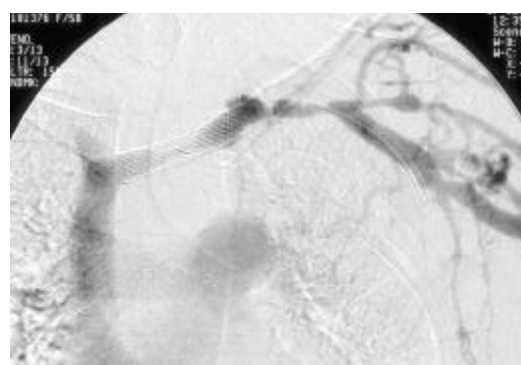


Fig 5a. Fistulogram shows marked stenosis of the intra-stent and subclavian veins with pronounced collateral flow in a patient complaining of arm swelling 5 month after deployment of a 12X40mm Niti-S stent.

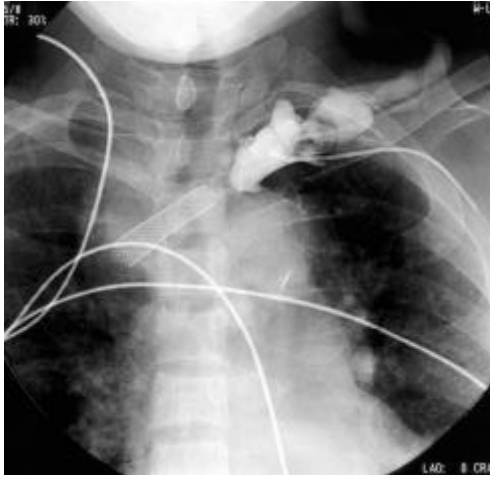


Fig 5b. Central fistulogram demonstrates complete obstruction of the distal stent margin in an arm swelling patient 11 months after deployment of a 14X40mm Wallstent.



Fig 6c. On the lateral spot film, the tip of trocar stylet overlaps with a headhunter catheter in the jugular vein.

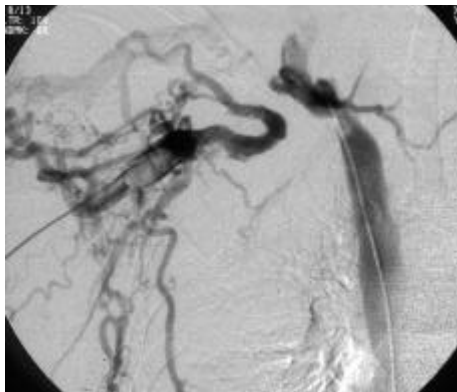


Fig 6a. Upper extremity venogram shows segmental occlusion of the right subclavian vein but no evidence of innominate vein stenosis.



Fig 6d. After angioplasty and placement of a self expandable stent, fistulogram shows patency of the venous shunt without extravasation.



Fig 6b. Spot film shows placement of a Rosch-Uchida curved stainless-steel cannula and trocar stylet in the right subclavian vein, directed toward a headhunter catheter in the jugular vein.

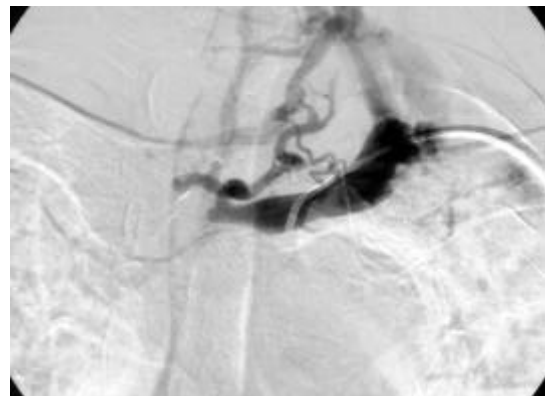


Fig 7a. Complete obstruction of the left innominate vein

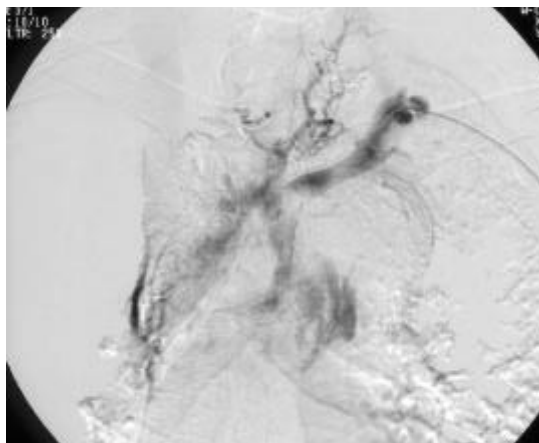


Fig 7b. During the procedure, venous rupture was induced by a guide wire and fistulogram revealed massive extravasation of contrast into the mediastinum.

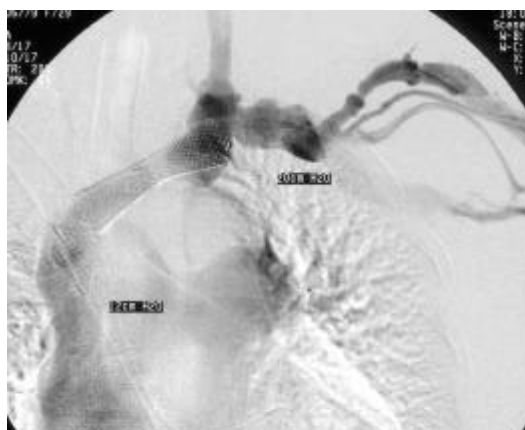


Fig 8a. Migrated stent in the SVC is noted in the post angioplasty fistulogram.



Fig 8b. A snare formed by looping a guide wire back on itself is used to help retrieve this self expandable stent. The snare has been created with the wire intentionally passed through the interstices of the stent to trap the stent on the snare.



Fig 8c. The snare is retracted, pulling the stent into the IVC, and it was removed through the femoral vein sheath.

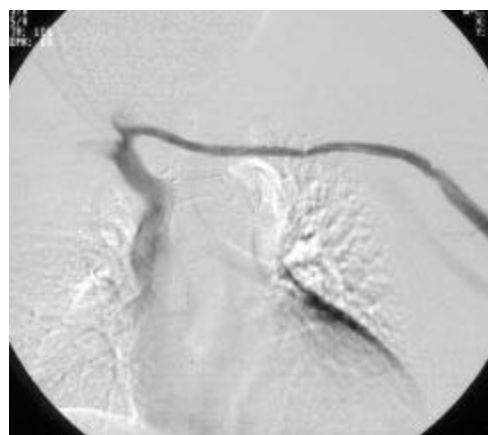


Fig 9. Surgical bypass between left proximal cephalic vein and right internal jugular vein.

# Congenital Tracheal Stenosis: Treatment with Balloon Posterior Tracheal Splitting and Temporary Placement of a Covered Retrievable Metallic Stent

Ji Hoon Shin / Jin Hyoungh Kim / Ho-Young Song

Departments of Radiology, Asan Medical Center

: Tracheobronchial tree, stenosis or obstruction

Interventional procedures, complications  
Balloon dilation

: A male infant

: A male infant weighting 2140g was born at 35 weeks' gestation. The Apgar scores were 9 at one minute and 10 at five minutes. The baby was discharged after one week but he had dyspnea and severe cyanosis when he cried and was transferred to our hospital at 29 days of age. He had a systolic murmur on physical examinations, but also had clear breath sounds. Echocardiography at our hospital showed a large ventricular septal defect, aortopulmonary window and left sided SVC.

He underwent total repair of the aortopulmonary window and right upper lobectomy at 36 and 42 days of age, respectively. At that time, cardiac problems and right upper lobar tracheal bronchus were mainly responsible for his respiratory problem, and the surgeons thought that the patient would not tolerate combined tracheal repair and aortopulmonary window repair or right upper lobectomy. However, there was no improvement in the dyspnea or CO<sub>2</sub> retention and he could not be weaned from the ventilation after surgery. Bronchoscopy confirmed tracheal stenosis from complete cartilaginous rings in the lower trachea.

At 61 days of age, the patient underwent balloon tracheoplasty under sedation in order to split and dilate the stenotic tracheal lumen. After balloon tracheoplasty, the ventilation setting improved, however, it was stationary after three days following the procedure.

Therefore, temporary stent placement for six months was performed to allow tissue healing around the torn tracheal wall.

After stent implantation, the patient's condition was improved and he had a stable ventilation setting. Five months after stent implantation, he had several episodes of pneumonia and culture of the endotracheal tube showed colonization of multiple bacteria. We thought that the stent would be an infection source and so removed it under bronchoscopic control. Although there was mild granulation tissue at both ends of the stent on bronchoscopy, the tracheobronchial lumen was completely patent. The stent was easily removed by pulling a retrievable lasso with bronchoscopic biopsy forceps. Seven weeks after stent removal, extubation was successfully achieved. He was transferred to a general ward two months after stent removal and was discharged one month later.

: congenital tracheal stenosis

Heart CT examinations, including two-dimensional (2D) - and three-dimensional (3D) - reconstruction airway images showed right upper lobar tracheal bronchus (the abnormal upper lobar bronchus originating from the trachea superior to its bifurcation) and a 13-mm segment of narrowing in the lower trachea (Fig. 1a). The diameter of the narrowed segment in the lower trachea was 3.5 mm, while that of the normal segment in the upper trachea was 6.5 mm. Emphysematous change was seen in the right upper lobe due to the air-trapping by the tracheal bronchus and mild collapse of the right middle and lower lobes on plain radiography (not shown).

Follow-up CT images obtained three and 12 months

after stent removal showed a widened lumen of the lower trachea (Fig 3).

**Balloon tracheoplasty technique :** A 6-mm (diameter) 2-cm (length) ballooncatheter (Cordis, Roden, the Netherlands) was advanced through the endotracheal tube (3.5 mm [inner diameter] - 10 cm [length]) and dilated the stenotic lumen up to the maximum pressure of 5 ATM. Initially, waist formation of the inflated balloon was noted and then the waist disappeared with an explosive sound (Fig 1b, 1c). There was no change of vital signs during and after balloon dilation. Post-procedure bronchoscopy showed disruption of the complete cartilaginous ring at the posterior aspect of the trachea minimal bleeding was also observed, however, there was no air leakage.

**Stent placement technique:** An 8-mm (diameter) 2 cm (length) polyurethane-covered retrievable self-expandable metallic stent with the retrieval lasso attached to the proximal end of the stent was used (Fig 2a). The stent was woven from a single thread of nitinol wire in a tubular configuration and the distal portion was flared distally to fit into the carina. Then, the stent was covered by using a dipping method with a 12% polyurethane solution. The stent and introducer set were constructed according to our specifications by a local manufacturer (Taewoong, Seoul, Korea). One week following balloon tracheoplasty, a 9-Fr sheath with a dilator was passed under fluoroscopic guidance over the guide wire into the trachea through the endotracheal tube (3.5mm, 10cm) and was advanced until the distal tip of the sheath reached the carina. Then the dilator and the guide wire were removed from the sheath. After that, a stent was compressed and loaded into the sheath and then positioned to cover the stenotic airway (Fig 2b). Immediately after the procedure, the stent was not fully dilated and the right lung began to collapse. We dilated the stent and both main bronchi using a 6 mm-diameter balloon catheter. We performed balloon dilation using 6 mm-diameter balloon catheter alternately in the right and left main bronchus with the proximal portion of the balloon within the stent. After balloon dilation, the stent was nearly fully dilated and the right lung was aerated (Fig 2c). Stent placement was also performed under sedation.

Infants born with congenital tracheal stenosis from complete cartilaginous rings often have respiratory distress which may be seen in isolation or in conjunction with other respiratory tract or cardiac anomalies (1,2). Since the early-1990s, posterior tracheal splitting by balloon dilation with or without assistance of temporary placement of an endotracheal tube, has been reported to be successful for maintaining the desirable lumen by Bagwell et al. and Messineo et al. (3,4). Their trial was based on the hypothesis that as the cartilaginous rings have a weak point in the posterior wall, aggressive balloon dilation would result in a posterior longitudinal splitting of the trachea and fibrous tissue could cover the split area a few weeks after placement of an endotracheal tube (3). However, keeping an endotracheal tube would be very annoying and difficult to maintain without sedation for an infant or child.

Recently, the uncovered metallic stents used in the vascular system have also been used in congenital tracheobronchial stenoses caused by cartilaginous rings (5-7). However, uncovered metallic stents have possible long-term risks of restenosis by recurrent granulation tissue with difficult or impossible removal, failure of tracheal growth with age, and tracheal erosion or penetration to the great vessels (5-7).

We initially planned to treat the patient with only rupture of the complete cartilaginous rings by balloon dilation because we agreed to the assertion by Bagwell et al. that disruption of the cartilaginous rings represents a prerequisite step for increase in the luminal diameter itself (4). This balloon posterior tracheal splitting carries the potential risks of free perforation of the trachea although the change to disastrous mediastinitis requiring surgical management has not been reported. In this patient, the widened tracheal lumen by balloon posterior tracheal splitting was not enough to maintain the functional patency of the lumen. We presumed that the free-flap-like, torn tracheal lumen probably caused disturbance of airflow, especially on expiration, as tissue healing around the splitting was delayed. Therefore, temporary placement of a covered retrievable self-expandable metallic stent was chosen to allow tissue healing to create new fibrous tracheal wall around the tear. A covered retrievable self-expandable metallic stent is very useful in that it can prevent the growth of gran-

ulation tissue through the stent wires and erosion or penetration of the stent to surrounding tissue in case of stent fracture. Moreover, the stent can easily be removed easily with bronchoscopic or interventional procedures after a given period of time, therefore, it can prevent complications associated with long-term stent placement, such as granulation tissue or infection around the stent and difficult stent exchange after increase of the tracheal diameter due to the normal growth of the infant. However, it is very difficult to determine the optimal time to remove a stent as the length and severity of the tear differ from patient to patient. We think that six months is enough for tissue to heal around the stent before encountering significant stent-related complications such as granulation tissue formation (8).

1. Berrocal T, Madrid C, Novo S, Gutierrez J, Arjonilla A, Gomez-Leon N. Congenital anomalies of the tracheobronchial tree, lung, and mediastinum: embryology, radiology, and pathology. *Radiographics* 2004;24:e17

2. Jaffe RB. Balloon dilation of congenital and acquired stenosis of the trachea and bronchi. *Radiology* 1997;203:405-9.

3. Messineo A, Forte V, Joseph T, Silver MM, Filler RM. The balloon posterior tracheal split: a technique for managing tracheal stenosis in the premature infant. *J Pediatr Surg* 1992;27:1142-4.

4. Bagwell CE, Talbert JL, Tepas JJ 3rd. Balloon dilatation of long-segment tracheal stenoses. *J Pediatr Surg* 1991;26:153-9.

5. Nicolai T, Huber RM, Reiter K, Merckenschlager A, Hautmann H, Mantel K. Metal airway stent implantation in children: follow-up of seven children. *Pediatr Pulmonol* 2001;31:289-96.

6. Maeda K, Yasufuku M, Yamamoto T. A new approach to the treatment of congenital tracheal stenosis: Balloon tracheoplasty and expandable metallic stenting. *J Pediatr Surg* 2001;36:1646-9.

7. Endo A, Watanabe K, Karasawa K, et al. Failure of stent implantation in an infant with congenital tracheal stenosis. *Pediatr Int* 2002;44:98-100.

8. Song HY, Shim TS, Kang SG, et al.

Tracheobronchial strictures: treatment with a polyurethane-covered retrievable expandable nitinol stent - initial experience. *Radiology* 1999;213:905-12.

Figure 1. CT image (a) before balloon tracheoplasty and fluoroscopic images (b, c) obtained during balloon tracheoplasty.

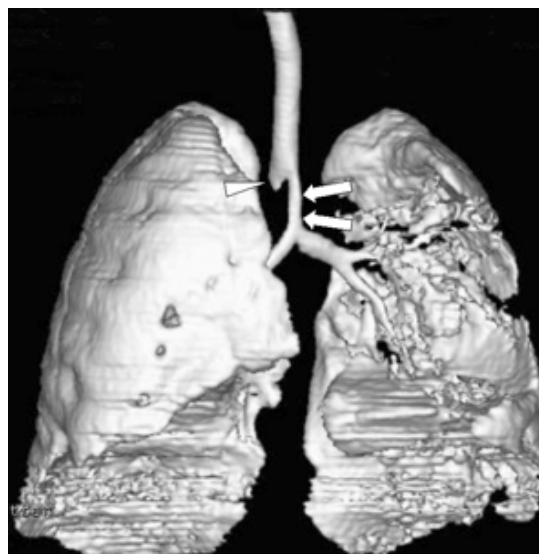


Fig. 1a. Three-dimensional (3D) reconstruction CT image, anteroposterior view, shows 13-mm segment of severe narrowing (arrows) of the lower trachea from below the tracheal bronchus (arrowhead) to the carina.



Fig. 1b. Formation of the waist is seen initially. A surgical clip after right upper lobectomy is seen. (b) Formation of the waist is seen initially. A surgical clip after right upper lobectomy is seen.



Fig. 1c. Suddenly, the balloon dilates to its full diameter (6 mm) with an explosive sound.

Figure 2. The stent and (a) and fluoroscopic images (b, c) obtained during stent placement.

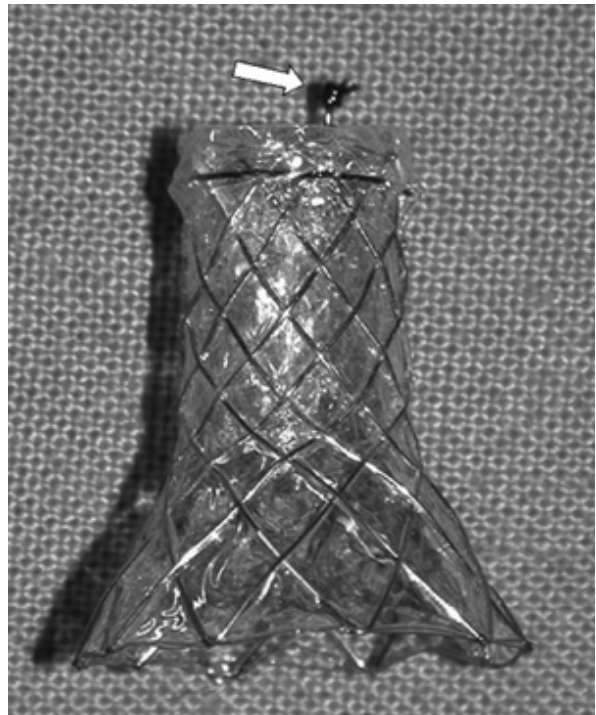


Fig. 2a. The stent is flared distally to fit into the carina. The retrieval lasso (arrow) is attached to the upper inner margin of the stent for bronchoscopic removal of the stent.

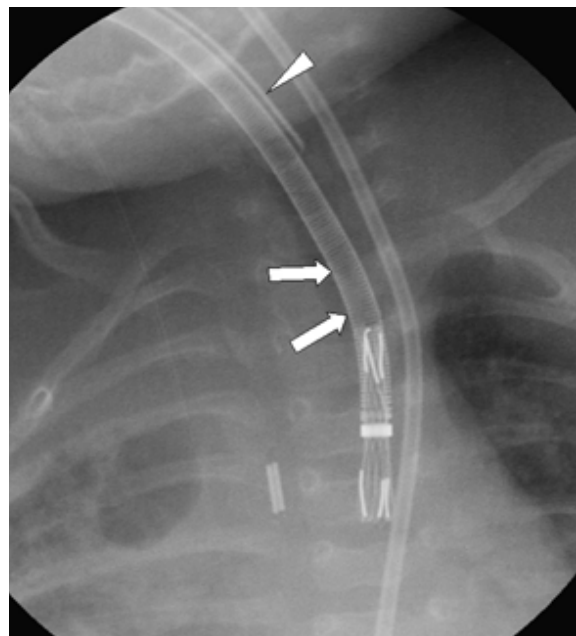


Fig. 2b. The stent is deployed as the sheath (arrows) is slowly withdrawn with one hand while the pusher catheter is held in place with the other hand. Stent placement was performed through the endotracheal tube (arrowhead).

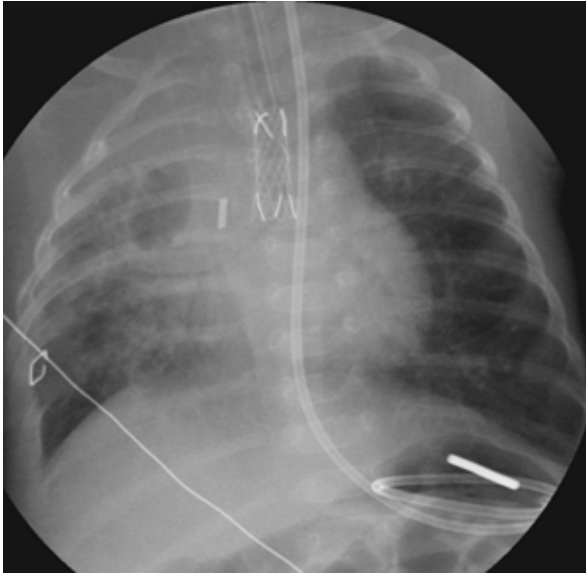


Fig. 2c. The stent is nearly fully dilated immediately following balloon dilation (not shown).

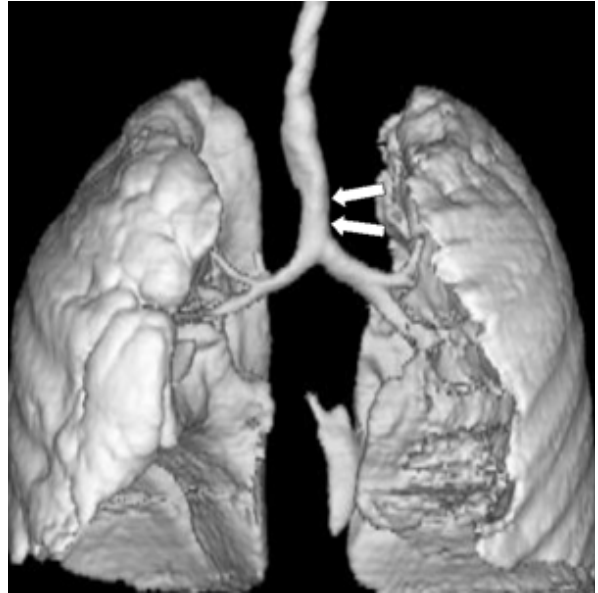


Fig. 3. Three-dimensional reconstruction CT image obtained 12 months after stent removal, anteroposterior view, shows a widened lumen (arrows) of the lower trachea. The diameter of the dilated lumen is 7 mm.



# Deep Tracheal Laceration with Pneumomediastinum after Tracheobronchial Balloon Dilation

Case **2**



Jin Hyoung Kim / Ji Hoon Shin / Ho-Young Song

Departments of Radiology, Asan Medical Center

: Tracheobronchial tree, stenosis or obstruction

Interventional procedures, complications

Balloon dilation

: 31-year-old woman

: Balloon dilation was performed in a 31-year-old woman for tuberculous tracheobronchial stenosis because of her recent symptoms such as aggravated cough, dyspnea, and 3 kg weight loss for seven months. Pre-balloon pulmonary function test (PFT) showed a forced expiratory volume in one second (FEV1) of 1.3 (45%, predicted) and a forced vital capacity (FVC) of 2.0 (54%, predicted).

Immediately after balloon dilation, she complained of mild chest pain and expectorated some blood-tinged sputum. On bronchoscopy (not shown) obtained immediately after balloon dilation, tracheal laceration at the posterior tracheal wall was observed. The length and depth were estimated as about 5 cm and 8 mm on bronchoscopy. Her vital sign was stable without fever or chills, and there was no change of hemoglobin level. Her chest pain and blood-tinged sputum disappeared within 24 hours. Therefore, she was prescribed only antibiotics to prevent possible infection and was discharged from hospital five days later.

Eight months after balloon dilation, her symptoms were much improved. Follow-up PFT eight months after balloon dilation showed a FEV1 of 1.8 (63%, predicted) and a FVC of 3.3 (89%, predicted); FEV1 and FVC increased as much as 18% and 45%, respectively, compared with those of the predilation PFT. She has maintained her symptomatic improvement without recurrence for ten months.

: Deep tracheal laceration with pneumomediastinum after balloon dilation

Four days before balloon dilation, chest CT including 3-dimensional (3D) reconstruction showed a 6-cm-long tracheal stenosis and a 1.5-cm-long right main bronchial stenosis, combined with tracheal and right main bronchial wall thickening (Fig 1). The diameters of the narrowed segment in the trachea and right main bronchus was 6 mm and 2 mm, respectively, while that of the normal segment in the trachea and right main bronchus was 16 mm and 11 mm, respectively.

CT immediately after balloon dilation revealed deep longitudinal laceration at the posterior tracheal wall and pneumomediastinum (Fig 3).

Follow-up CT scans (Fig 4) obtained eight months following balloon dilation, the deep laceration completely healed and the widened tracheal lumen was maintained.

Topical anesthesia of the oropharynx was achieved prior to the procedure with an aerosol spray of lidocaine hydrochloride (Dai Han, Seoul, Korea). With bronchoscopic guidance, a 0.035-inch exchange guide wire (Terumo, Tokyo, Japan) was inserted across the stenoses in the trachea and right main bronchus into the distal portion of them through the working channel of the bronchoscope. After withdrawing the bronchoscope while the guide wire was in place, a straight 5-F graduated sizing catheter (Cook Bloomington, IN) was passed over the guide wire to the distal portion of the stenoses in order to measure their length. Using fluoroscopic guidance, the location of the narrowed tracheal

and bronchial lumen were marked on the patient's skin with radiopaque markers. After measuring the length of the stenoses, we initially dilated the right main bronchial stenosis, and subsequently the tracheal stenosis. A 6-mm-diameter balloon catheter was used first in a severe right main bronchial stenosis to provide for passage of the larger balloon catheter. Then, the balloon (Boston Scientific/Mediatech, Watertown, Mass; 10 mm in diameter and 4 cm long for bronchial stenosis, 18 mm in diameter and 10 cm long for tracheal stenosis) was slowly inflated manually with a diluted water-soluble contrast medium. One session of balloon inflation was performed for the right main bronchial stenosis with balloon inflation time of two minutes. While, four sessions of balloon inflation were performed at a time for the tracheal stenosis with each balloon inflation time of 30 seconds, therefore, the total inflation time was two minutes. There was waist formation of the inflated balloon catheter at the stricture segment, however, the waist became disappeared soon without much resistance (Fig 2).

Previous reports have stated that afibrotic process may be more amenable to successful balloon dilation than other processes such as inflammation or calcification (3,6). Although the predominant fibrotic process can be easily dilated and can suggest good clinical outcome, there may be potential complication such as laceration or even free perforation after sudden balloon dilation of fibrotic stenosis because of its hardness or stiffness. In this patient in our report, the history of tuberculosis was more than ten years and the predominant fibrotic process was confirmed on bronchoscopy.

Previously, clinical outcome and follow-up data of deep tracheal or bronchial laceration has not been documented in detail. In our case, interestingly, the long and deep tracheal laceration as well as pneumomediastinum disappeared completely during the follow-up of ten months after balloon dilation. Lee et al (7) also stated briefly that two deep lacerations with pneumomediastinum left no subsequent clinical sequelae without any further description. We assumed that even though deep laceration occurs after dilation of fibrotic stenosis, good clinical outcome, in some cases, can be achieved because the lumen of stenotic segment may be widened enough after the tear of fibrotic tissue, thereby

rendering deep laceration, and deep laceration may heal soon with growth of granulation tissue. Balloon dilation for congenital tracheal stenosis is another illustration of the same point; rupture of the complete cartilaginous rings by balloon dilation represents a prerequisite step for increase in the luminal diameter itself (13).

In our case, bronchoscopy immediately after balloon dilation was very useful for early detection of the deep tracheal laceration and CT including 3D reconstructions was very helpful to delineate the extent of the deep laceration as well as pneumomediastinum.

1. Ferretti G, Jouvan FB, Thony F, Pison C, Coulomb M. Benign noninflammatory bronchial stenosis: treatment with balloon dilation. *Radiology* 1995; 196:831-834
2. Sheski FD, Mathur PN. Long-term results of fiberoptic bronchoscopic balloon dilation in the management of benign tracheobronchial stenosis. *Chest* 1998; 114:796-800
3. Lee KH, Ko GY, Song HY, Shim TS, Kim WS. Benign tracheobronchial stenoses: long-term clinical experience with balloon dilation. *J Vasc Interv Radiol* 2002; 13:909-914.
4. Brown SB, Hedlund GL, Glasier CM, Williams KD, Greenwood LH, Gilliland JD. Tracheobronchial stenosis in infants: successful balloon dilation therapy. *Radiology* 1987; 164:475-8.

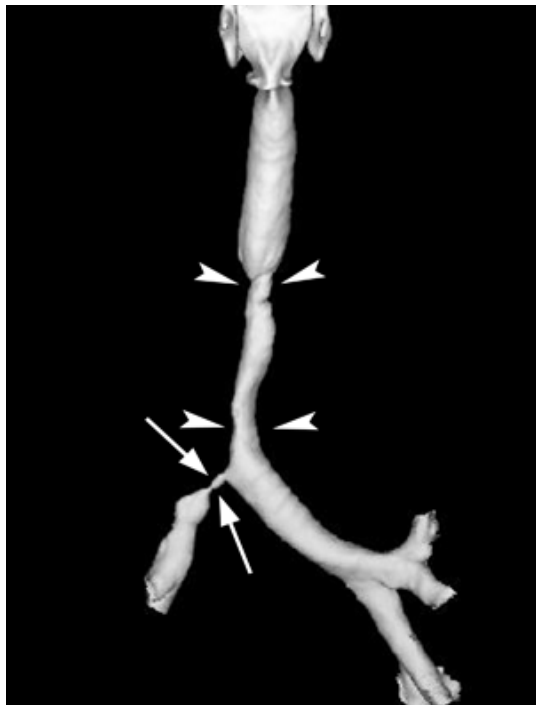


Fig. 1a. Anteroposterior view of three-dimensional (3D) reconstruction CT shows a 6-cm-long tracheal stenosis from mid-trachea to carina and a 1.5-cm-long right main bronchial stenosis.



Fig. 1b. Axial CT scan at the level of mid trachea shows tracheal stenosis (arrow) with wall thickening (arrowheads).

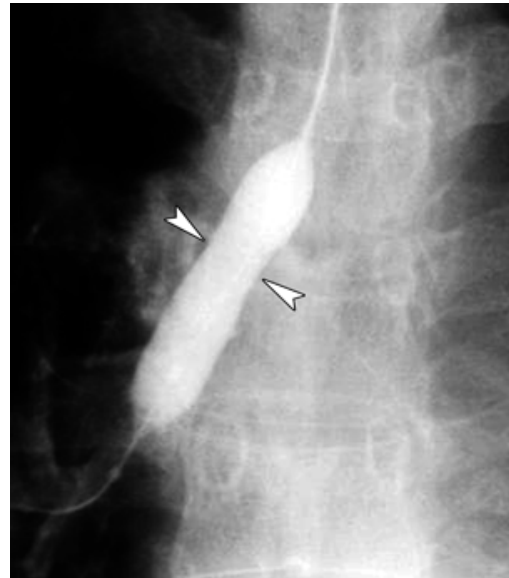


Fig. 2a. Initially, right main bronchial stenosis (arrowheads) is fully dilated with a 4-cm-long and 10-mm-diameter balloon.

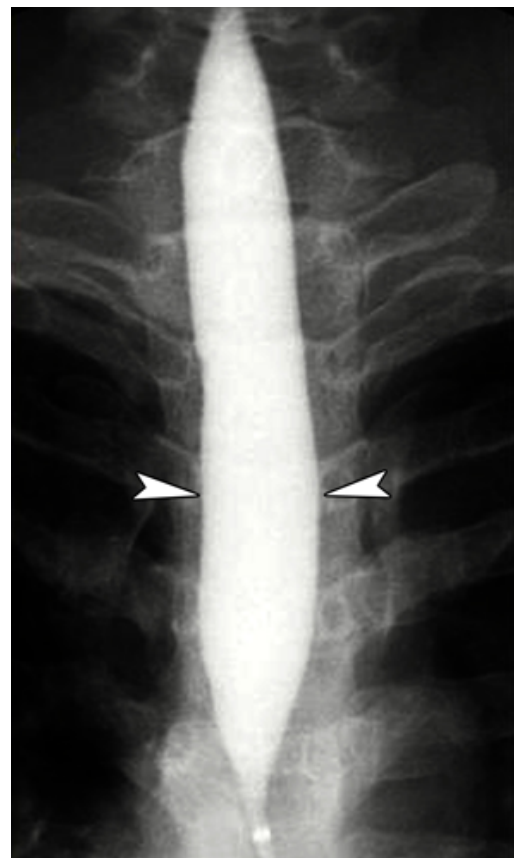


Fig. 2b. Tracheal stenosis (arrowheads) is then fully dilated with a 12-cm-long and 18-mm-diameter balloon.

Figure 3. A long and deep laceration (arrowheads) at the posterior tracheal wall with pneumomediastinum(B) (arrows) is well visualized in lateral view of 3D reconstruction(A).

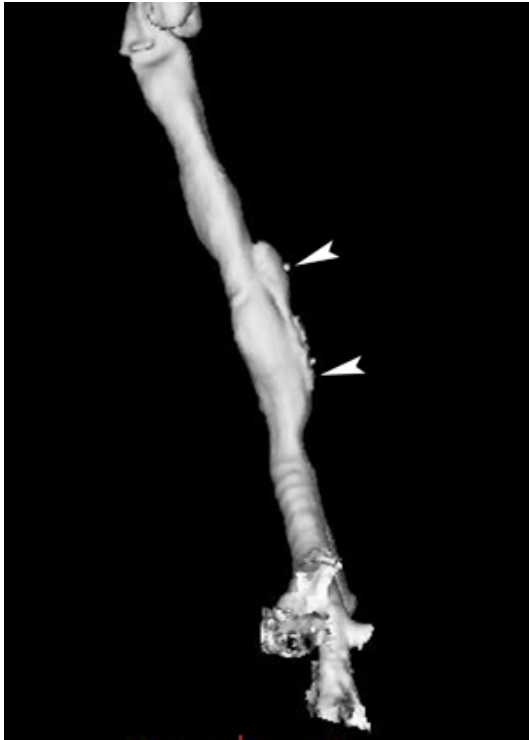


Fig. 3a. 3-D reconstruction image.

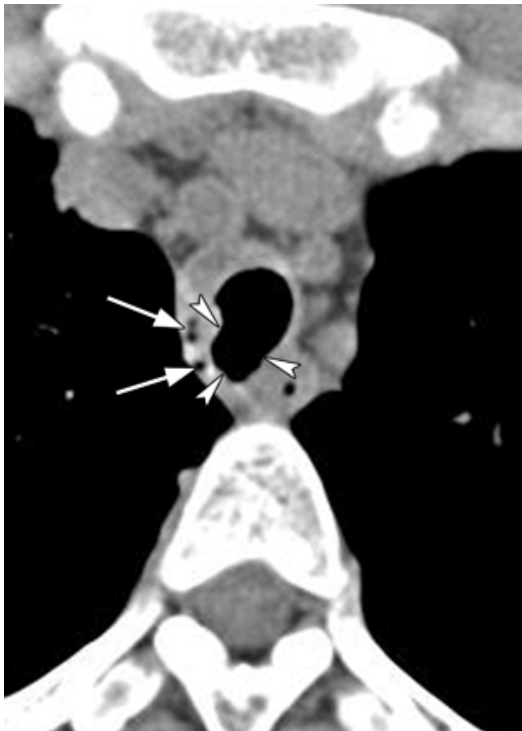


Fig. 3b. Pneumomediastinum

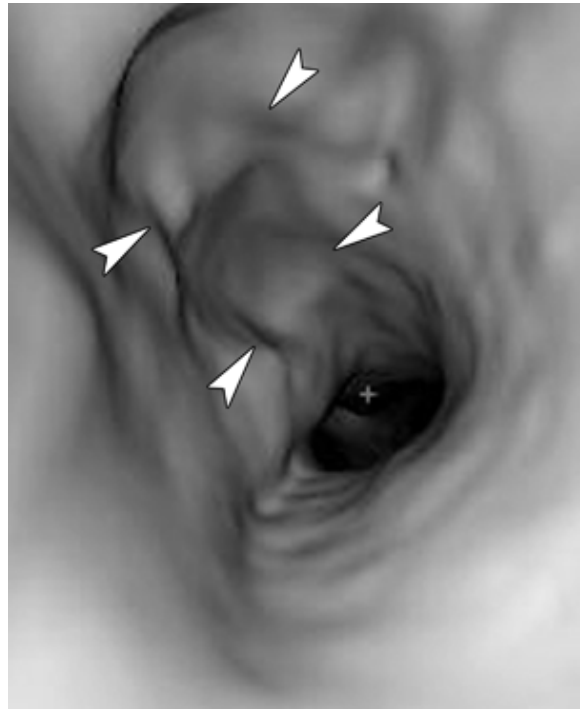


Fig. 3c. Virtual bronchoscopy image.

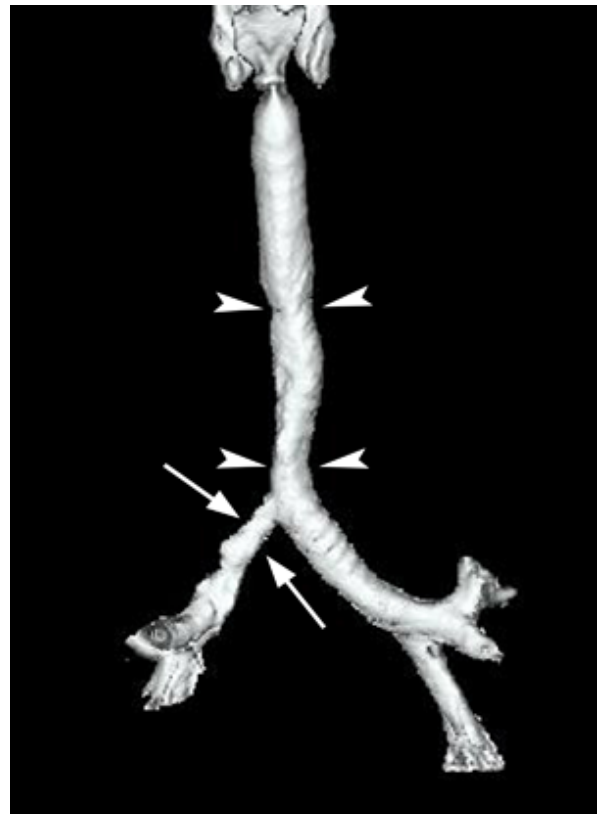


Fig. 4a. Anteroposterior view of 3D reconstruction CT shows improved right main bronchial (arrows) and tracheal stenosis (arrowheads).

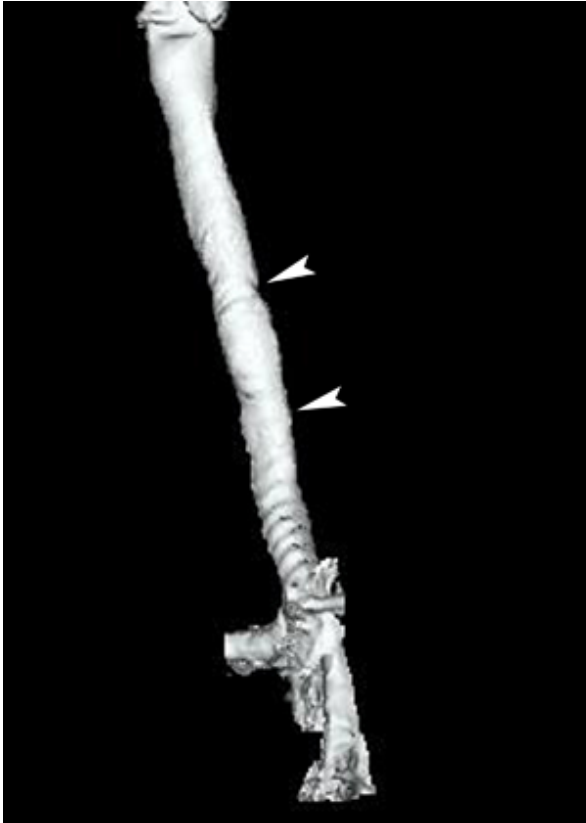


Fig. 4b. Lateral view of 3D reconstruction CT demonstrates disappeared deep laceration at the posterior tracheal wall (arrowheads).



Fig. 4c. Axial CT scan at the level of mid trachea shows the improvement of the stenosis (arrow) and wall thickening (arrowheads) in the involved trachea.

## Hepatic Lymphatics Demonstrated during PTBD

/ / / /

: Lymphography, Lymphatic system  
 Bile ducts, interventional procedure  
 : 57 /  
 :  
 :

가

(Fig. 1).  
 가 (hilum)  
 가 (Fig. 2).

22G Chiba needle

가 (centripetal)  
 가  
 가  
 가 T12

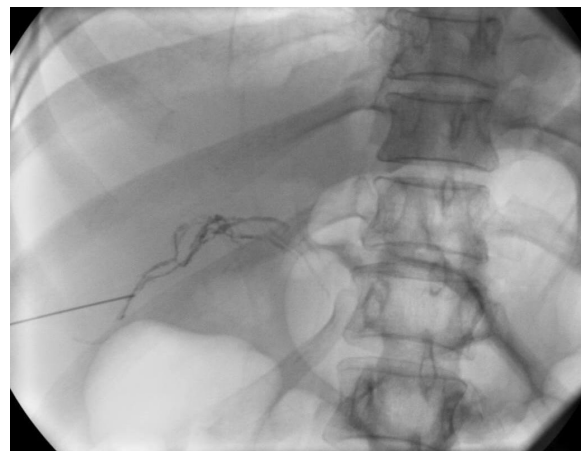


Fig. 1. Beaded irregular shaped, multiple lymphatic channels are visualized. They are drained to the region of the liver hilum and extended outside the boundaries of the liver to the region of the T12 vertebral body.

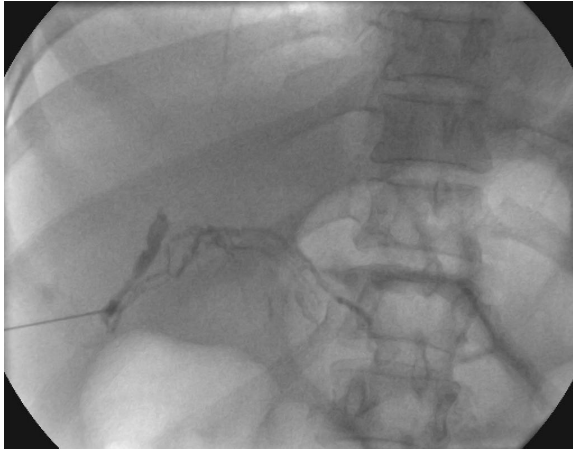


Fig. 2. After modulation of the needle tip, the bile duct is visualized.

1. Okuda K, Sumikoshi T, Kanda Y, Fukuyama Y, Koen H. Hepatic lymphatics as opacified by percutaneous intrahepatic injection of contrast medium. Analysis of hepatic lymphograms in 125 cases. *Radiology* 1976; 120:321-326.

2. Goldberg HI, Dodds WJ, Lawson TL, Stewart ET, Moss AA. Hepatic lymphatics demonstrated by percutaneous transhepatic cholangiography. *AJR* 1975 123:415-419.

3. Percutaneous transhepatic lymphography method to image and treat intra-abdominal lymph node metastasis in patients with unresectable hepatobiliary pancreatic cancer. *Surgery*. 2002 May; 131(5):529-33.

## Covered Metallic stent

### Covered Metallinc stent in the Treatment of Esophagojejunal Anastomotic Leak

/ / / /

: Fistula, gastrointestinal tract , CT 가 ,  
 Esophagus, Grafts and Protheses retrieval set ,  
 : 32 / ,  
 : , , . (Fig 5. A & B)

: - (Esophagojejunal  
 anastomotic leak)

4% 17%  
 40% .

CT - ,  
 가 ,  
 . (Fig. 1A & B) Covered metallic stent

Pigtail (Boston Scientific, Indiana, USA) 10F

. (Fig. 2)

(Fig. 3) covered metallic stent

. covered metallic stent  
 7%  
 Covered metallic stent

가

2  
 covered metallic stent

17.5 2

Terumo (Terumo, Tokyo,  
 Japan) Cobra  
 (Cook, Bloomington, USA) . Cobra

. Cobra

long stiff guide wire . Stiff guide  
 wire 18 mm X 6 cm, Song retrievable covered  
 esophageal stent (Taewoong, Seoul, Korea)

Covered metallic stent

. (Fig. 4)



1. Roy-Choudhury SH, Nicholson AA, Wedgwood KR, et al. Symptomatic malignant gastroesophageal anastomotic leak: management with covered metallic esophageal stents. *AJR Am J Roentgenol.* 2001 Jan;176(1):161-5.

2. Doniec JM, Schniewind B, Kahlke V, Kremer B, Grimm H. Therapy of anastomotic leaks by means of covered self-expanding metallic stents after esophagogastrectomy. *Endoscopy.* 2003 Aug;35(8):652-8.

3. Shin JH, Song HY, Ko GY, Lim JO, Yoon HK, Sung KB. Esophagorespiratory Fistula: Long-term Results of Palliative Treatment with Covered Expandable Metallic stents in 61 Patients. *Radiology.* 2004 Jul;232(1):252-9. Epub 2004 May 27.

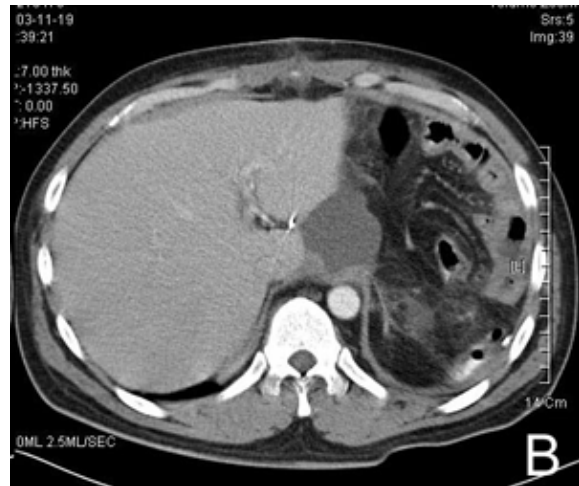


Fig. 1b. CT scan on the lower level reveals fluid collection in the perihepatic space, adjacent to the caudate lobe.

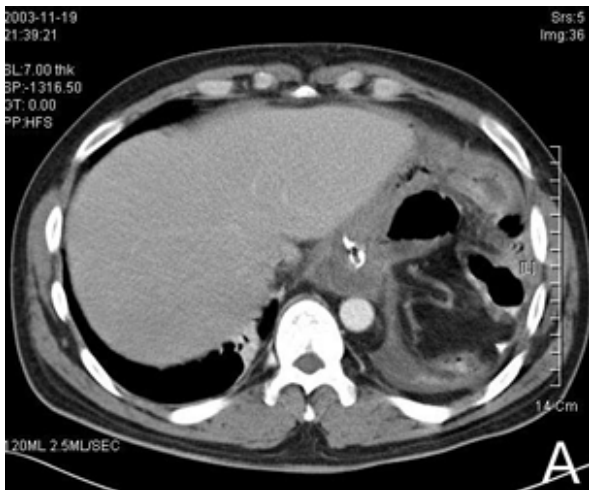


Fig. 1a. CT scan on the level of esophagojejunal anastomosis site shows fluid collection around the anastomotic suture material and in the left pleural cavity.



Fig. 2. Tubogram with 10F pigtail catheter for percutaneous abscess drainage shows decreased size of abscess around the anastomosis and filling of contrast material in jejunum.



Fig. 3. Esophgogram after revision operation shows fistula between esophagus and abscess cavity and contrast filling in abscess cavity.

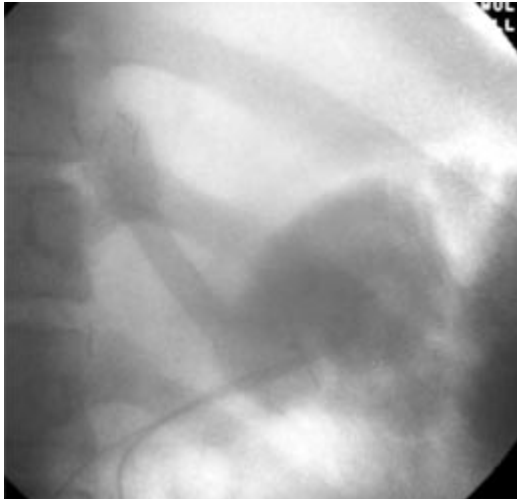
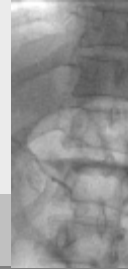


Fig. 4. Covered metallic stent is deployed and esophagogram shows no leakage of contrast media and good passage of contrast material through the stent.



Figure 5. (a) After the hook stent hooked onto the draw-string of covered stent, the sheath with the hook stent was pulled out of stent. (b) Esophagogram after retrieval shows patent esophagojejunal anastomosis and no definite leakage of contrast media.



## Double-J

### Removal of Double-J Stent with Bended Guide Wire in Severe Hydronephrosis

가

: Hydronephrosis

Kidney, interventional procedures

double-J

가

Ureter, stenosis or obstruction

Ureter, stents

(Fig. 3A).

8 Fr

: 14 /

(sheath)

snare kit (Microvena,

:

White Bear Lake, MN, USA)

double-J

double-J

가

Omni Flush catheter (Angiodynamics, Queensbury, NY, USA)

grade 5,

(twist)

double-J

가

grade 4

3

double-J

(Fig. 3B, C).

double-J

가

Safe-T-J

curved fixed core wire guides (Cook, Bloomington, IN, USA)

:

90o

(Fig 4).

가

double-J

(Fig 5A, B).

8.5 Fr

가

(grade 5).  
(Fig. 1).

grade 4

Double-J

(1). Double-J

8.5 Fr

(DM, Cook, Bloomington, IN, USA)

2 6 Fr, 24 cm double-J

(Cook, Bloomington, IN, USA) (Fig 2).

2

double-J

(2,3).

Double-J

X - 가 (4).

가 X- 25-35 mm gooseneck (5).

가 가

가

0.038 20-30

mm 가 .

double-J

가 , X-

가

가 가 .

double-J 가

90o

double-J 가

가 double-J



Fig. 1. Voiding cystoureterogram shows severe hydronephroureter of both kidneys and ureters.

1. Double-J 가 . 1998  
39:82-86
2. . 1996; 35:605-611
3. Double-J .  
1997; 38:410-415
4. X - . 1999; 40:  
851-855
5. 2002;47:69-76



Fig. 2. To prevent stenosis of the vesicoureteral anastomosis after ureteral reimplantation for vesicoureteral reflux, antegrade placement of the double-J stent was done via percutaneous nephrostomy tract, which had been made 2 days ago.

Figure 3. The first trial of removal with an Omni Flush catheter

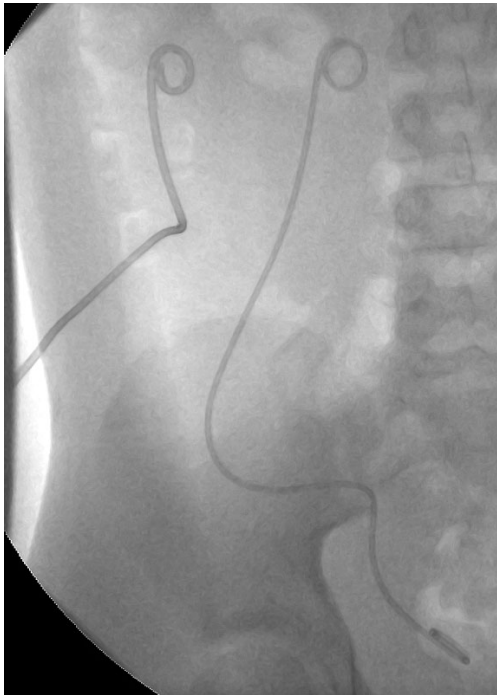


Fig. 3a. Follow-up image obtained at six weeks after placement shows migration of the head portion of the double-J stent to medial side (A).

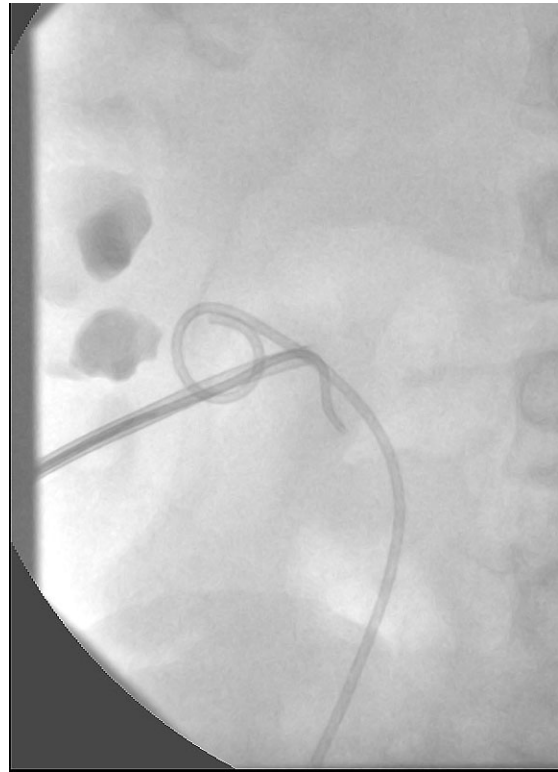


Fig. 3c. Although removal was failed because of untwisting between the Omni Flush catheter and the double-J stent, the head portion was migrated to renal pelvis (C).



Fig. 3b. Removal of the double-J stent via tract of percutaneous nephrostomy was tried by twisting with the Omni Flush catheter (B).

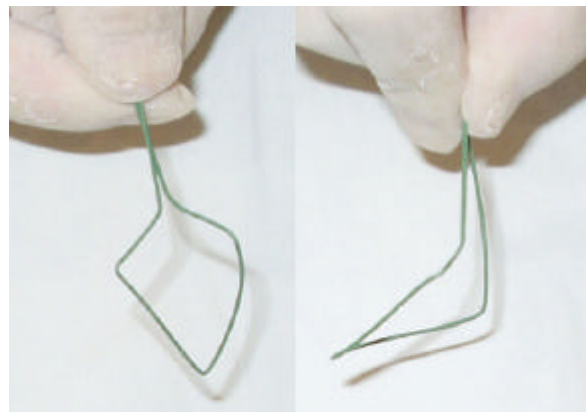


Fig. 4. Snare made by bending of safe-T-J curved fixed core wire guides.

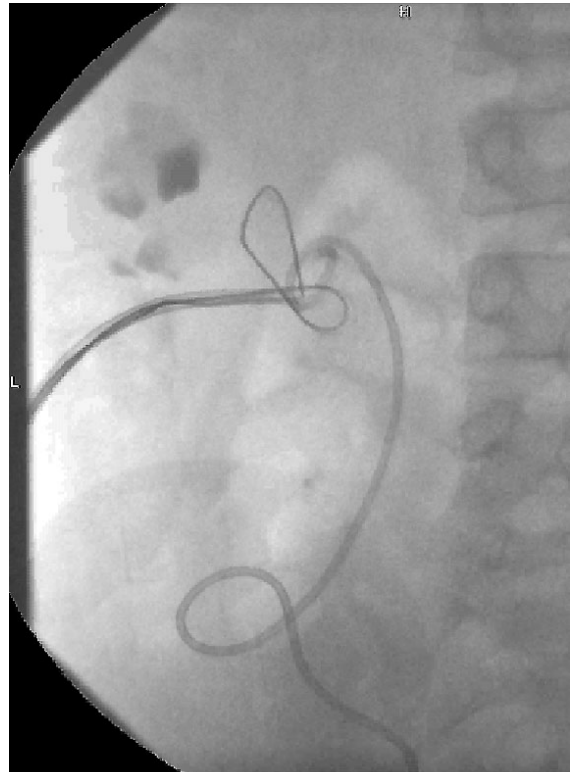
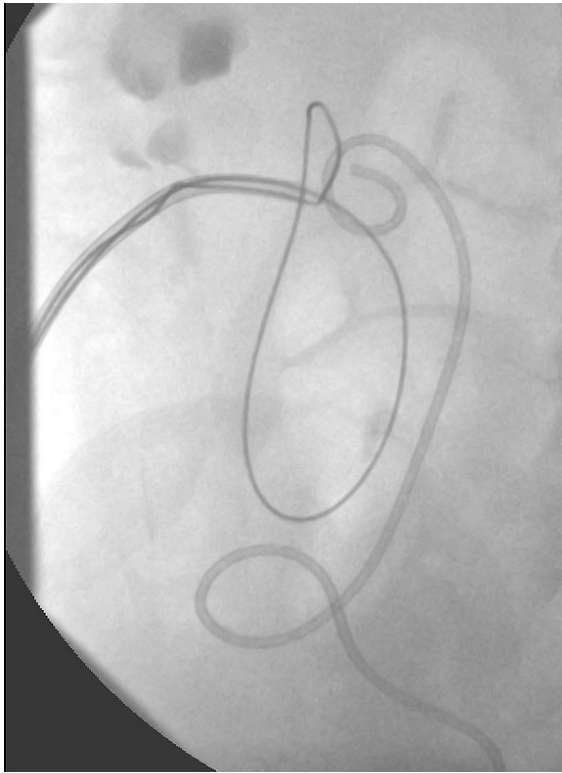


Fig. 5 a, b. Double-J catheter was successfully captured by newly designed snare.

## stent - graft

## Stent-graft repair of tracheo-innominate artery fistula after tracheostomy

/ / / /

: innominate artery  
tracheostomy  
stent graft  
: 35 /  
:  
5  
5  
2200cc  
:  
(Fig.1).

10mm  
(Fig.3). Stent - graft

CT stent - graft  
12mm - 4cm  
(Fig.5).

Jo stent graft  
50  
stent - graft  
(Fig.4),  
(Fig.6)

1100cc,  
30 - 80%,  
70%  
가  
end - to end anastomosis,  
20 - 40%  
stent graft  
stent - graft  
(patency) 89 - 100%  
가  
stent - graft 14  
50

Angiocatheter  
Jo stent graft(JOMED, GmbH, German)  
4cm  
10mm, 31mm  
10mm,  
loading

가 2.5 \* 1.5  
 cm                    stent                    3cm  
 stent-graft가  
 stent-graft                    stent  
 stent-graft

1. Seth B. Blattman, Gregg S. Landis, Mark Knight, et al. Combined endovascular and open repair of a penetrating innominate artery and tracheal injury, Ann Thorac Surg 2002;74:237-9
2. Juno Deguchi, Takatoshi Ruruya, Nobutaka Tanaka, et al. Successful management of tracheo-innominate artery fistula with endovascular stent graft repair, J Vasc Surg 2001;33:1280-2
3. Paul R. Hilfiker, Mahmood K. Razvi, Stephen T. Kee, et al. Stent-traft therapy for subclavian artery aneurysms and fistulas : Single-center mid-term re- sults, JVIR 2000;11:578-584



Fig 1. thoracic aortogram, the cuff of the tube compressed the Rt. innominate artery mildly, but, bleeding focus was not seen.



Fig. 2. after the balloon of endotracheal tube was de- flated, massive gush-out of contrast material was seen at the Rt. proximal innominate artery.



Fig. 3. Jo stent-graft was inserted at the Rt. innominate artery injury site.



Fig. 4. 50days after stent-graft repair, neck CT scan shows contrast material leakage behind the stent-graft site.



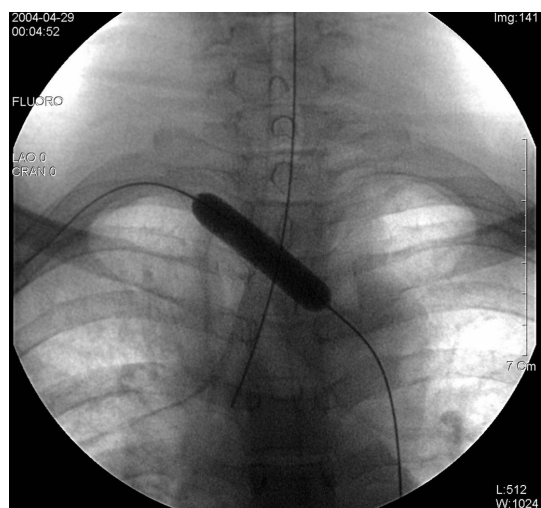
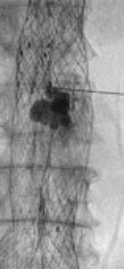


Fig. 5. the stent was expanded using the 12mm-4cm ballooning catheter in order to stop rebleeding.



Fig. 6. after 12mm ballon angioplasty, no extravasation is detected on the thoracic aortogram



# Case 7

## Type B

가

(Treatment of progressive dilatation of abdominal false lumen in patient with stent-graft treatment for Type B aortic dissection)

/ / / /

: type B aortic dissection, stent-graft, entry tear, reentry tear

: 54 /

: 6 (Abdominal dis-comfort) (pulsating abdominal mass) . 5 type B (aortic dissection)

(stent-graft)

가 (abdominal aortic false lumen) . (Fig. 1 A)

: Type B aortic dissection

re-entry tear

endoleak

12 x 80 mm, 8 x 70 mm coil

2 (common femoral artery) 22F Keller-Timmerman Sheath(Cook, Bloonington, IN, USA) (28mm x 5.6cm)

Nitinol-PTFE covered, S & G ) (24mm x 5.6cm) 1cm , (12mm x 6.2 cm) 1cm ,

reentry leakage tear가 6 CT re-entry 가 (thrombosis) (Fig 4) 가

5 CT primary entry tear 가 Type B 가 (Fig. 1 A).

CT 가 (false lumen) (true lumen) (re-expansion) (Fig. 1 B) (remodeling)

가 4.8 x 4.3 cm 6.5 x 5.1 cm (Fig. 2)

primary entry tear re-entry tear가 (celiac artery) 3cm , 3cm, 가 re-entry tear (Fig. 3).

Nienaber Dake (stent-graft) (stent-graft) neck

type B 가 . Type B (strategy) pri- 가 (rupture) 가 re-entry tear

가  
가  
가  
re-entry tear  
(branch)  
가 re-entry tear  
가  
re-entry tear  
가  
CT (high frame rate)  
. hd

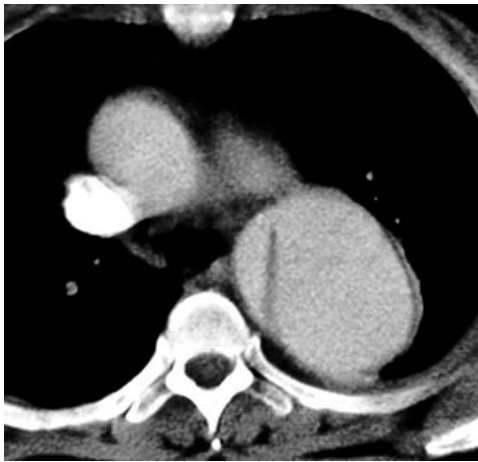


Fig. 1a. Contrast enhanced CT scan, which performed before the stent graft insertion at the descending thoracic aorta, shows DeBakey type III aortic dissection with a intimal flap (arrow) and large false lumen (white arrow).

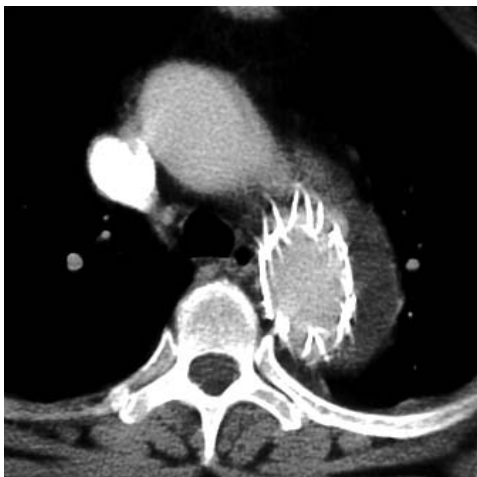


Fig. 1b. After the successful deployment of stent-graft at primary entry tear, follow up CT scan have shown complete thrombosis of the thoracic false lumen and expansion of true lumen for 5 years.

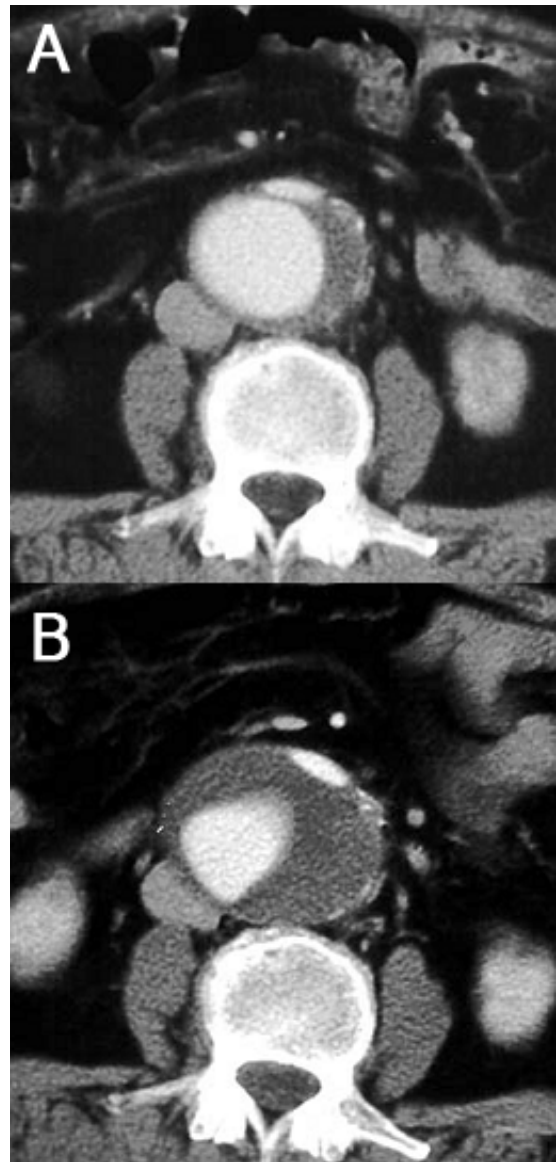


Figure. 2. Contrast CT scan taken before (A) and 5 years after (B) the stent-graft at primary entry tear show progressive dilatation of abdominal false lumen. The maximal diameter of abdominal aorta including false lumen is increased from 4.8 x 4.3 cm to 6.5 x 5.1 cm.

Figure 3. False lumen blood flow through each re-entry tears are noted.

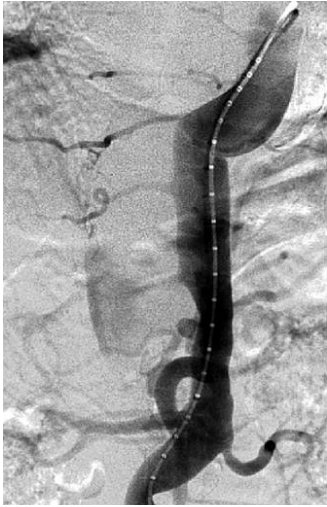


Fig. 3a. Digital subtraction angiography, which performed on admission, shows three reentry tear sites (arrows) at 3cm above the celiac truck.



Fig. 3b. 3cm below the renal artery.

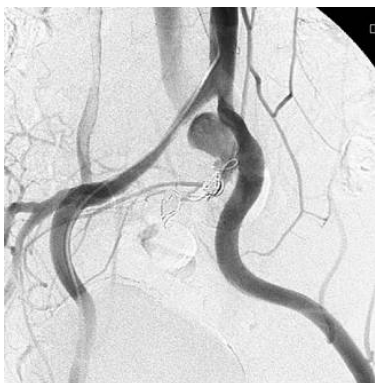


Fig. 3c. The bifurcation of left common iliac artery.

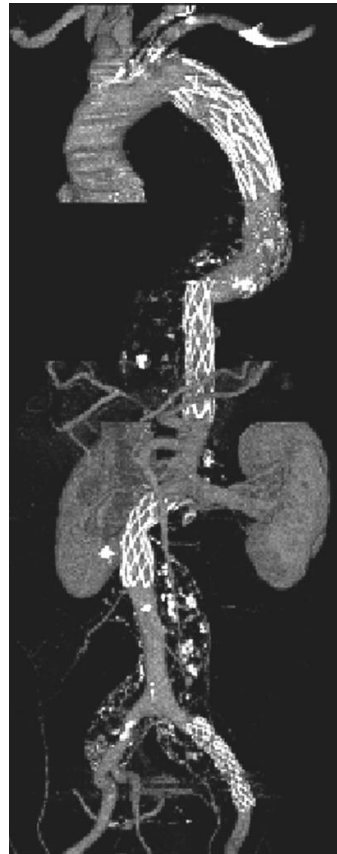


Figure 4. 3-D volume rendering reconstruction image of CT angiography shows 4 stent-grafts deployed in thoracic, abdominal aorta and left common iliac artery. Complete exclusion of thoracic and abdominal aortic false lumen is noted. Intact blood flows of thoracic and abdominal aortic branch vessels are shown.

1. Dake MD, Kato N, Mitchell RS, et al. Endovascular stent-graft placement for the treatment of acute aortic dissection. *N Engl J Med* 1999; 340:1546-1552.

2. Kato N, Hirano T, Shimono T, et al. Treatment of chronic aortic dissection by transluminal endovascular stent-graft placement: preliminary results. *J Vasc Interv Radiol* 2001; 12:835-840.

3. Lopera J, Patio JH, Urbina C, et al. Endovascular Treatment of Complicated Type-B Aortic Dissection with Stent-Grafts: midterm results. *J Vasc Interv Radiol* 2003; 14:195-203.

4. Won JY, Lee DY, Shim WH, et al. Elective endovascular treatment of descending thoracic aortic aneurysms and chronic dissections with stent-grafts. *J Vasc Interv Radiol* 2001; 12:575-582.

# Penetrating Atherosclerotic Ulceration 가 Stent - Graft

Case 8

## Percutaneous Endovascular Stent-Graft Insertion in Penetrating Atherosclerotic Ulceration with Pseudoaneurysm

/ / / /

: Aorta, rupture

Aorta, grafts and prostheses

: 56 /

: 15

CT

가

가

CT

: Penetrating atherosclerotic ulceration with  
pseudoaneurysm.

가

20mm balloon (XXL Ballon catheter,  
Boston Scientific, Galway, Ireland)

(Fig. 2 B & C), Pigtail

12F Introducer sheath (Cordis,  
Johnsonand Johnson Medical, Roden, Netherland)

CT

가

2.2 cm

가

가

. (Fig. 1 A

& B)

Penetrating atherosclerotic ulceration

가

, 가

(가

stent-graft

5F Introducer sheath

(Terumo, Tokyo, Japan)

5F Pigtail

(Cook, Bloomington, USA)

(Terumo, Tokyo,

Japan)

가

가

. (Fig. 2 A)

Lunderquist

(Cook, Bloomington, USA)

24mm x 4cm aortic

stent graft device (S&G Biotech, Seoul, Korea)

Pigtail

stent graft device

3%

13%

6.9%

60%

Penetrating atherosclerotic ulceration

가

가

가

가

12.5%

4%가

0%

Brittenden Penetrating athero-  
sclerotic ulceration 가  
stent-graft 1  
, Shoder  
penetrating atherosclerotic  
ulceration 가 7  
423 (264-690 )  
, 7 1  
..  
Penetrating atherosclerotic  
ulceration

1. Schoder M, Grabenwoger M, Holzenbein T, Domanovits H, Fleischmann D, Wolf F, Cejna M, Lammer J. Endovascular stent-graft repair of complicated penetrating atherosclerotic ulcers of the descending thoracic aorta. *J Vasc Surg.* 2002 Oct;36(4):720-6.

2. Murgo S, Dussaussois L, Golzarian J, Cavenaile JC, Abada HT, Ferreira J, Struyven J. Penetrating atherosclerotic ulcer of the descending thoracic aorta: treatment by endovascular stent-graft. *Cardiovasc Intervent Radiol.* 1998 Nov-Dec;21(6):454-8.

3. Hayashi H, Matsuoka Y, Sakamoto I, Sueyoshi E, Okimoto T, Hayashi K, Matsunaga N. Penetrating atherosclerotic ulcer of the aorta: imaging features and disease concept. *Radiographics.* 2000 Jul-Aug;20(4):995-1005.

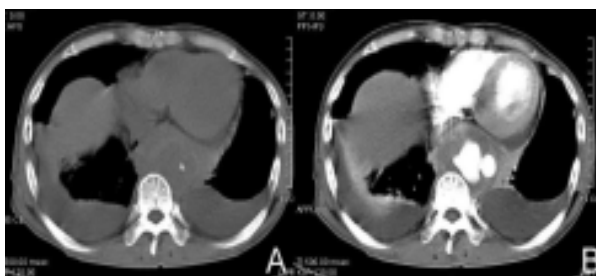


Fig.1 A & B. Pre-enhancing chest CT scan at aortic hiatus

level shows small atheromatous calcification on right side wall of descending thoracic aorta and fluid collection in both pleural cavities, left pericardial space, and posterior mediastinum (A). About 2.2cm sized pseudoaneurysm is seen in right side of descending thoracic aorta on early arterial phase CT (B).

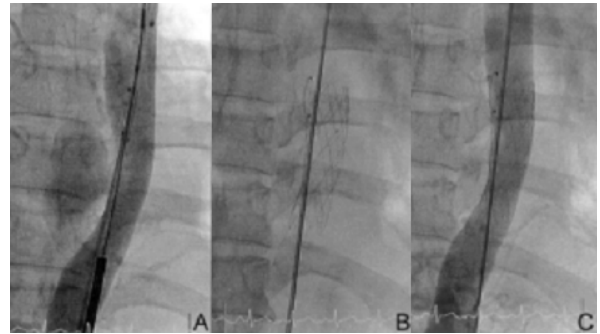


Fig.2 A, B, & C. Aortography reveals aortic wall defect and pseudoaneurysm in aortic hiatus level (A). A 24 mm X 4 cm stent-graft is deployed at pseudoaneurysm site of descending aorta (B). Aortography after deploying of stent-graft shows intact lumen of descending thoracic aorta without visualization of pseudoaneurysm (C).

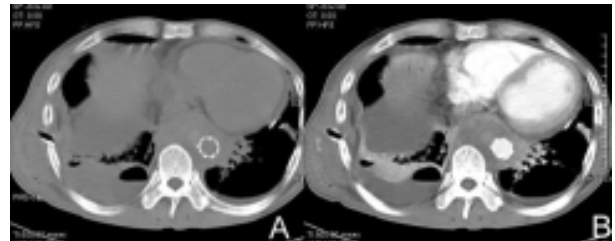
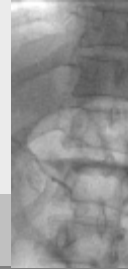


Fig.3 A & B. Follow-up CT scan 2 days after stent-graft insertion. Pre-enhancing scan shows stent-graft in aorta and slightly high attenuation, maybe thrombosis in pseudoaneurysm, in right side of descending thoracic aorta. Fluid collection in left pleural cavity and pericardial space is improved and no interval change is seen in fluid collection in right hemithorax (A). Enhanced CT scan shows no definite contrast leakage into pseudoaneurysm (B).



## endoleak

## Translumbar embolization of type II endoleak after stent-graft treatment of abdominal aortic aneurysm

/ / / / / /

: Aortic aneurysm, abdominal

Embolization

Endoleak

Stent-graft

: 70 /

: 6

5

가

(stent-graft)

. 1

type II endo-

leak

: Type II endoleak after stent-graft treatment of abdominal aorta aneurysm,

1

(sac)

(aortic bifurcation)

(lumbar artery)

(leak)

가

(Fig. 1A,B).

(lumbar artery)

(sac)

type II endoleak

(Fig.2 A,B).

5F

endoleak

(lumbar artery)

22G

(needle)

endoleak

n-bu-

tyl cyanoacrylate (NBCA; Cordis, FL, USA) 1cc + lip-iodol 1cc (Fig.3). 3

type II endoleak

(Fig. 4A,B)

:

endoleak

(aneurysm sac)

가

. 10% (8~44%)

가

type II endoleak

Type II endoleak

가

가

(transarterial approach)

coil

(trans-lumbar direct puncture)

coil

가

(transarterial approach)

(catheter)

가

가

Baum  
approach)

(transarterial ap-

80%

(trans-lumbar direct puncture)

8%

endoleak

(feeding and draining vessel)

(arteriovenous malformation)

(central nidus)

가

endoleak

(trans-lumbar direct puncture)

1. Baum RA, Stavropoulos S, Fairman RM, et al. Endoleaks after endovascular repair of abdominal aortic aneurysms. J Vasc Interv Radiol 2003;14:1111-1117
2. Baum RA, Carpenter JP, Golden MA, et al. Treatment of type II endoleaks after endovascular repair of abdominal aortic aneurysms: comparison of transarterial and translumbar techniques. J Vasc Surg 2002;35:23-29
3. Martin ML, Dolmatch BL, Fry PD, et al. Treatment of type II endoleaks with Onyx. J vasc Interv Radiol 2001;12:629-632

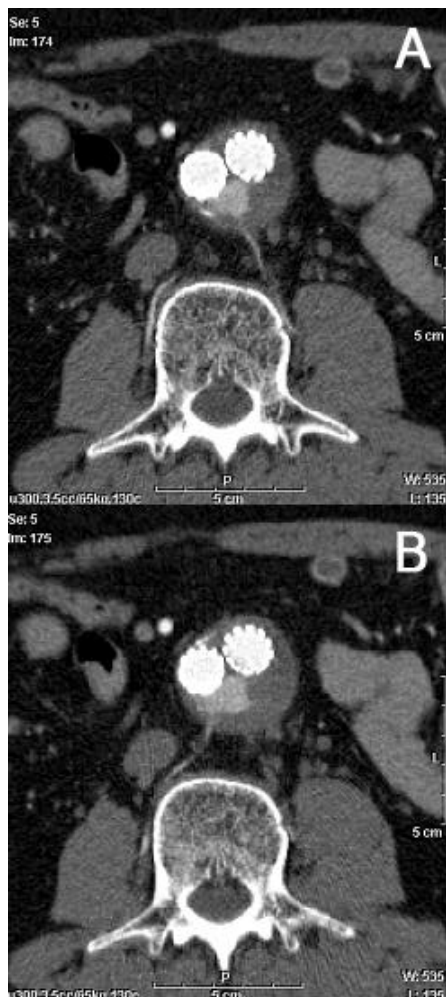


Fig.1A, B. Abdominal CT shows type II endoleak supplied from both lumbar artery (arrows) just below the level of stent-graft bifurcation.

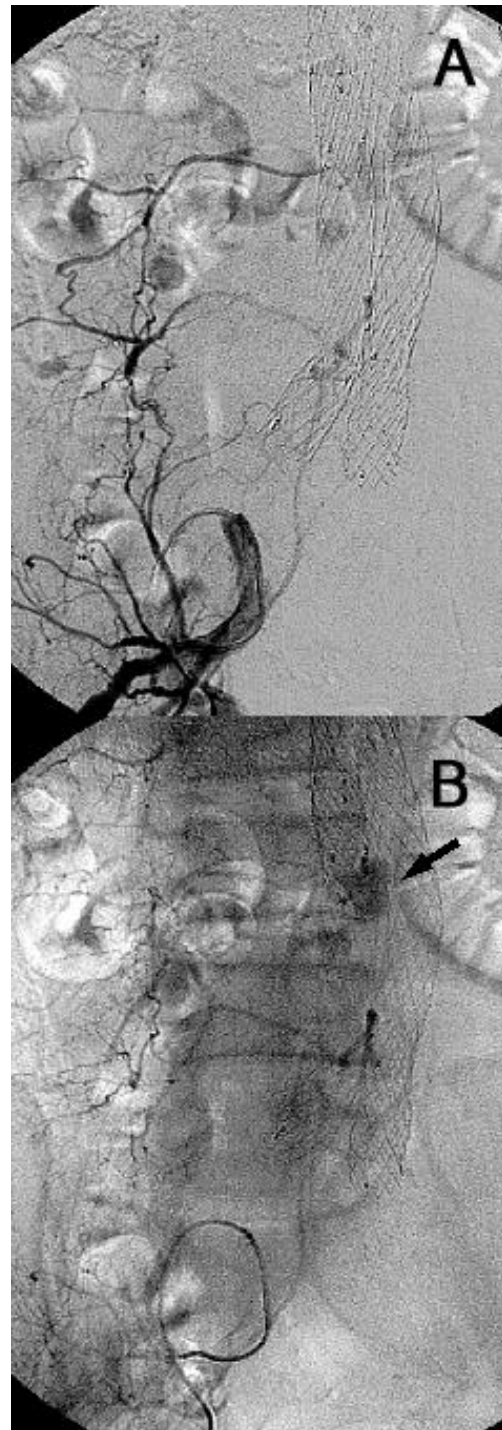


Fig.2 A,B. Right internal iliac artery angiogram shows endoleak (arrow, B) filling from fine collaterals of lumbar arteries.



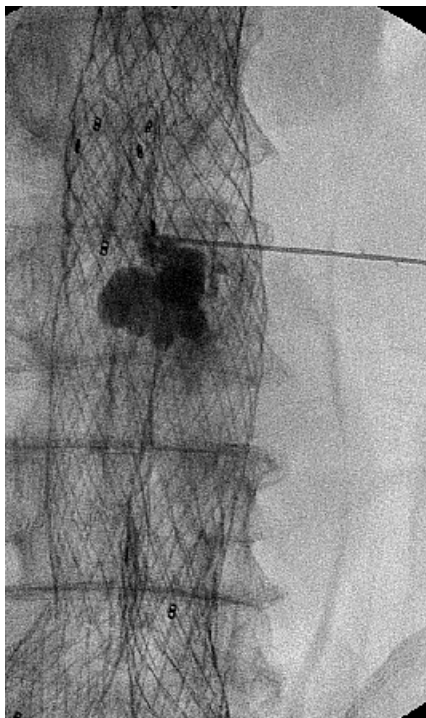
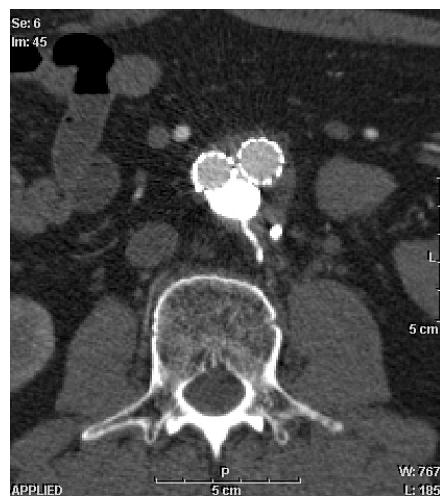


Fig.3. Under prone position, percutaneous translumbar puncture with 22G fine needle was followed by NBCA+lipiodol 1:1 mixture embolization into the endoleak.

Fig.4A,B. Follow-up CT shows complete embolization of endoleak. Bilateral feeding lumbar arteries are also obliterated by NBCA.



# Case 10

## graft - stent

Aortic graft-stent insertion in patient with retroperitoneal malignancy.

: 40 /  
: 40 가 8 retro -  
peritoneal mass excision inverted Y shap -  
ed bi-iliac gotex bypass graft  
가 가 ,  
CT re -  
curred malignant fibrous histiocytoma

: Recurred malignant fibrous histiocytoma with  
obliterated and abutting parent abdominal  
aorta.

CT(Fig.1)

section) CT(Fig.2) . 2 (partial re -  
가 bypass graft encasement patent

12Fr sheath introducer  
20mm -5cm graft - stent( , ,  
; Dacron graft, 1cm bare seg -  
ment) infrarenal aorta graft  
(Fig.3). CT graft - stent

(Fig.4 a,b)

Retroperitoneum 가  
retroperitoneal organ 가  
extrinsic compression invasion

graft - stent

1. Lee JT, Donayre CE, Walot I, Kopchok GE, White RA. Endovascular exclusion of abdominal aortic pathology in patients with concomitant malignancy. Ann Vasc Surg 2002;16;150 -156.

2. Kerwin G, Silverstein M, Lewis C. Percutaneous stent treatment for arterial occlusion caused by retro - peritoneal fibrosis. AJR 2000; 175; 1283 -1285.



Fig. 1. Initial CT shows active bleeding(arrow) from abdominal aorta into the soft tissue mass which is encasing the aorta.

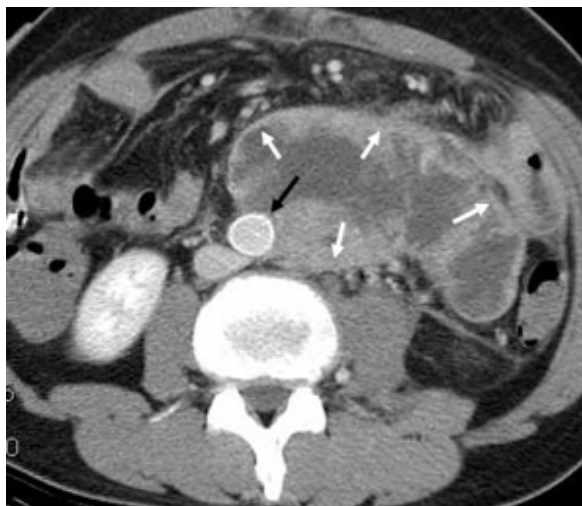


Fig. 2. Post-op followup CT shows an interposed graft(black arrow) in the aortic lumen and huge soft tissue mass(white arrows) which is partially abutting to aortic wall.

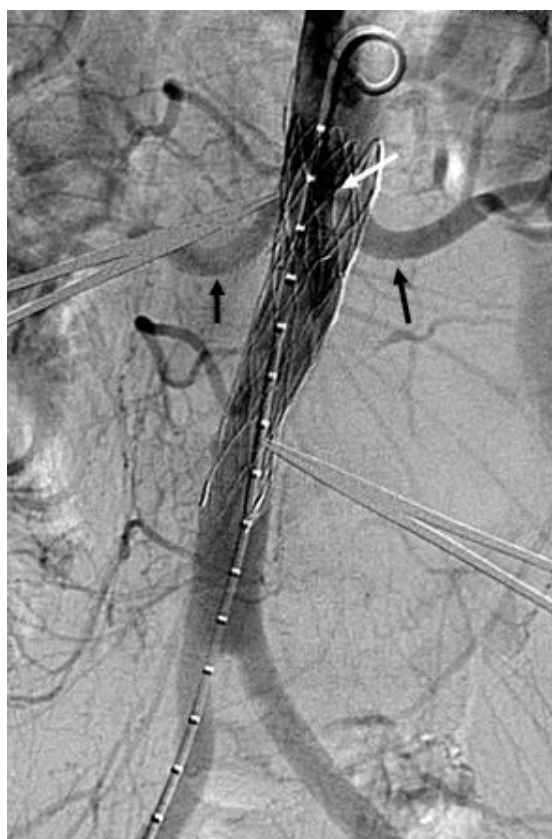


Fig. 3. Aortogram after insertion of graft-stent shows a patent SMA(white arrow) and both renal arteries(black arrows).



Fig. 4a. Followup CT after 2 days later shows a graft - ent within the surgical graft and somewhat decreased soft tissue mass.

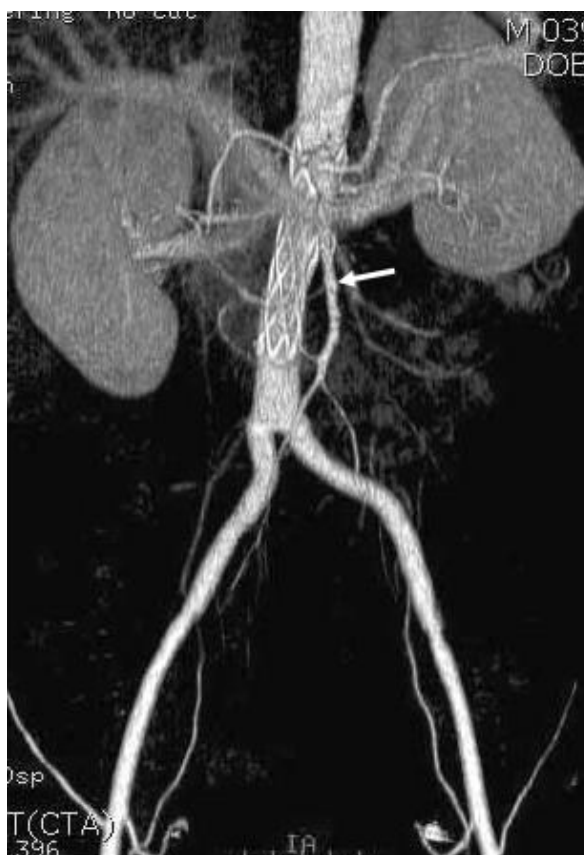


Fig.4 b. CTA shows a patent SMA(arrow) and both renal arteries.

## Coil Embolization of Aortopulmonary Shunt

: Arteries, therapeutic embolization

Lung, congenital malformation

: 12

: murmur가 mild pulmo-  
nary congestion congestive heart failure

: Aberrant systemic arterial supply to the left  
lower lobe

( Fig. 7). 19

embolization coils가

( Fig. 8) .

(Chest CT)

가

(Fig. 1, 2 ). CT

descending thoracic aorta

anomalous artery가 left inferior pulmo-

nary vein abnormal connection

Aortopulmonary shunt (Fig. 3, 4 ).

Right femoral artery 5F cobra catheter

aorta aberrant systemic artery selection

embolization coils 9 embolization

. 10

shunt가

가 embolization

embolization coil 가 aorta lu-

men free floating vascular for-  
cep( Cook, Bloomington, USA )

(Fig 5) . Post embolization Aortogram sys-  
temic pulmonary artery arterial flow

( Fig. 6 ),

congenital heart fail-

ure

Chest CT

em-

bolization coil

major aortopulmonary collateral arteries(MAPCA),  
pulmonary sequestration, anomalous systemic arterial  
supply to lung parenchyma .

major aortopulmonary collateral artery

congenital heart disease가 TOF 가

pulmonary atresia steno-  
sis가 aorta systemic artery pulmonary  
artery multiple collateral vessel .

pulmonary artery connection TOF

Blalock - Taussig(B - T) shunt

collateral vessel (1).

Isolated MAPCA

congestive heart failure

descending thoracic aorta

pulmonary vein aortopulmonary shunt iso-

lated MAPCA 가

Pulmonary sequestration intralobar type pulmo-  
nary vein drainage (2) CT abnormal

lung parenchymal mass bronchial atresia가

pulmonary sequestration 가

pulmonary seques-  
tration lung parenchyma systemic  
supply 가

involve hemoptysis, chest  
pain, exercise-related dyspnea or murmurs

(3 - 5).

murmur가

congestive heart failure

systemic

pulmonary artery

Systemic pulmonary artery                      pulmo-  
 nary sequestration      pulmonary arteriovenous fistula  
    가                      embolization coil  
    detachable coils      balloon, PVA particle      Glue  
    가                      embolic material      pulmonary vein  
  
    coil  
    distal embolization                      가  
    snare wire      vascular forcep



Fig. 1. Initial chest PA shows marked enlarge cardiac shadow and pulmonary congestion.

Ramsay JM, Macartney FJ, Haworth SG. Tetralogy of Fallot with major aortopulmonary collateral arteries Br Heart J. 1985 Feb;53(2):167-72

Dinkel HP, Hoppe H, Striffeler HU, Triller J. Preoperative arterial embolization of intralobar lung sequestration Radiologe. 2001 Nov;41(11):1001-4

Ashizawa K, Ishida Y, Matsunaga N et al. Anomalous systemic arterial supply to normal basal segments of left lower lobe: characteristic imaging findings J Comput Assist Tomogr. 2001 Sep-Oct;25(5):764-9.

Bruhlmann W, Weishaupt D, Goebel N, Imhof E. Therapeutic embolization of a systemic arterialization of lung without sequestration. Eur Radiol. 1998;8(3):355-8.

Chabbert V, Doussau-Thuron S, Otal P et al Endovascular treatment of aberrant systemic arterial supply to normal basilar segments of the right lower lobe: case report and review of the literature Cardiovasc Intervent Radiol. 2002 May-Jun;25(3):212-5

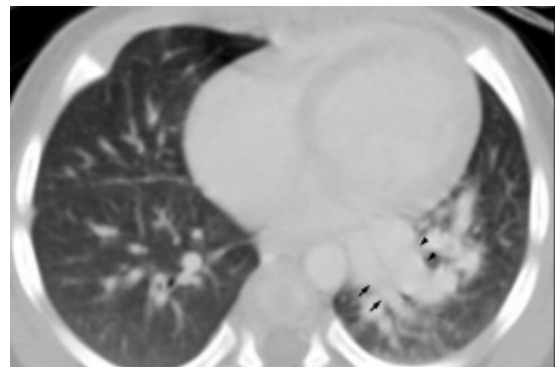


Fig. 2. There are two large dilated vessel on chest CT( arrow: systemic pulmonary artery, arrowhead : dilated pulmonary vein)



Fig. 3. Aortogram shows aberrant systemic pulmonary artery origin from descending thoracic aorta and marked dilated pulmonary vein

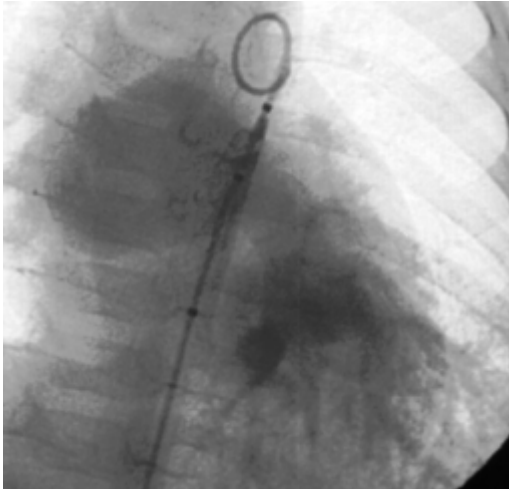


Fig. 4 Aortogram shows aberrant systemic pulmonary artery origin from descending thoracic aorta and marked dilated pulmonary vein



Fig.8 The patient had dramatic improvement of congestive heart failure and follow up chest PA shows normal heart shadow and normal vascularity of left lung.

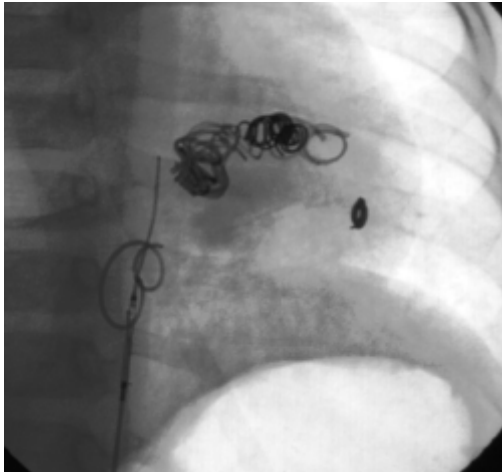


Fig. 5. During coil embolization, coil displaced in aorta lumen. Removal of coil using vascular forcep was done.

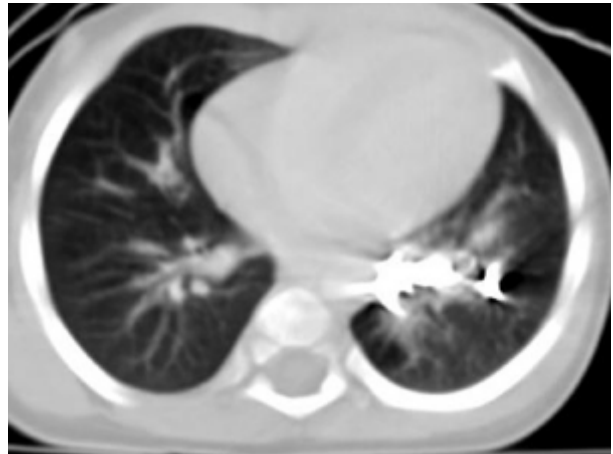


Fig. 7. Immediate follow up CT scan showing multiple coils in systemic pulmonary artery, disappeared aorto-pulmonary shunt.

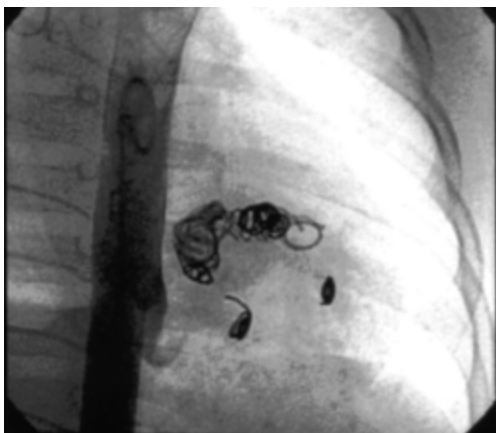


Fig. 6. Aortogram after embolization of systemic pulmonary artery shows no arterial flow in the systemic pulmonary artery



/ /

: Arteries, bronchial  
Arteries, therapeutic embolization  
: M/64  
:

200cc/

tinged sputum  
300cc/

blood  
가 1

. BAAO T4-T6  
aorta, thyrocervical trunk, subclavianartery, internal  
mammary artery, innominate artery, pericardiophrenic  
arteryt, inferior phrenic artery

left gastric artery bronchial artery가  
가 .

CPA  
(Fig 1).

1 T6

(Fig 2a),

250~355um polyvinyl alcohol (PVA)  
gelfoam

(Fig. 2b).

1 1  
2

(Fig. 3a).

1  
가

(Fig. 3b),

1. Sancho C, Escalante E, Mominguez J et al.  
Embolization of bronchial arteries of anomalous origin.  
Cardiovasc intervent Radiol 1998; 21:300-304

2. Sellas N, Bellic A. Non-bronchial collateral  
supply form the left gastric arteryin massive  
haemoptysis. Eur Radiol 2001; 11:76-79

3. , , .  
:  
2001; 45:589-596

4. Han MC, Park JH. Interventional radiology.  
Seoul: Ilchogak. 1999: 24-29.

2 bronchial arteries of  
anomalous origin (BAAO) non-bronchial collaterals



Fig. 1. Plain chest demonstrates chronic tuberculous lesions involving the right upper lobe and destructive change of the left lung.



Fig. 2a. Right intercostobronchial arteriography demonstrates abnormal parenchymal hyperemia with systemic-pulmonary arterial shunts in right upper lobe.



Fig. 2b. Right inferior phrenic arteriography demonstrates abnormal parenchymal hyperemia with severe shunts in left lower lobe, supplied by left pericardiophrenic artery.



Fig. 3a. Left gastric arteriography demonstrates left bronchial artery anomalously originating from left gastric artery, which ascends in the mediastinum, enters left lung via hilum and courses along left lobar bronchi. Abnormal parenchymal hyperemia of left lung is noted.



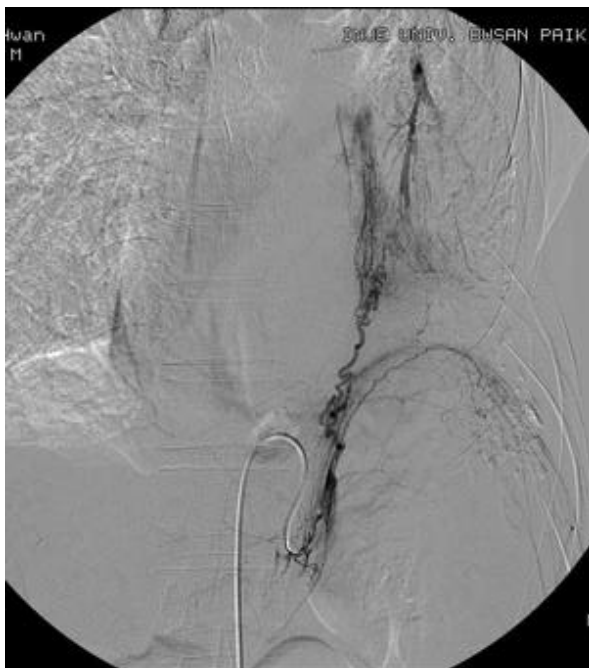


Fig. 3b. Left inferior phrenic arteriography demonstrates abnormal parenchymal hyperemia with shunts in left lower lobe.

## Gelform Embolization of Bronchial Artery Bleeding in Active Cavitory Pulmonary Tuberculosis

: Bronchial artery  
Embolism, therapeutic

: 42 /

:

: Bronchial artery bleeding in active pulmonary tuberculosis

5, 6  
intercostobronchial trunk

CT 4.5cm

(Fig. 1a).

가 (Fig. 1b,  
1c).

가  
Gelform polyvinylalcohol(PVA) 가  
200-250um  
spinal feeder

4F Yashiro (Terumo, Tokyo, Japan)

Microferret (Cook, Bloomington, IN, USA)  
gelform (Fig. 1b).

가 (Fig.  
1c).

가  
, 90%

1. Woong Yoon, Jae Kyu Kim, Yun Hyun Kim, Tae Woong Chung and Heoung Keun Kang. Bronchial and nonbronchial systemic artery embolization for life-threatening hemoptysis: a comprehensive review. Radiographics 2002; 22: 1395-1409

2. HaponikEF, Fein A, Chin R. Managing life-threatening hemoptysis : has anything really changed? Chest 2000; 118: 1431-1435

3. Najarian KE, Morris CS, Arterial embolization in the chest. J Thoracic Imaging 1998; 13:93-104

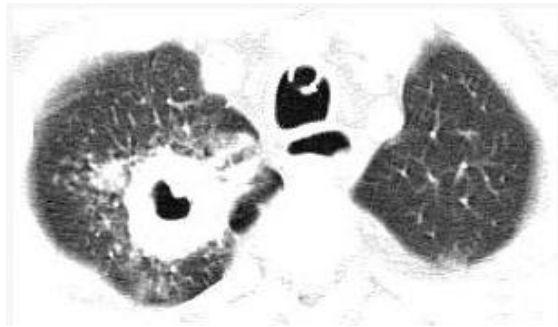


Fig. 1a. Chest CT shows a thick-walled cavitary lesion with multiple tiny satellite nodules in right upper lobe.



Fig. 1b. Right intercostobronchial arteriogram shows blood supply to the cavitary lesion in right upper lung from right bronchial artery.

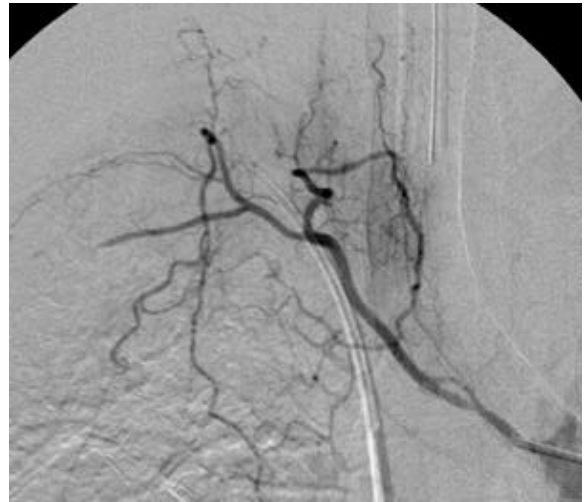


Fig. 1c. Post-embolization arteriogram shows complete occlusion of right bronchial artery and no residual hyper-vascular stain in the cavitary lesion.

# Case 14

## Embolization for intercostal artery bleeding after thoracentesis

: Thoracentesis  
 Intercostal arteries, bleeding  
 Intercostal arteries, therapeutic blockade  
 : 48 /  
 :  
 가 10.4 -> 5.9  
 chest tube bloody  
 fluid가  
 : Intercostal artery bleeding after thoracentesis

pneumothorax  
 chest tube  
 bleeding from lacerated intercostal vessel, re-expansion pulmonary edema, inadvertent liver or spleen puncture, air embolism

가  
 Intercostal artery laceration

가 CT 10  
 (Fig 1).

가 intercostal artery tortuosity가  
 old age  
 가  
 posterior intercostal artery collateral intercostal artery가

가 가

8-12 , 12  
 10  
 (Fig 2). 3 F  
 12  
 Gelfoam pledget  
 (Fig 3). 2 chest tube se-  
 rosanguineous fluid가 10.5  
 가

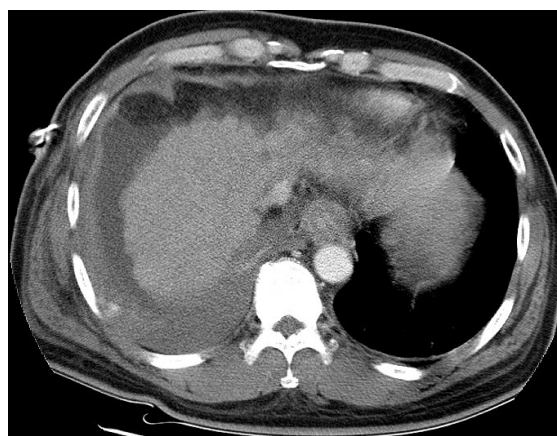


Fig. 1. CT scan shows contrast leakage into right pleural space around the junction between posterior and lateral arc of 10th rib.

21 22 G,  
 16 18 G  
 pneumothorax, local pain, vasovagal reflex, sub-cutaneous hematoma, cough



Fig. 2. Selective arteriogram of right 12th intercostal artery shows contrast extravasation from an unusual branch of 12th intercostal artery, which runs superiorly and laterally to right 10th intercostal space.

1. Jones PW, Moyers JP, Rogers JT et al. Ultrasound- guided thoracentesis: is it a safer method Chest 2003;123(2): 418-423

2. Da Rocha RP, Vengjer A, Blanco A et al. Size of the collateral intercostal artery in adults: anatomical considerations in relation to thoracocentesis and thoracoscopy Surg Radiol Anat 2002; 24(1): 23-26

3. Carney M, Ravin CE. Intercostal artery laceration during thoracentesis: increased risk in elderly patients. Chest 1979; 75: 520-522



Fig. 3. After embolization, Contrast extravasation is no longer seen on selective arteriogram of right 12th intercostal artery.

# Case 15

## Aberrant right bronchial artery originating from left subclavian artery

: arteries, bronchi bronchi, anatomy bronchi, interventional procedures

: 54 /

mammary artery, thyrocervical trunk, subclavian artery, costocervical artery, brachiocephalic artery, lower thoracic aorta, abdominal aorta

(nonbronchial systemic artery)

10

500 mL

가

가

Massive hemoptysis due to chronic tuberculosis

CT

(Figure 1).

Yoon W, Kim JK, Kim YH, Chung TW, Kang HK. Bronchial and nonbronchial systemic artery embolization for life-threatening hemoptysis: a comprehensive review. *RadioGraphics* 2002; 22: 1395-1409.

(Figure 2)

bra type

GLB

fluoroscopy

. 5 Fr co-

(Figure 3)

(Figure 4)

polyvinyl alcohol

5

6

(anomalous origin)

8-35%

aortic arch, internal



Fig. 1. Contrast-enhanced axial CT scan shows dilated bronchi within airspace consolidations in right upper lobe.



Fig. 2. Thoracic aortogram fails to reveal enlarged bronchial arterial structure but shows only enlarged right upper intercostal artery (arrow).

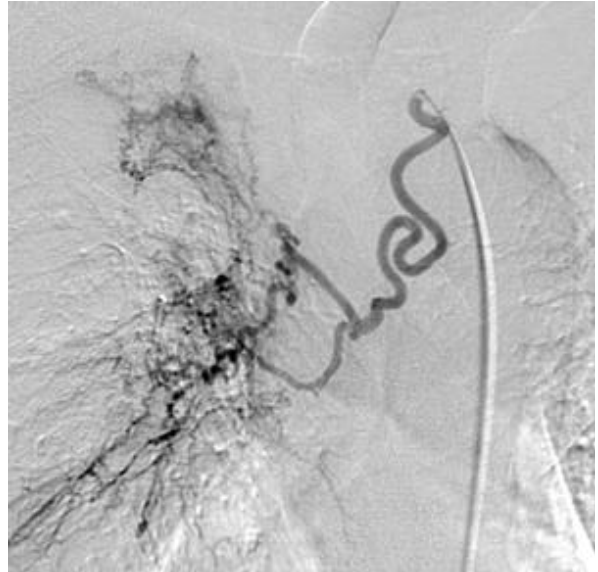


Fig. 4. Image obtained after selective injection of an aberrant bronchial artery shows hypertrophic artery that supplies hypervascular lesions in right upper lobe.



Fig. 3. Left subclavian arteriogram shows an aberrant bronchial artery (arrows) that arises from the proximal portion of left subclavian artery.

# Case 16

## Intimal hyperplasia after stent insertion of left subclavian artery

: Stent and prosthesis  
 Angioplasty, subclavian artery  
 : 54 /  
 : 가  
 TFCA left subclavian  
 artery stenosis stent in-  
 section 6  
 F/U angiography intimal hyperplasia  
 : intimal hyperplasia after stent insertion of left  
 subclavian artery



Fig. 1. left proximal subclavian artery의 focal severe stenosis

Guiding catheter left subclavian artery  
 left proximal subclavian  
 artery focal severe stenosis ( 1). stent  
 catheter가 stenotic portion stenosis  
 가 microwire preballoon angioplasty  
 ( 2). exchange wire left brachial  
 artery balloon-expandable stent sten-  
 otic portion deployment ( 3).  
 stent 6 angiography stent  
 가  
 . stent  
 ( 4).



Fig. 2. Preballoon angioplasty





Fig. 3. Balloon-expandable stent deployment



Fig. 4. Intimal hyperplasia

80%  
6.7%  
3-6  
vessel wall  
recoil, intimal dissection, plaque dislodgement  
intimal hyperplasia  
30 pack year  
3-4.5 /  
plavix astrix  
lescol  
AST, ALT가 가 total cholesterol

F/U  
6

1. Gordon McLennan, Scott O. Trerotola, Mitchell Forney, Brian Jellison, Robert G. Dreesen, and Jerry Tennery Short-term Patency and Safety of an Expanded Polytetrafluoroethylene Encapsulated Endoluminal Device at the Venous Anastomosis of a Canine Arteriovenous Graft Model J Vasc Interv Radiol 2001 12: 227-234.

2. Robert M. Conroy, Ian L. Gordon, Jonathan M. Tobis, Takafumi Hiro, Shunji Kasaoka, Edward A. Stemmer, and S. Eric Wilson Angioplasty and Stent Placement in Chronic Occlusion of the Superficial Femoral Artery: Technique and Results J Vasc Interv Radiol 2000 11: 1009-1020.

3. Johannes Lammer, Michael D. Dake, Jacques Bleyn, Barry T. Katzen, Manfred Cejna, Philippe Piquet, Gary J. Becker, and Richard A. Settlage

Peripheral Arterial Obstruction: Prospective Study of Treatment with a Transluminally Placed Self-expanding Stent-Graft Radiology 2000; 217: 95-104.

4. BJ de Smet, RE Kuntz, YJ van der Helm, G Pasterkamp, C Borst, and MJ Post

Relationship between plaque mass and neointimal hyperplasia after stent placement in Yucatan micro-pigs

Radiology 1997; 203: 484-488.

5. Manfred Cejna, Johannes M. Breuss, Helga Bergmeister, Rainer de Martin, Zhongying Xu, Mario Grgurin, Udo Losert, Hanns Plenk, Jr, Bernd R. Binder, and Johannes Lammer Inhibition of Neointimal Formation after Stent Placement with Adenovirus-mediated Gene Transfer of IB in the Hypercholesterolemic Rabbit Model: Initial Results Radiology 2002 223: 702-708; published online as 10.1148/radiol.2233011002

## Splenic artery; Extrahepatic collateral in hepatocellular carcinoma

: liver neoplasms, blood supply, liver neoplasms, therapeutic radiology

: 44 /

: 2  
CT

: Hepatocellular carcinoma

(1).

(1) supply  
가

가

CT

가  
가

(Fig 1).

1. Chung JW. Extrahepatic collaterals in hepatocellular carcinoma. In Han MC, Park JH. Interventional radiology. Seoul : Ilchokak 1999:355 - 363

가 (Fig 2).  
4F (Terumo)

가 가 (Fig 3)  
(Fig 4). 5F

(Cook) 가 (Fig 5) 3F

(Fig 6,7).

(Fig 8) 1 CT  
(Fig 9).



Fig. 1. Contrast-enhanced CT scan (early phase) demonstrates large lipidolized mass in right hepatic lobe with enhancing lipiodol defect area in anterior aspect of main mass. Note the two enhancing structures suggesting vessels, anterior to viable portion.

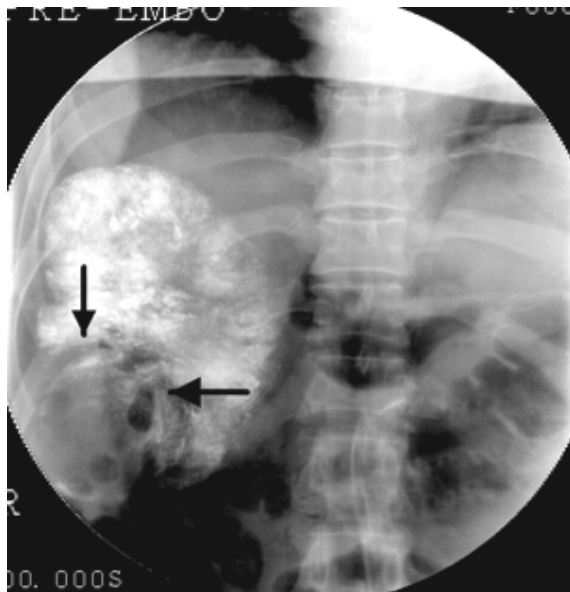


Fig. 2. Preembolization scout image of 2nd TACE shows area of nodular lipiodol defect area (arrows).



Fig. 4. On delayed phase of celiac angiogram, there are viable tumor stainings in medial aspect and inferolateral aspect of lipiodolized mass in right hepatic lobe.



Fig. 3. Celiac angiogram in early arterial phase shows viable tumor staining in medial margin of lipiodolized HCC in right hepatic lobe. Note the arterial structure crossing the lipiodolized mass.



Fig. 5. Selective angiogram of splenic artery shows aberrant branch originating from proximal portion of splenic artery.



Fig. 6. Superselctive angiogram shows aberrant branch of splenic artery crossing the lipiodolized mass (Fig. 6) and tumor staining (Fig. 7)

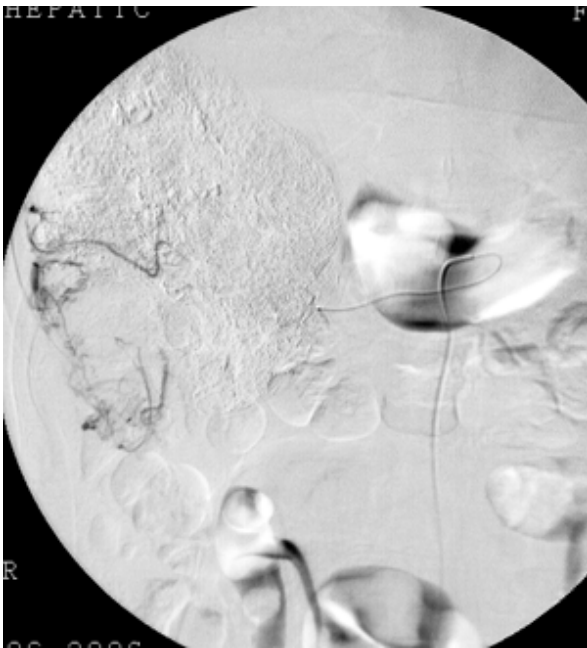


Fig. 7. Superselctive angiogram shows aberrant branch of splenic artery crossing the lipiodolized mass (Fig. 6) and tumor staining (Fig. 7).

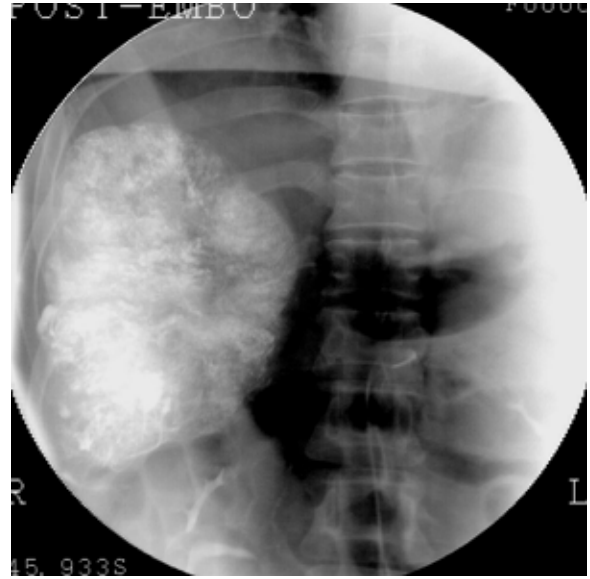


Fig. 8. Postembolization scout image of 2nd TACE shows compact nodular lipiodol uptake in previous defect area.

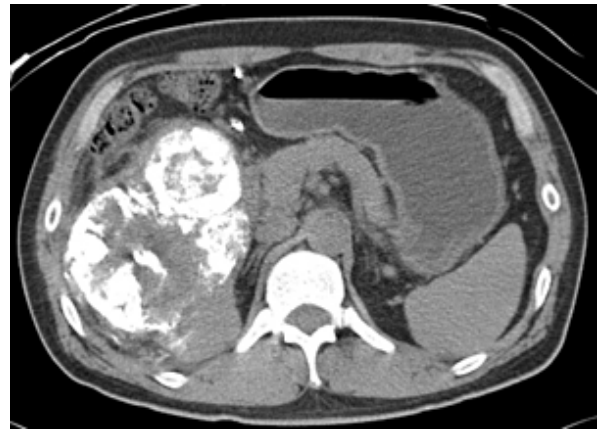


Fig. 9. One month follow-up CT scan shows nodular compact lipiodol uptake in embolized area fed by a branch of splenic artery. Note the lipiodol retention in aberrant branch of splenic artery.

# A New Tip-Fixation Technique without Coil Embolization in Percutaneous Implantation of a Port-catheter System for Hepatic Arterial Infusion Chemotherapy

/ / / / / / /

: Hepatic artery, hepatocellular carcinoma,  
port catheter.

: M/60

: 13 B

, 2

CT

: massive hepatocellular carcinoma (HCC)

CT

가  
(Fig. 1).

Deltec, St Paul, MN, U.S.A.)

. Chemoport

(sub-cuta-

neous pocket)

(closure) (Fig 5).



Fig. 1. Massive HCC is noted on both lobes of liver with portal vein invasion.

. 5F (Cook, Bloomington, IN, USA)

(celiac artery)

(Fig. 2),

(common hepatic artery)

(guide wire)

(gastroduodenal artery)

. 5.8 F polyurethane

(Port - A - Cath

Deltec, St Paul, MN, U.S.A.)

2

(proper hepatic artery)

(Fig. 3).

wedging

(Fig. 4)

(sub-cutaneous fat layer) Chemoport (Port - A - Cath,

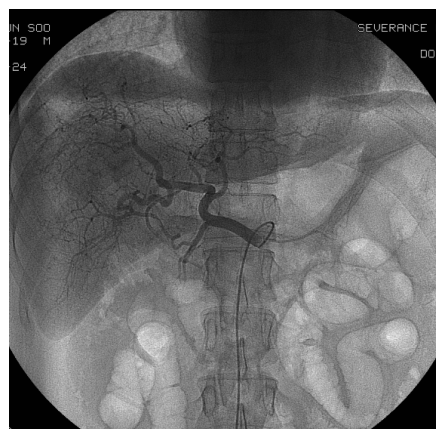


Fig. 2. Common hepatic angiography with 5-Fr catheter shows normal anatomy of proper hepatic artery and gastroduodenal artery.



Fig. 3. After measuring the length of gastroduodenal artery with guide wire and making two side holes of 5.8 F polyurethane catheter, catheter is inserted into gastroduodenal artery. Only the hepatic artery is opacified through the side-holes with slow injection of contrast material.

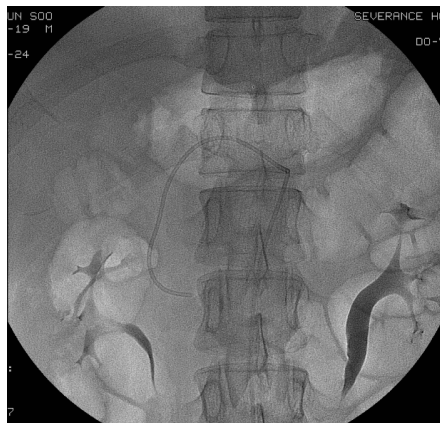


Fig. 4. Tip of the port catheter is wedged into the far distal gastroduodenal artery without embolization.

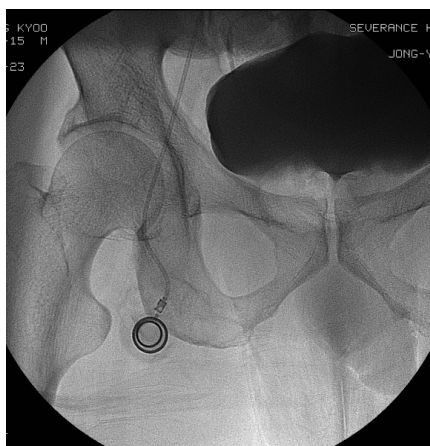


Fig. 5. Chemoport chamber is implanted in the subcutaneous fat layer of thigh or abdominal wall

1950 Klopp  
가 . 가  
(hepatic arterial infusion chemotherapy)  
coil NBCA (n-butyl cyanoacrylate)  
(catheter tip)  
(port-catheter system) (dislocation)  
가 , , 가  
가 가  
가  
34 coil  
(Rt  
gastroepiploic artery) wedging  
(technical success  
rate) 100% . 33  
( 58 ) , (1-14 ,  
6.3 ) (patency rate) 92%  
1 , 2  
(  
5.6 - 43.8%, coil (2%),  
0 - 22%, 1.6 - 2.6%)  
.  
.  
1. , , .  
: 110  
. 2000;43 :417-422  
2. Yamagami T, Nakamura T, Yamazaki T, et al. Catheter-tip fixation of a percutaneously implanted port-catheter system to prevent dislocation. Eur. Radiol. 2002 12:443-449  
3. Yamagami T, Kato T, Iida S, et al. Value of transcatheter arterial embolization with coils and n-butyl cyanoacrylate for long-term hepatic arterial infusion chemotherapy. Radiology 2004; 230:792-802

: 2

## Percutaneous transhepatic stent placement of extrahepatic portal vein stenosis: 2 cases

/ / / / / /

: portal vein, interventional procedure  
pancreatic cancer  
liver transplantation

resection anastomosis  
postoperation 16 follow up CT portal  
vein stenosis .

1 : 46 /

: portal vein stenosis of recurrent lymphadenopathy after whipple operation  
:  
2 pancreatic cancer whipple operation .

3 portal vein. focal severe  
stenosis collateral vessel (Fig.2 - a).

denopathy portal vein stenosis가 (Fig.1 - a).  
3 portal vein focal stenosis가  
(Fig.1 - b).

1 portal vein  
obstruction  
10mm - 6cm Zilver stent(Cook, Bloomington, IL, U.S.A.)  
가 8mm - 4cm  
synergy balloon(Medi - Tech, Watertown, MA, U.S.A.)  
0 mmHg .

21G chiba needle right posterior portal  
vein puncture 7 - Fr introducer sheath  
0.035 inch guide wire (Terumo, Tokyo, Japan)  
5 - Fr cobra catheter (Cook, Bloomington, IL, U.S.A.)  
stenotic portion .

(extrahepatic portal vein stenosis)  
(thrombosis), ,

: 6mmHg, 11mmHg - 5mmHg). 14mm - 6cm Wallstent  
(Medi - Tech, Watertown, MA, U.S.A.)  
0 mmHg .  
MWCE - 35 - 4 - 3 coil (Cook, Bloomington, IL, U.S.A.) 4

가

1

2 : 64 /

: portal vein stenosis after distal pancreatectomy and portal vein anastomosis  
: Pancreatic tail cancer distal pancreatectomy hepatic artery portal vein

Yamakado

100%  
(splanchnic vein) 14%  
. Funaki

1. Brian Funaki, Jordan D. Rosenblum, Jeffrey A. Leef, et al. Percutaneous Treatment of Portal Venous Stenosis in Children and Adolescents with Segmental Hepatic Transplants: Long-term Results.

Radiology 2000; 215: 147-151.

2. Koichiro Yamakado, Atsuhiro Nakatsuka, Naoshi Tanaka, et al. Portal Venous Stent Placement in Patients with Pancreatic and Biliary Neoplasms Invading Portal Veins and Causing Portal Hypertension: Initial Experience

Radiology 2001; 220: 150-156.

1

Figure 1. Recurrent lymphadenopathy causing portal vein stenosis in a 46-year-old woman.

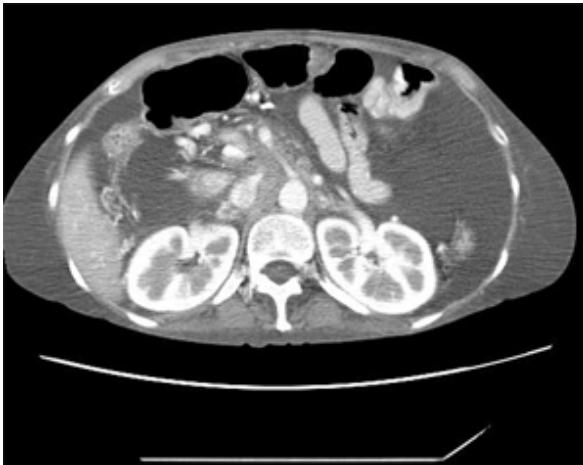


Fig. 1a. Abdominal enhanced CT scan shows lymphadenopathy encasing portal vein with stenosis.

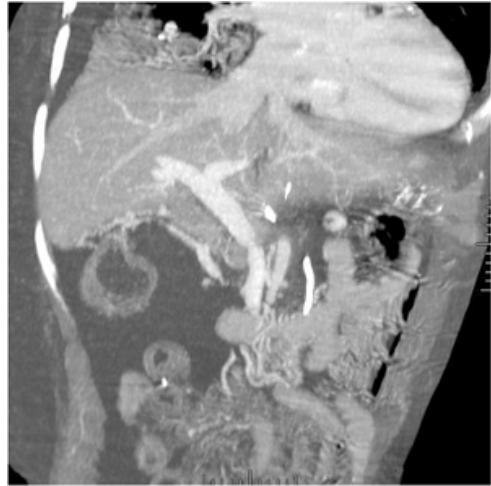


Fig. 1b. 3D reconstruction image shows focal mild stenosis of portal vein.



Fig. 1c. Transhepatic portography confirms the presence of a focal mild stenosis of the portal vein.



Fig. 1d. Portography after stenting shows disappearance of the stenosis.



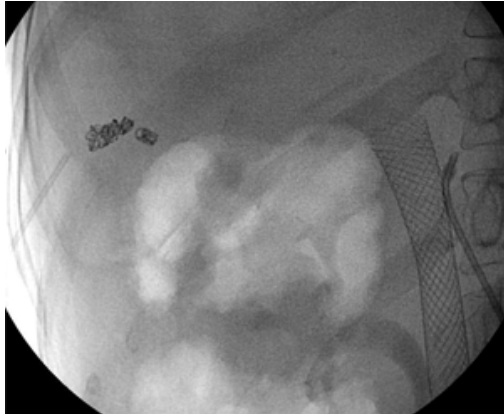


Fig. 1e. Parenchymal track was closed by coils.

2

Fig. 2. postoperative anastomotic stricture of portal vein in a 64-year-old woman.



Fig. 2c. Photography after stent placement shows stenosis remained.

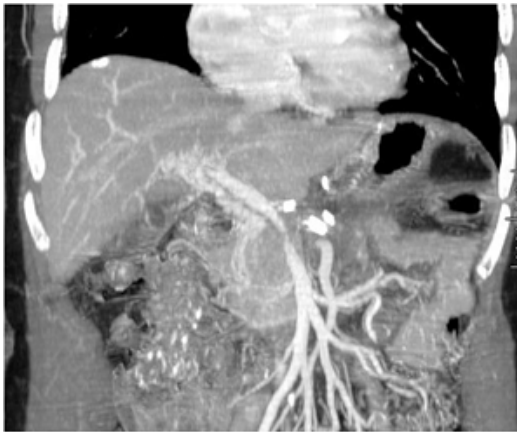


Fig. 2a. 3D reconstruction image shows a severe focal stenosis of the portal vein.at anastomotic site

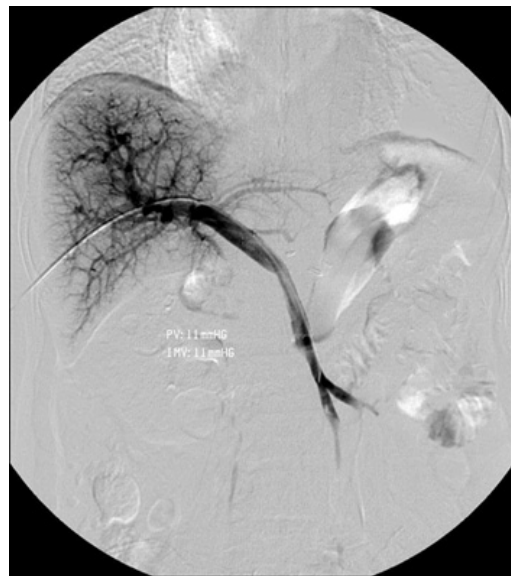


Fig. 2d. Final portography shows marked improvement in luminal caliber after balloon angioplasty, but persistent luminal narrowing still was noted.



Fig. 2b. Transhepatic portography shows complete obstruction of the portal vein with collateral vessels.

## Case 20

### Extrahepatic portal venous stenosis: Treatment with Percutaneous Transhepatic Stent Placement

: Hypertension, portal  
Portal vein stenosis  
Stents and Prostheses  
Hypertension, portal  
Portal vein stenosis  
Stents and Prostheses

: 54 /

Extrahepatic portal venous stenosis.

: 8 Whipple

4

2-3

8

Whipple

4

2-3

CT

(Fig 1 A, B).

. (Fig 1 C.)

가 10mm X 4cm Smart

10mm x 2cm

21G

7F

. 5F cobra

가

1cm

가

10mm X 4cm Smart

10mm x 2cm

25%가

5-10%

가

가

가

가

TIPS가

Yamakado

2)

3)

1)

4)

5)

가

1

60%

가

21G

7F

. 5F cobra

가

1cm

5-10%





Fig. 1c. SMA portography shows focal stenosis at extrahepatic portal vein.

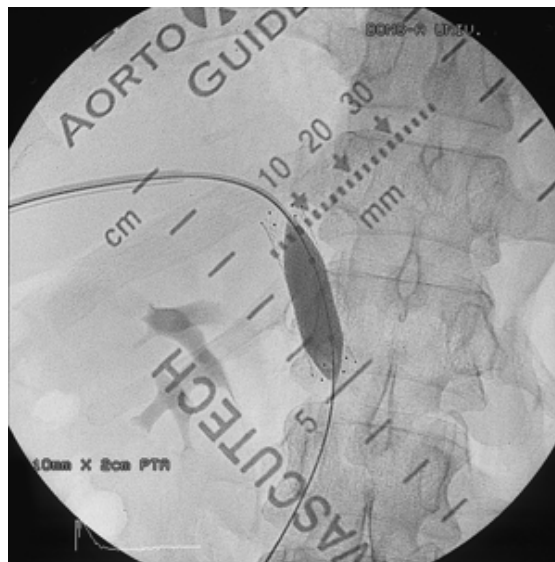


Fig. 2b. 10mm X 4cm Smart stent was inserted and 10mm X 2cm balloon angioplasty was done.

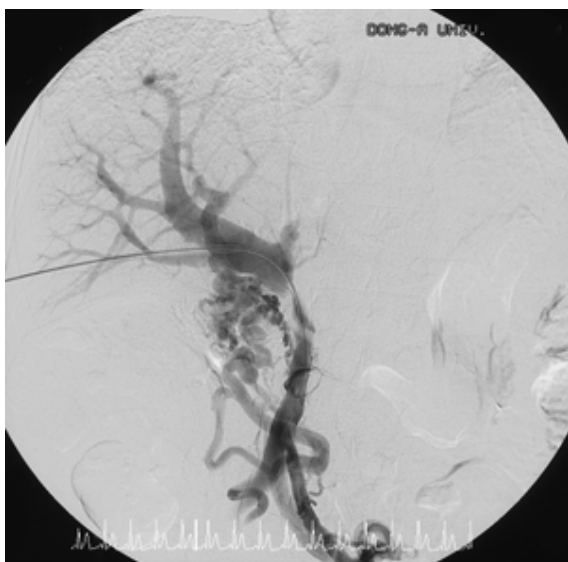


Fig. 2a. Transhepatic portography shows focal stenosis of extrahepatic portal vein and filling of collateral veins.

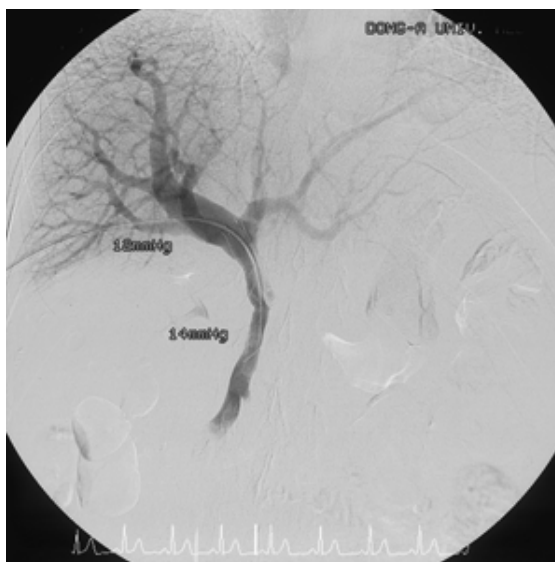


Fig. 2c. Portogram obtained after stent placement shows disappearance of collateral veins. C) Portogram obtained after stent placement shows disappearance of collateral veins.



## Treatment of Spontaneously Ruptured Intraperitoneal Metastases secondary to Ruptured Hepatocellular Carcinoma

: , , .

: 56 /

: Spontaneous rupture of intraperitoneal metastases of ruptured hepatocellular carcinoma

: A 56 year old male was referred for evaluation of sudden onset abdominal pain. He has been diagnosed an alcoholic hepatitis before 5 years. On admission, the serum level of alpha-fetoprotein (AFP) was 237.9 ng/ml and HBsAg was positive. Hemoglobin level was 8.1 g/dL and hematocrit was 24.3. Mild hepatic dysfunction was detected. Clinically rupture of HCC was suspected. Transarterial chemoembolization (TACE) was done after confirmation of hepatoma rupture on angiography. The patient was clinically improved and discharged 2 weeks later. Seven months later, the patient was readmitted due to newly developed abdominal pain. After detection of the intraperitoneal metastatic nodules, TACE was repeated. Two months later after 2nd TACE, the patient complained of abdominal distension with pain. The patient expired two weeks later finally.

On initial abdominal CT scan, two hypervascular tumor nodules were demonstrated in the right lobe of the liver with hematoma in the perihepatic space suggestive of hepatoma rupture (Fig1a-c). Homogeneous lipiodol uptakes in tumor nodules were shown on follow-up CT scan after TACE (Fig1-d). Seven months later, three intraperitoneal metastatic nodules were detected on CT scan (Fig2). One of them revealed a large hematoma

around the tumor nodule representing rupture. Abdominal angiography was performed to evaluate the tumor lesions and for TACE. Selective gastroduodenal arteriography reveals three extrahelic intraepitoneal tumor nodules compatible with the CT findings. Two of them were supplied by the distal omental branch of gastroduodenal artery. The large one with hemorrhage was supplied directly by multiple fine & small branches of the gastroduodenal and the proximal omental arteries (Fig3). Finally a huge enlargement of the mass, up to 23 cm in diameter, was noted on the follow-up CT scan two months later (Fig4).

Initial TACE was performed for ruptured HCC in the liver. After superselection of the feeding arteries with microcatheter (Renegade, Boston-Scientific, USA), chemoinfusion, mixture of Adriamycin 30 mg and lipiodol 6 cc, with gelfoam embolization was done. Seven months later two of three peritoneal metastatic nodules can be partially chemoembolized. But embolization of the large one with spontaneous rupture could not be made.

Spontaneous rupture of HCC with intraperitoneal hemorrhage is reported in the incidence of 12-14.5%. Prognosis of ruptured HCC is generally poor. Many malignant cells are thought to disperse into the peritoneal cavity or pleural cavity during HCC rupture. A well-enhanced mass with central low-attenuation representing intratumoral necrosis and engorgement of adjacent omental vessels were reported in some patients as the imaging findings of intraperitoneal seeding from HCC by Kim et al. The omental metastases are usually

supplied by omental and mesenteric arteries on angiography. Several treatment have been proposed for spontaneous rupture of HCC including surgical or radiological intervention. In our case, tumors were supplied directly by fine branches of omental and gastroduodenal arteries which made complete TACE difficult or impossible. Therefore aggressive surgical intervention is the choice of treatment. Due to prolonged survival in the patients with ruptured HCC by radiologic intervention, early detection through a periodic surveillance of disseminated metastases and aggressive surgical intervention can provide the best chance for longer survival.

1. Kim TK, Han JK, Chung JW, et al. Intraperitoneal Drop Metastases from Hepatocellular Carcinoma: CT and Angiographic Findings. *J Comput Assist Tomogr* 1996;20(4):638 - 642
2. Marini P, Vilgrain V, Belghiti J, et al. Management of Spontaneous Rupture of Liver Tumors. *Dia Surg* 2002;19(2):109 - 113
3. Uneishi T, Kubo S, Hirohashi K, et al. Successful Surgical Control for Hepatocellular Carcinoma Disseminated to the Peritoneum. A Case Report. *Hepatogastroenterology* 2002;49(44):532 - 534
4. Kosaka A et al. Successful Surgical Treatment for Implanted Intraperitoneal Metastases of Ruptured Small Hepatocellular Carcinoma: Report of A Case. *Surg Today* 1999;29(5):453 - 437

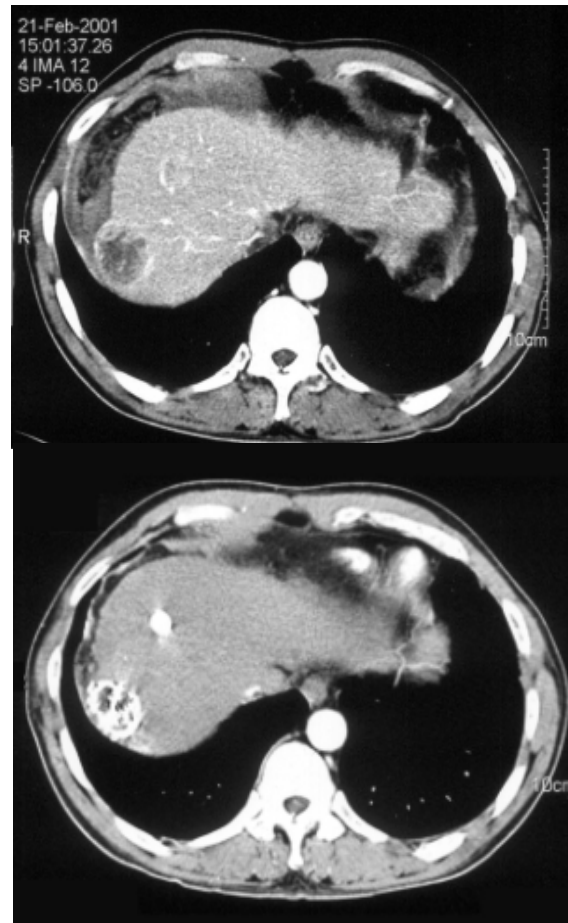
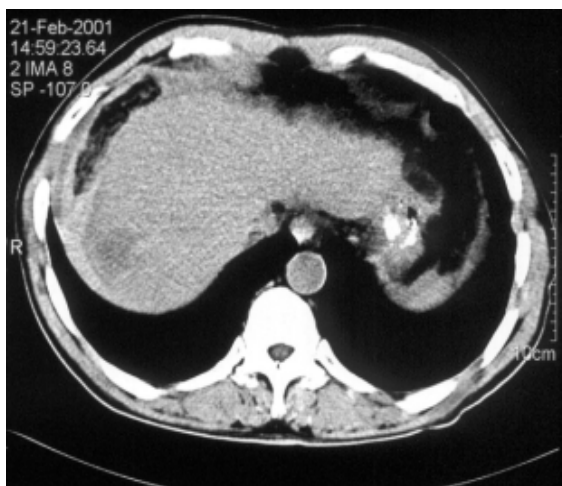
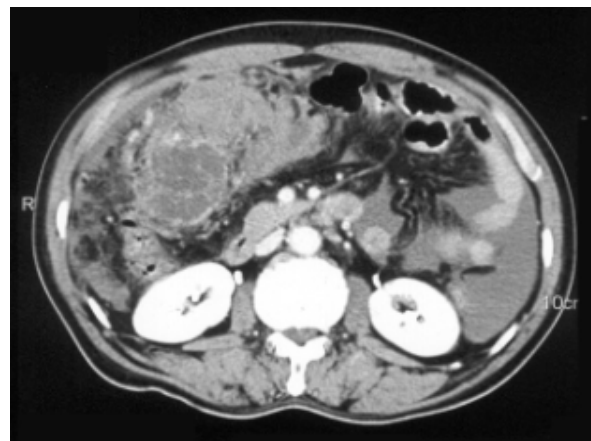


Fig. 1. Two tumor nodules with hemorrhage are seen on abdominal CT scan (non-enhanced, early arterial and portal phases). On follow-up CT scan after TACE, good lipiodol uptakes are shown in the tumor nodules.



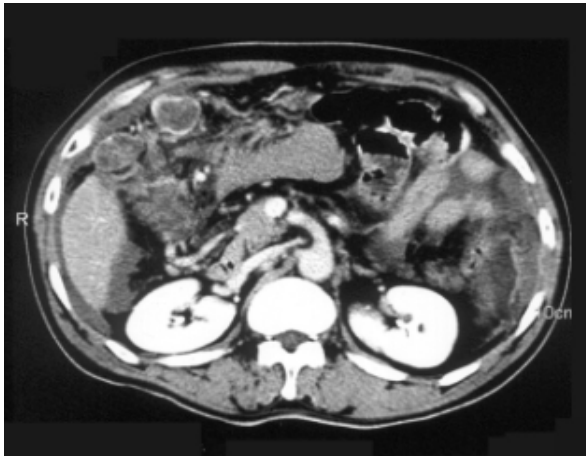


Fig. 2. Peritoneal implanted metastatic nodules are detected with hemorrhage on abdominal CT scan(7 months later)



Fig. 3. A faint tumoral staining in the subhepatic space is shown on selective angiography of the gastroduodenal artery. The tumor is supplied by directly from multiple fine branches of both gastroduodenal and omental arteries.

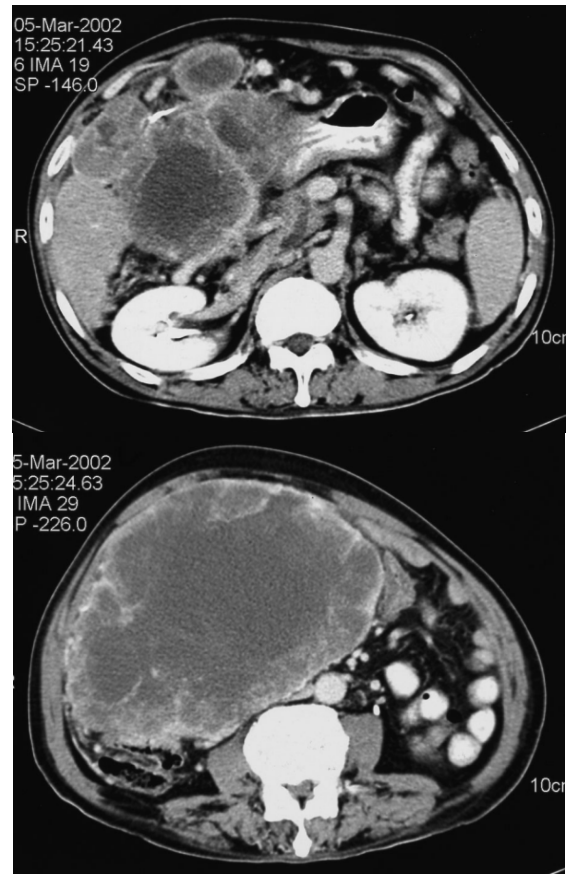


Fig. 4. Abdominal CT scan(9 months later) shows enlargement of the metastatic nodules(Fig4-a). The largest one is up to 23 cm in diameter(Fig4-b).

## Balloon occluded retrograde transvenous obliteration for gastric variceal bleeding in a patient of portal vein occlusion with hepatoma

: Stomach ,varix, Balloon occluded retrograde transvenous obliteration, Portal vein thrombosis.

: 66 /

: 10 C , 3  
12

가 가

:Multiple Hepatoma with portal vein thrombosis and gastric varix.

(Fig 6). 3

(2)

(3)

CT

가

(Fig 1,2).

가

가

5Fr

(Cook)

(3),

7F

(Boston scientific)

가

CT

가

가

(Fig 6).

가

(Fig 3). Hirota

(1) grade 3

7mm/2cm

(Fig 4)

가 가

5% ethanolamine oleate, lipiodol 5:1

12ml

30

8ml

가

가 30

가

(Fig 5).

CT

1.Hirota S, Matsumoto S, Tomita M, Sako M, Kono M. Retrograde transvenous obliteration of gastric varices. Radiology 1999;211:349-356.

2. Hur J, Lee K, Lee JH, Yu J, Won JY, Lee D.



Stent-Graft for TIPS in a Hepatocellular Carcinoma Patient with Main Portal Vein Invasion. *Am. J. Roentgenol* 2004;182:1301-1304

3. Romano M, Gioielli A, Capuano G, Pomponi D, Salvatore M. Partial splenic embolization in patients with idiopathic portal hypertension. *Eur J Radiol* 2004;49:268-73.

4. Tetsuya Fukuda, Shozo Hirota, and Kazuro Sugimura. Long-term Results of Balloon-Occluded Retrograde Transvenous Obliteration for the Treatment of Gastric Varices and Hepatic Encephalopathy. *J Vasc Interv Radiol* 2001;12:327-336.



Fig. 1. Contrast-enhanced CT scan (portal phase) demonstrates multiple HCC in both lobes of liver. Note the fundal and gastric varices.



Fig. 2. Venous thrombosis of Lt and main portal vein is noted in the lower level CT scan. Note the gastrorenal shunt in the left side of aorta.

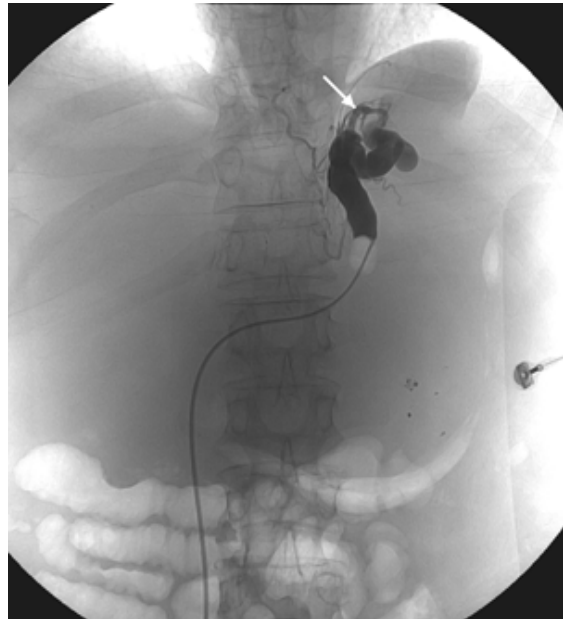


Fig. 3. Venography of gastric varices shows main and accessory (arrow) gastroduodenal shunts with moderate degree of collateral veins.

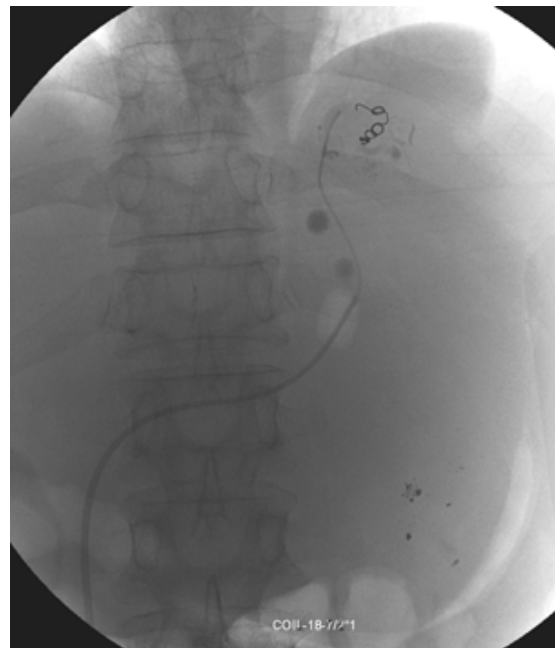


Fig. 4. Coil embolization of accessory gastroduodenal shunt has performed to increase transit time of sclerotic agent in gastric varices.

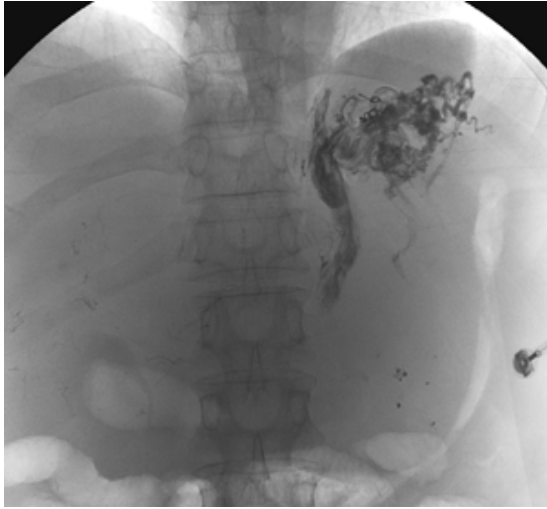
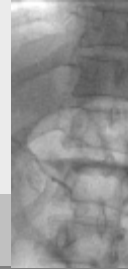


Fig. 5. Scout image after sclerotherapy of 20ml ethanol-amine oleate and lipiodol mixture shows contrast stagnation of gastric varix and gastrosplenic shunt.



Fig. 6. Follow-up CT scan in one week shows complete exclusion of gastric varices with retention of lipiodol.



# Balloon-Occluded Retrograde Transvenous Obliteration (BROTO) of Gastric Varix

/ / / /

: Stomach, varices, Stomach, bleeding, Veins,  
therapeutic blockade

: 67 /

: (melena)  
drowsy mental status

: Gastric fundal varix with hemorrhage

TIPS

hepatic encephalopathy

40-50%

BROTO gastrorenal shunt

gastric varix

varix

TIPS

, hepatic encephalopathy

BROTO

가

. Gastrorenal shunt가

gastric varix hemody-

namics

varix가

Liver CT  
gastrorenal shunt가

gastric fundal varix  
(Fig.1).

mm occlusion balloon catheter 10 F sheath 20  
gastrorenal shunt catheter bal-

loon inflation inferior phrenic vein (Fig. 2)

leakage가 gastric varix가

coil gelfoam

gastric varix가 (Fig. 3). Occlusion balloon  
catheter 30cc (5% ethanolamine ole-

ate) BROTO . 4 CT  
varix (Fig. 4), 6

CT varix

(Fig. 5).

ix varix가 , var -

가

. BROTO

가

가

가

1. Hirota S, Matsumoto S, Tomita M, Sako M, Kono M. Retrograde transvenous obliteration of gastric varices. Radiology 1999;211:349-356

2. Fukuda T, Hirota S, Sugimura K. Long-term results of balloon-occluded retrograde transvenous obliteration for the treatment of gastric varices and hepatic encephalopathy. J Vasc Interv Radiol 2001;12:327-336

3. Yamagami T, Kato T, Iida S, Tanaka O, Nishimura T. Change in the hemodynamics of the portal venous system after retrograde transvenous balloon occlusion of a gastrorenal shunt. AJR 2003;181:1011-1015

3-30% 가 30%

1

45-55%

, TIPS

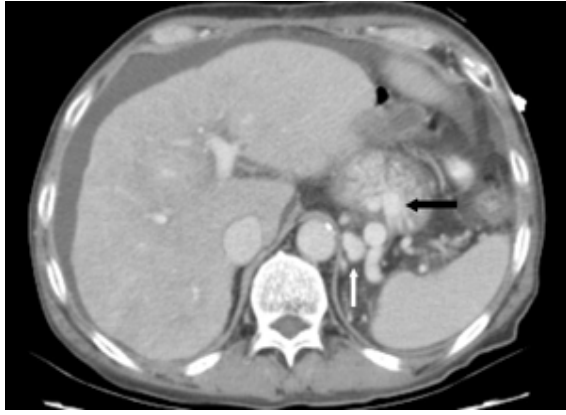


Fig. 1. Contrast-enhanced CT scan shows enhancement of the gastric fundal varices (black arrow) and gastrorenal shunt (white arrow). Contrast-enhanced CT scan shows enhancement of the gastric fundal varices (black arrow) and gastrorenal shunt (white arrow).

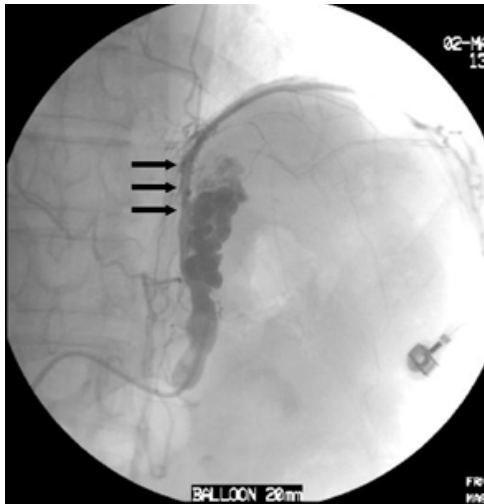


Fig. 2. Left adrenal venogram fails to delineate gastric fundal varices due to leaking inferior phrenic vein (arrows). Left adrenal venogram fails to delineate gastric fundal varices due to leaking inferior phrenic vein (arrows).

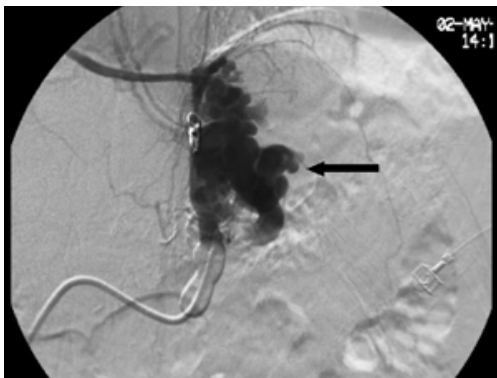


Fig. 3 . Venogram obtained after selective embolization of the inferior phrenic vein shows whole extent of gastric fundal varices (arrow). Venogram obtained after selective embolization of the inferior phrenic vein shows whole extent of gastric fundal varices (arrow).



Fig. 4. Follow-up CT scan obtained 4 days later shows complete thrombosis of the gastric fundal varices. Follow-up CT scan obtained 4 days later shows complete thrombosis of the gastric fundal varices.

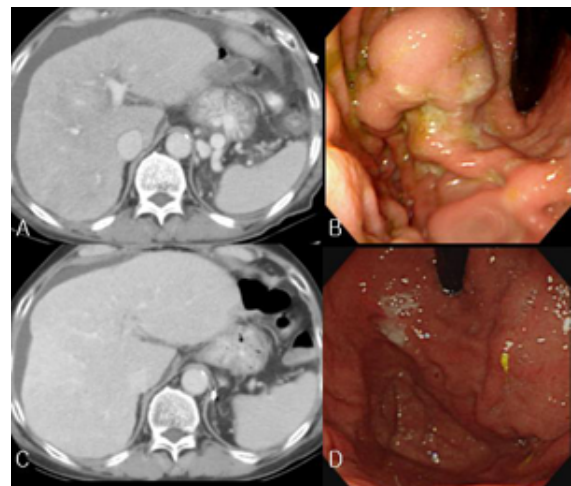


Fig. 5. Both follow-up CT scan (C) and endoscopy (D) obtained 6 months after BRTD reveals no recurrence of the gastric varix. (A), (B) = before BRTD.

# Hepatic arterial embolization and partial splenic embolization for gastric variceal bleeding due to severe arterioportal shunt of hepatocellular carcinoma.

: liver neoplasm, chemotherapeutic infusion, portal hypertension, splenic embolization.  
 : 30 /  
 :  
 8.1mg/dl, 3.4/dL, PT 74%,  
 FP: 6600 ng/ml 가  
 Child-Pugh B7  
 Transjugular intrahepatic portosystemic shunt(TIPS)  
 Balloonoccluded retrograde transvenous ob-  
 literation(BRTO)  
 가  
 40%  
 hypersplenism  
 2 가 , 2 30-40%  
 50-60%  
 30-80% 가  
 가  
 가  
 가  
 (EVL)  
 TIPS BRTO  
 poietin 가가 thrombo-  
 ( ) Histoacryl(n-butyl cya-  
 noacrylate, B Braun) lipiodol 1:3  
 Adriamycin 20mg lipiodol 3cc  
 가  
 hepatopedal flow가  
 Gelfoam pledget  
 80%

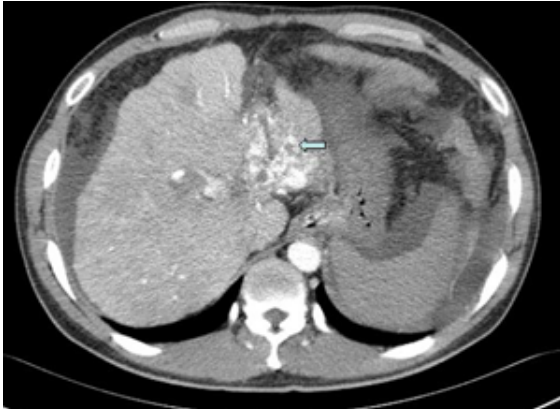


Fig. 1a. Tumor thrombus at left PV with massive AP shunt(open arrow) is noted on early arterial phase of postenhanced CT.

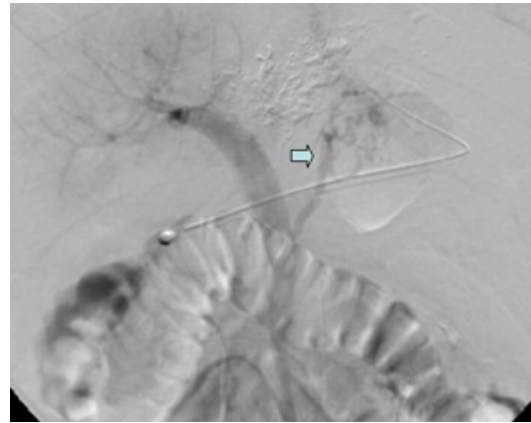


Fig. 2b. Hepatopedal flow without reverse flow is noted on SMA portography. Left gastric v. is noted(open arrow).

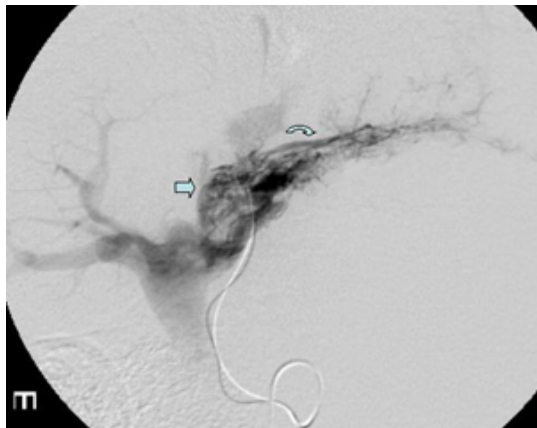


Fig. 1b. Thread & streak sign(open arrow) with AP shunt (curved arrow) at tumor thrombus at left portal vein & reversed portal flow on hepatic arteriography is noted.

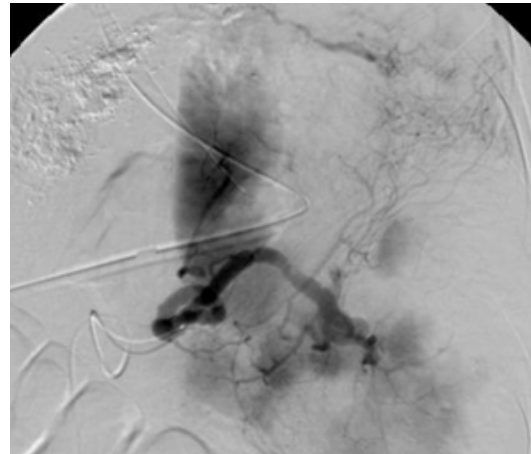


Fig. 3. Patchy parenchymal staining is noted on splenic angiography after postsplenic embolization(80%). Avoid short gastric artery & branch of pancreatic artery.

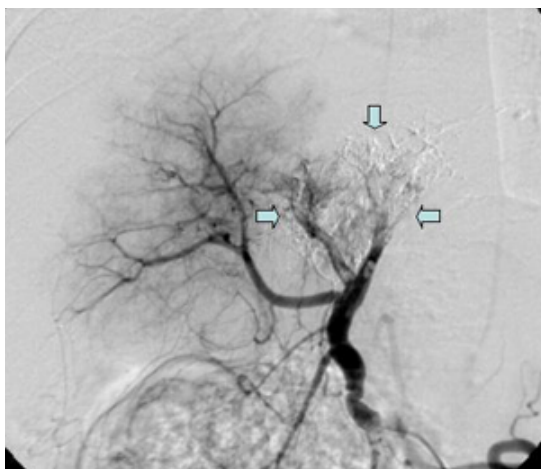


Fig. 2a. Celiac angiography is noted after obliteration of AP shunt with glue(open arrow).

1. Shah SR, Pramesh CS, Deshmukh HL, Mathur SK, Splenic artery embolization for variceal hemorrhage following blocked distal splenorenal shunt. *Hepatogastroenterology*. 2003 Jul-Aug;50(52):1167-8.
2. Rui-Yun Xu, Bo Liu, Nan Lin, Therapeutic effects of endoscopic variceal ligation combined with partial splenic embolization for portal hypertension. *World J Gastroenterol* 2004 April 1;10(7):1072-1074.
3. Abraldes JG, Tarantino I, Turnes J, Garcia-Pagan JC, Rodes J, Bosch J. Hemodynamic response to pharmacological treatment of portal hypertension and long-term prognosis of cirrhosis. *Hepatology*. 2003 Apr;37(4):902-8.

: Gastrointestinal tract, hemorrhage  
Embolism, therapeutic

: 39 /

: (4 )

Dieulafoy

가

(Hb 7.6 g/dl, BP 90/50

mmHg).

: Dieulafoy lesion in stomach

가

1/3

(lesser curvature)

(Fig. 1)

(left gastric artery)

(Fig. 2,3),

(Fig. 6).

(Fig. 4,5)

5F Yashiro ( , )

3F

Microferret (Cook, Bloomington, USA)

가

(Fig. 2,3).

3/2 Tornado (Cook, Bloomington, USA) 1

가 Gelform

(Fig. 4,5).

(Fig. 6).



Fig. 1. Except for a slit-like mucosal defect, the protruding, ruptured vessel is surrounded by a normal mucosal surface without sign of ulceration.

Dieulafoy

Gallard (1884) G. Dieulafoy (1896)

T.

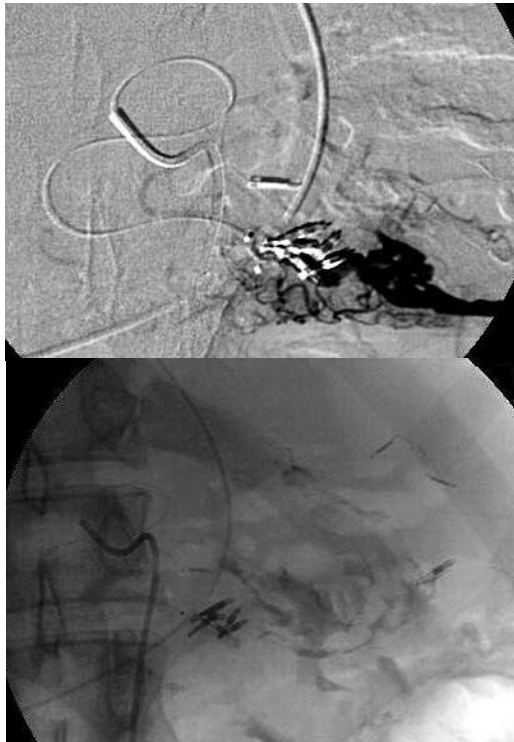


Fig. 2,3. A,B. After superselection of left gastric arterial branch, focus of bleeding is identified. Contrast media is extravasated to the lumen of stomach and gastric rugae are evident.

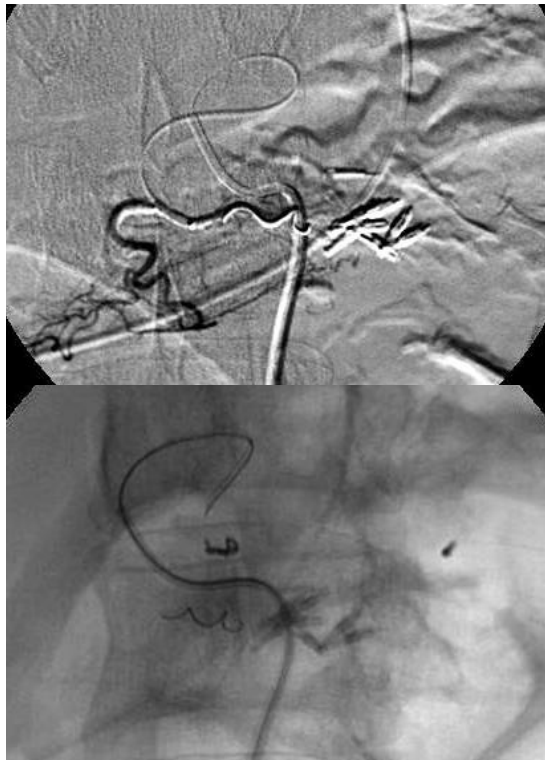


Fig. 4,5. Coil embolization is tried. 3/2 Tornado coil 3ea and gelform are applied.

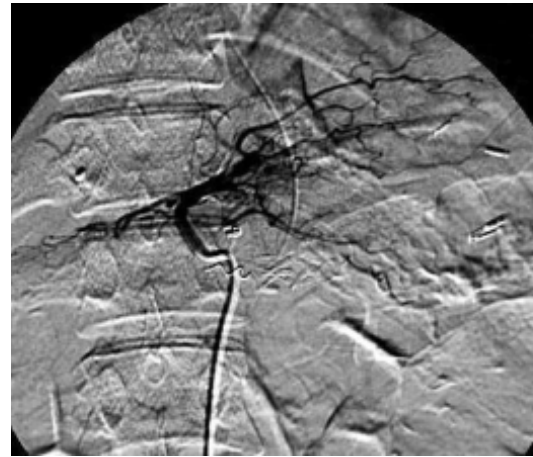


Fig. 6. After successful coil embolization, extravasation is not visible on angiography.

1. Lee KS, Moon YJ, Lee SI, Park IS, Sohn SK, Yu JS, Kie JH. A case of bleeding from the Dieulafoy lesion of the jejunum. *Yonsei Med J.* 1997 Aug; 38(4):240-4.
2. Lije C, Greiner P, Reide UN, Sontheimer J, Brandis M. Dieulafoy lesion in a one-year-old child. *J Pediatr Surg.* 2004; 39(1):133-134
3. Pitcher GJ, Bowley DM, Chasumba G, Zuckerman M. Life-threatening haemorrhage from a gastric Dieulafoy lesion in a child with haemophilia. *Haemophilia.* 2002; 8(5):719-720.



# Coil embolization for gastric ulcer bleeding from intercostal artery after esophagectomy and gastric reconstruction.

1 / 2 / 3 / 4

1 2

: Stomach, ulcer; interventional procedures  
esophagectomy  
: 70 /  
: 5

5F RH (Cook)

1

(Microferret, Cook)  
(superselection)

가 2  
(Cordis) (Cook) 1

70 mmHg, 116  
23%

(Cordis) 2 (Cook)

:

가  
(reconstructed gastric tube)

114  
54 (47%)  
3.5 %

(Fig. 1) (celiac trunk) 10.5% , 35.1%  
(right gastroepiploic artery) , 6.1%  
(stomach) (truncal vagotomy)

(feeding vessel)  
(intercostobronchial trunk)  
(Fig. 2). 가 2,

1.

, 3,  
(aortogastric fistula)4,5, (gastrotracheal fistula)6,  
(gastropericardial fistula)7 가

1

가

가

가

가

1. Motoyama S, Saito R, Kitamura M, et al. Prospective endoscopic follow-up results of re-constructed gastric tube. *Hepatogastroenterology* 2003; 50:666-669.

2. Maier A, Tomaselli F, Sankin O, et al. Acid-related diseases following retrosternal stomach interposition. *Hepatogastroenterology* 2001; 48:899-902.

3. Uchida Y, Tomonari K, Murakami S, Hadama T, Shibata O, Shirabe J. Occurrence of peptic ulcer in the gastric tube used for esophageal replacement in adults. *Jpn J Surg* 1987; 17:190-194.

4. Katsoulis IE, Veloudis G, Exarchos D, Yannopoulos P. Perforation of a gastric tube peptic ulcer into the thoracic aorta. *Dis Esophagus* 2001; 14:76-78.

5. Deutsch A A, Reisee R. Aortogastric fistula: an unusual complication of the thoracic portion of the stomach. *Arch Surg* 1978; 113:537 (letter).

6. Tsujinaka T, Ogawa M, Kido Y, Shiosaki H, Takesada M. A giant tracheogastric tube fistula

caused by a penetrated peptic ulcer after esophageal replacement. *Am J Gastroenterol* 1988; 83:862-864.

7. Shima I, Kakegawa T, Fujita H et al. Gastropericardial and gastrobrachiocephalic vein fistulae caused by penetrating ulcers in a gastric pedicle following esophageal cancer resection: a case report. *Jpn J Surg* 1991; 21:96-99.

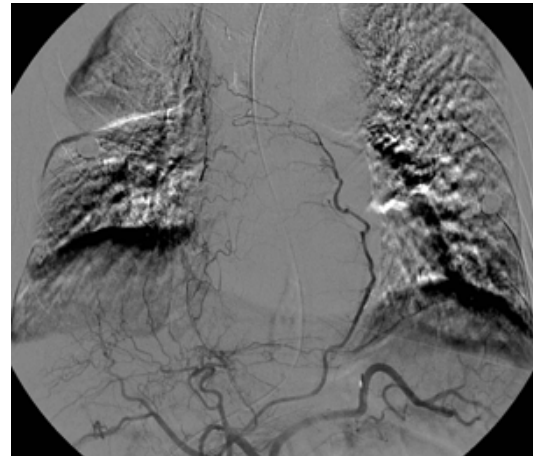


Fig. 1. Celiac trunk arteriography shows the trifurcation of replaced right hepatic artery, common hepatic artery, and splenic artery. Right gastric and right gastroepiploic arteries go through posterior mediastinum, but any bleeding site is not seen.

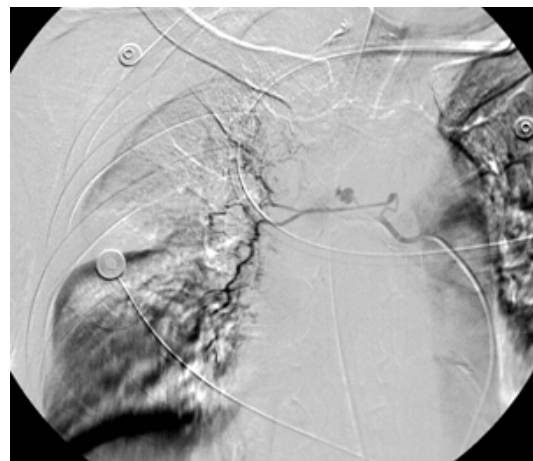


Fig. 2A. Right intercostobronchial artery originates from right side wall of aorta at the level of left main bronchus. Active contrast leakage from intercostal artery is noted.

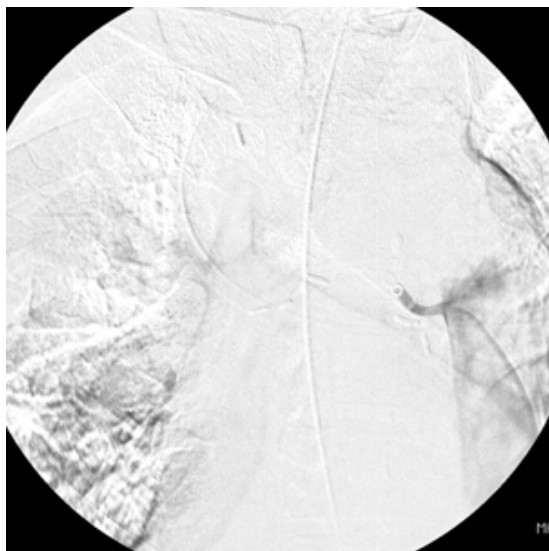


Fig. 2B. After embolization with gelfoam and microcoils, no more contrast leakage is seen.

## Embolotherapy of Gastroduodenal Arterial Bleeding by Gall bladder Cancer Invasion

: Gastrointestinal tract, Hemorrhage  
Gallbladder cancer  
Embolism, therapeutic

: 55 /

:

: GB cancer and duodenal invasion with bleeding

weiss tear,

, ( ), ,  
( , )

가

가

CT (duodenal  
bulb) (duodenal 2nd portion)  
(Fig. 1)  
(Fig. 3).

가

가

4F Yashiro ( , )

( )

(Fig. 2).

Microferret (Cook, Bloomington, U.S.A)  
( )  
(Fig. 3)

( , collateral circulation)

Tornado

(3/2) 3  
( ) Tornado 3  
(Fig. 4,5).

(Fig. 6).

1. Alaint. Drooz, Curtis A.Lewis, Timothy E. Allen et.al : Quality improvement guidelines for percutaneous transcatheter embolization. JVIR 2003 ;14;S237-S242

2. Luc Defrey, Peter vanlangenhove, Martine DeVos. et.al : Embolization as a first approach with endoscopically unmanageable acute nonvariceal gastrointestinal hemorrhage. Radiology 2001;218;739-748

3. Geoffrey S. Hastings. ; Angiographic localization and transcatheter treatment of gastrointestinal bleeding. Radiographics 2000 ;20 ;1160-1168

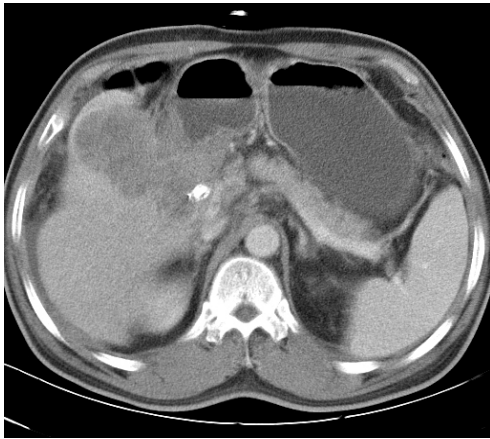


Fig. 1. Axial CT scan shows invasion of recurrent GB cancer into 1st and 2nd portion of duodenum.



Fig. 4. Gastroduodenal artery distal to the bleeding focus is embolized using Tornado Coil.



Fig. 2. Celiac angiography shows irregular narrowing of gastroduodenal artery.



Fig. 5. Proximal gastroduodenal artery is also embolized using Tornado coils.



Fig. 3. Gastroduodenal arteriography shows extravasation of contrast media.



Fig. 6. Completion angiography shows no further extravasation.

## Embolotherapy of Left Gastric Arterial Bleeding due to Metastasis of Ovarian Cancer to Lesser Sac

: Ovarian cancer

Gastrointestinal tract, Hemorrhage

Embolism, therapeutic

: 62 /

:

(perihepatic space)

(lesser

sac)

85%  
3%

5%,

:

가

CT

(Fig. 1,2)

가  
가

(Fig. 3).

coaxial microcatheter

가

4F Pigtail  
가

derlying disease

un -

(Fig. 3).RH

(Cook, Bloomington, U.S.A)가

3 F Microferret

Simmons (Cook,  
. Microferret

Bloomington, U.S.A)

gelfoam

(Fig. 4).

Microferret  
Bloomington, U.S.A)

3/2 Tornado (Cook,

(Fig. 5)gelfoam  
culation)

(collateral cir-  
(Fig. 4)

(Fig. 6).

1. Matthew P. Schenker, Richard Duszak, Jr, Michael C. Soulen, et al.Upper gastrointestinal hemorrhage and transcatheter embolotherapy : Clinical and technical factors impacting success and survival. JVIR 2001;12:1263-1271

2. Kelemouridis V, Athanasoulis CA and Waltman AC. Gastric bleeding sites : an angiographic study Radiology. 1983 ;149: 643-648

3. Rima Aina, Vincent L. Eric Therasse et. al : Arterial embolotherapy or upper gastrointestinal hemorrhage: Outcome assessment. JVIR 2001;12: 195-200



Fig. 1,2. CTscan shows huge ovarian cancer in pelvic cavity and metastatic mass in lesser sac, which invades posterior wall of the stomach.



Fig. 3. Left gastric arteriography through RH catheter shows a round ulcer crater containing extravasated contrast media.



Fig. 4. Selective angiography shows extravasation from a branch of left gastric artery.

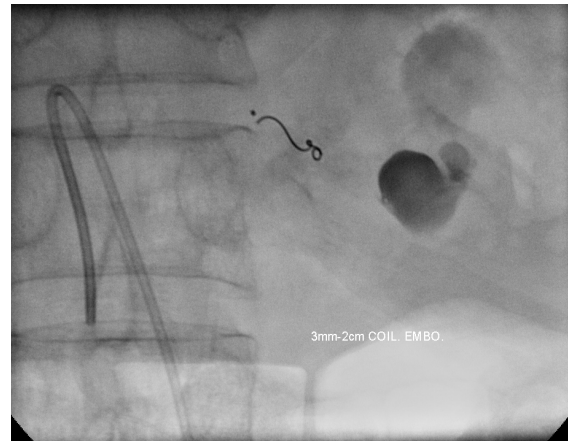


Fig. 5. 3/2 Tornado coil is deployed for embolization of a small branch of left gastric artery.



Fig. 6. Completion angiography after coil and gelfoam embolization shows no further contrast extravasation and obstructed left gastric artery.

## Transarterial Coil Embolization of Pseudoaneurysm in Chronic Pancreatitis

: Pseudoaneurysm  
Embolism, therapeutic

가

(Fig. 3b).

: 42 /

: melena

7.6, 80/60 mmHg

가

: 가

가 (40%)

(Fig. 1a,b).

(Fig. 2a,b).

, gelform  
가

79%

가

(collateral circulation)

. 4F Yashiro seldinger 4F sheath  
( )

(Fig. 2a,b), 3F Microferret (Cook,  
Bloomington, IN, U.S.A) 가  
6/2 Tornado microcoil (Cook,  
Bloomington, IN, U.S.A)

Microferret (Cook, Bloomington, IN, U.S.A)  
6/2 Tornado microcoil 가

(Fig. 3a). 7  
가

가

(Fig. 3b).

1. Lileswar Kaman, Sudip Sanyal, Somasekhar R, Menakuru, Rajinder Singh. Pseudoaneurysm of the superior pancreaticoduodenal artery, a rare cause of hemosuccus pancreaticus: report of a case. Surg today 2004; 34: 181-184

2. Takaaki Sugiki, Takashi Hatori, Toshihide Imaizumi, Nobuhiko Harada et al. Two cases of hemosuccus pancreaticus in which hemostasis was achieved by transcatheter arterial embolization. J Hepatobiliary Pancreat Surg 2003; 10: 450-454

3. Krejci T, Hoch J, Leffler J. Massive hemorrhage from a pancreatic pseudocyst into the duodenum. Rozhl Chir. 2003 Aug ;82(8) :413-7





Fig. 1a Contrast enhanced CT scan shows scattered calcification of pancreas and low density cystic lesion in body of pancreas.

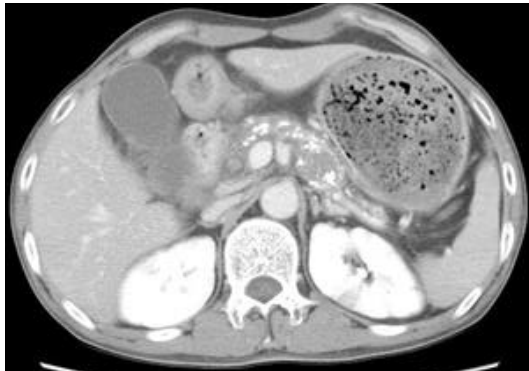


Fig. 1b Contrast enhanced CT scan shows scattered calcification of pancreas and low density cystic lesion in body of pancreas.

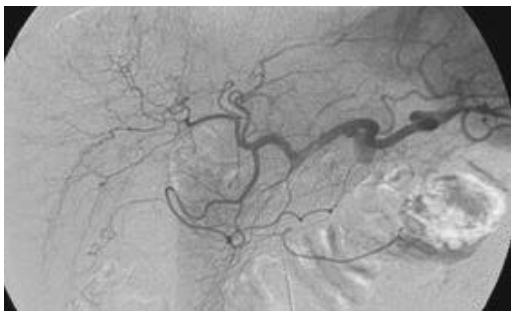


Fig. 2a Early (a) and delayed celiac angiograms (b) show pseudoaneurysm arising from splenic artery.

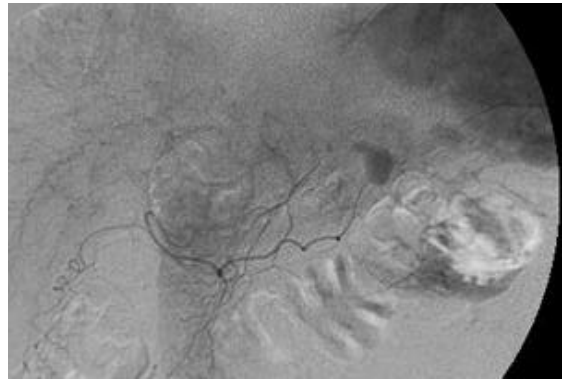


Fig. 2b Early (a) and delayed celiac angiograms (b) show pseudoaneurysm arising from splenic artery.

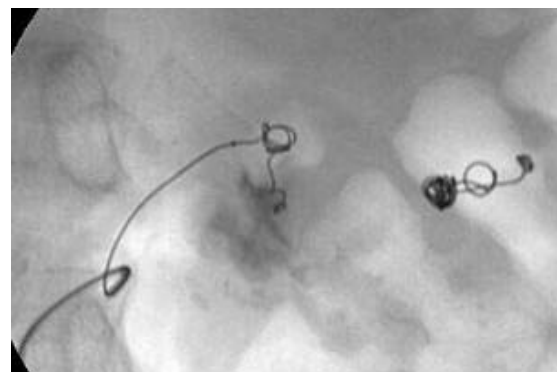


Fig. 3a Transarterial coil embolization of neck portion of pseudoaneurysm and segmental artery of splenic artery.



Fig. 3b Transarterial coil embolization of neck portion of pseudoaneurysm and segmental artery of splenic artery.

# Coil embolization of a giant gastroduodenal artery pseudoaneurysm caused by chronic pancreatitis

/ /

:Arteries, gastroduodenal.

(Fig 6).

Therapeutic blockade

Pseudoaneurysm

M/77

:

2

Hb.

7.9mg/dL

:

가

(GDA)

erosion  
erosion 가  
가  
가  
5~10% , 가  
15~20% 가  
splenic artery, gastroduodenal artery, pan-  
creaticoduodenal arteries . Visceral artery 가  
가 80%  
가 가

CT

GDA

가

가

(Fig 1) 가

5 Cm

가

가

가

GDA

(Fig 2)

(Fig 2). GDA

가

가

(Fig 3)

anterior superior  
pancreaticoduodenal artery (ASPD) right gastro-  
epiploic artery (RGEA)가 가

5F RH catheter GDA

3F microcatheter (Renegade, Boston-Scientific,  
Natick, MA, U.S.A.) co-axial anterior su-  
perior pancreaticoduodenal artery right gastroepiploic  
artery microcoils (Tornado, Cook,  
Bloomington, IN, U.S.A.) , GDA

microcatheter

Tornado microcoils (Cook)

GDA (Fig 4) SMA angiography (Fig 5)

가

. 7

CT

가

, collateral

coil 가

NBCA

1. Bakal CS, Silberzweig JE, Cynamon J, Sprayregen S. Vascular and interventional radiology: principles and practice. New York: Thieme. 2002: 359-373

2. Kaufman JA, Lee MJ. Vascular and interventional radiology: the requisites. Philadelphia: Mosby. 2004: 314-317.

3. Han MC, Park JH. Interventional radiology. Seoul: Ilchogak. 1999: 39-52.

4. Yamakado K, Nakatsuka A, Tanaka N et al. Transcatheter Arterial Embolization of Ruptured Pseudoaneurysms with Coils and n-Butyl Cyanoacrylate. J Vasc Interv Radiol 2000 11: 66-72.



Fig. 1. Enhanced abdominal CT scan shows strong enhancement of a large (approximately 5cm in diameter) pseudoaneurysm (arrow) in the pancreatic head abutting the gastroduodenal artery (arrowhead) as well as multiple parenchymal calcifications and pancreatic duct dilatation.



Fig. 2. Gastroduodenal angiography showed a large pseudoaneurysm (arrow). Gastroduodenal angiography showed a large pseudoaneurysm (arrow).



Fig. 3. An extravasation of contrast medium (arrow) through the neck of the psuedoaneurysm is well demonstrated. Bifurcation (arrowhead) of the gastroduodenal artery (GDA) to the anterior superior pancreaticoduodenal artery (ASPDA) and the right gastroepiploic artery (RGEA) is well demonstrated. An extravasation of contrast medium (arrow) through the neck of the psuedoaneurysm is well demonstrated. Bifurcation (arrowhead) of the gastroduodenal artery (GDA) to the anterior superior pancreaticoduodenal artery (ASPDA) and the right gastroepiploic artery (RGEA) is well demonstrated.

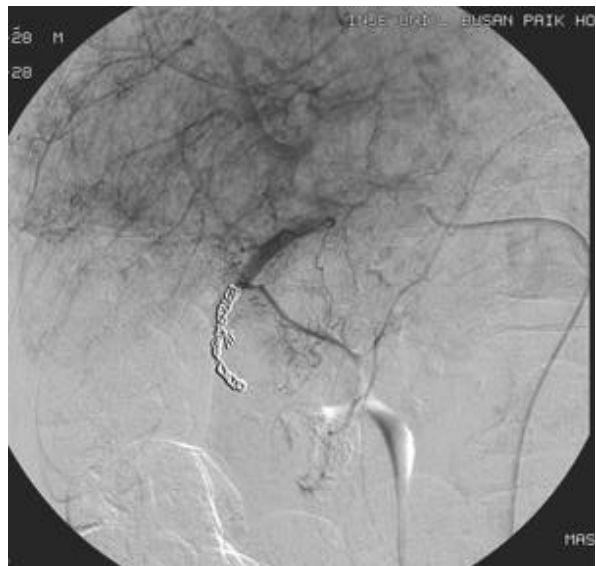


Fig. 4. Post-embolization gastrodeudenal demonstrated complete exclusion of the pseudoaneurysm. Post-embolization gastrodeudenal SMA angiography demonstrated complete exclusion of the pseudoaneurysm.

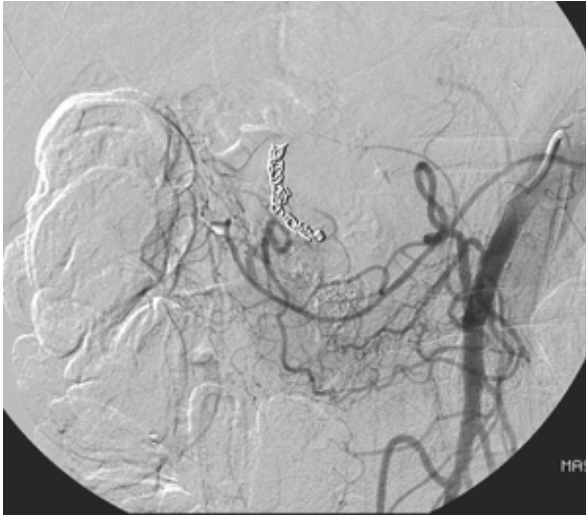


Fig. 5. Post-embolization SMA angiography demonstrated complete exclusion of the pseudoaneurysm. Post-embolization SMA angiography demonstrated complete exclusion of the pseudoaneurysm.



Fig. 6. Follow-up CT scan 1 week after embolization demonstrated complete thrombus filling in the pseudoaneurysm. Follow-up CT scan 1 week after embolization demonstrated complete thrombus filling in the pseudoaneurysm.

## Angiographic Diagnosis and Embolization of Massive Spontaneous Retroperitoneal Hemorrhage originated from Adrenal Gland

:  
: 51 /  
: Adrenal hemorrhage  
: A 51-year-old woman was brought to the emergency department by hypovolemic shock. The patient was stabilized after embolization of the adrenal artery. No adrenal insufficiency or other complications were noted.

Abdominal and pelvic CT scan showed a large retroperitoneal hematoma extending from the right upper quadrant to the pelvis (Fig 1a-b). The abdominal aortography appeared normal. Active bleeding was confirmed by leakage of contrast media from the adrenal gland on selective angiography of the right inferior phrenic artery (Fig 2-a).

The right inferior phrenic artery and two adrenal branches were embolized with microcoils (3mm to 2mm (n=5), 4mm to 2mm (n=5), 5mm to 2mm (n=3)) (VortX, Target Therapeutics Inc., USA) (Fig 2-b). The inferior adrenal artery originated from the right renal artery was intact.

Adrenal hemorrhage is a rare condition in adults, occurring in association with trauma, severe physical stress, surgery, anticoagulation therapy, septicemia,

hypotension or tumor (pheochromocytoma, metastases, carcinoma or adenoma). Vella Adrian et al. proposed a mechanism of the susceptibility of adrenal gland to massive intraglandular bleeding which is probably related to the complex vascular supply. Although high resolution CT scan or MRI is sensitive for investigation of retroperitoneal hemorrhage, adrenal hemorrhage could be overlooked in the presence of massive retroperitoneal hemorrhage. As seen in this case, even thoracic or abdominal aortography may not reveal the bleeding from the small distal branches which supply the terminal organs or tissue. Therefore careful investigation of each systemic arterial branches is required. Selective angiography of adrenal gland should be included in evaluation of massive retroperitoneal hemorrhage by unknown origin. Furthermore the bleeding can be successfully treated by transarterial embolization.

1. Akira Kawashima, Carl M, Sandler, et al. Imaging of Nontraumatic Hemorrhage of Adrenal Gland. *Radiographics* 1999;19:949-963

2. Hoeffel, C., Legmann, P., Luton, J.P., et al. Spontaneous Unilateral Adrenal Hemorrhage: Computerized Tomography and Magnetic Resonance Imaging Findings in 8 Cases. *The Journal of Urology* 1995;154:1647-1651

3. Igwilo, Obinna C., Sulkowski, Robert J., Shah, Manoj R., et al. Embolization of Traumatic Adrenal Hemorrhage. *The Journal of Trauma* 1999;47:1153-1158

4. Dinc, H., Simsek, A., Ozyavux, R., et al. Retroperitoneal Haemorrhage due to Inferior Adrenal

Injury: A Case Report. Acta radiologica 2002;43:326-328

5. Vella, Adrian., Nippoldt, Todd B., Morris, John C. III. Adrenal Hemorrhage: A 25-Year Experience at the Mayo Clinic. Mayo Clinic Proceedings 2001;76:161-168



Fig. 1 a,b. A large retroperitoneal hematoma extending from the right upper quadrant to the pelvis is shown.

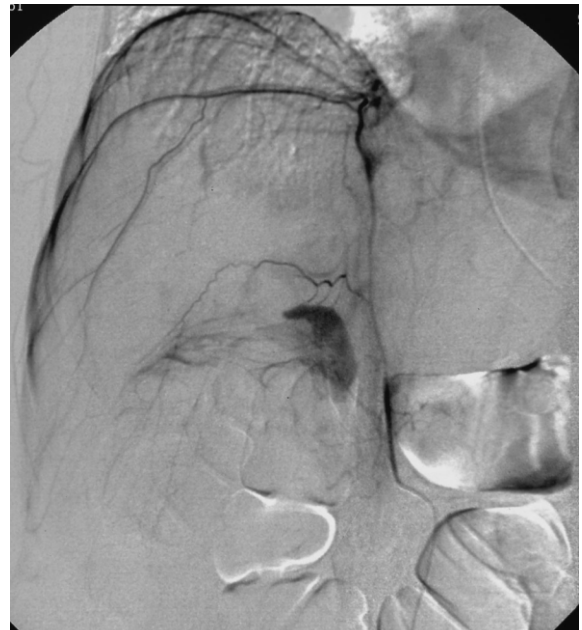


Fig. 2a. A leakage of contrast media from the adrenal gland on selective angiography of the right inferior phrenic artery is shown.



Fig. 2b. The right inferior phrenic artery and its adrenal branches are embolized with microcoils.

: Uterine arteries  
 Embolization, uterus  
 Myoma, uterus  
 : 32 /  
 :

MRI 5.8 x 4.9 x 5.6 cm (83.3

cc)

. 3Fr Microcatheter (Renegade, Boston, USA), Polyvinyl alcohol particle (350-500 µm)

cer -  
 vicovaginal branch lower uterine segment

2

6

40% . 6  
 MRI , 3.7 x 3.6 x 4.0 cm (27.9cc)

66.5 %

40.7 %

MRI



Fig. 1a. Preprocedural MRI On T2-weighted sagittal image (1-a) and gadolinium enhanced T1-weighted image (1-b), submucosal myoma is demonstrated in uterine fundus with contrast enhancement.



Fig. 1b. On T2-weighted sagittal image (1-a) and gadolinium enhanced T1-weighted Image (1-b), submucosal myoma is demonstrated in uterine fundus with contrast enhancement.





40  
(hysterectomy)  
3 1  
15  
25%  
6  
1995 Ravina  
가 , Goodwin ,  
84-90 % 가  
Walker 400  
84%가  
, 97%가  
1%  
1. Ravina JH, Herbreteau D, Ciraru-Vigneron N,  
et al. Arterial embolisation

to treat uterine myomata. Lancet, 1995; 346:  
671-672  
2. Worthington-Kirsch RL, Popky GL, Hutchins FL.  
Uterine arterial  
embolization for the management of leiomyomas:  
Quality-of-Life  
assessment and clinical response. Radiology, 1998;  
208:625-629  
3. Goodwin SC, McLucas B, Lee M, et al. Uterine  
artery embolization for the  
treatment of uterine leiomyomata; midterm results.  
JVIR, 1999; 10:1159-1165  
4. Walker WJ, Pelage JP. Uterine artery embolisation  
for symptomatic fibroids: clinical results in 400 women  
with imaging follow up. BJOG. 2002  
Nov;109(11):1262-72.  
5. Spies JB, Ascher SA, Roth AR, Kim J, Levy EB,  
Gomez-Jorge J.  
Uterine artery embolization for leiomyomata. Obstet  
Gynecol. 2001;98(1):29-34.

## / / / / /

Renal arteries, stent or prosthesis

•

•

, crea -

1.2mg/dl

1

DTPA

(Fig.5)

2 11-39%

9cm

(Fig.3).

90%

mm, "Osteal stenosis", 10% 1cm "proximal stenosis".

1) degree of luminal narrowing (50-75%), 2) post-stenotic dilatation, 3) slow flow distal to the lesion, 4) the presence of collateral circulation, and 5) decreased renal mass

가 10mmHg

가

90% , delayed nephrogram

heparin 3000 IU

0.038inch Stiff ter -

5mm.

4cm balloon cathe-

6mm

90%

170/100mmHg    Adalat 60mg 1T qid

2

150/90mmHg

1) residual

osteal lesion

pre -

Osteal lesion      가

.가

1.5-2cm 가

plaque

30%

가 가

5-7mm

mm

6

CT,  
osteal stenosis  
가

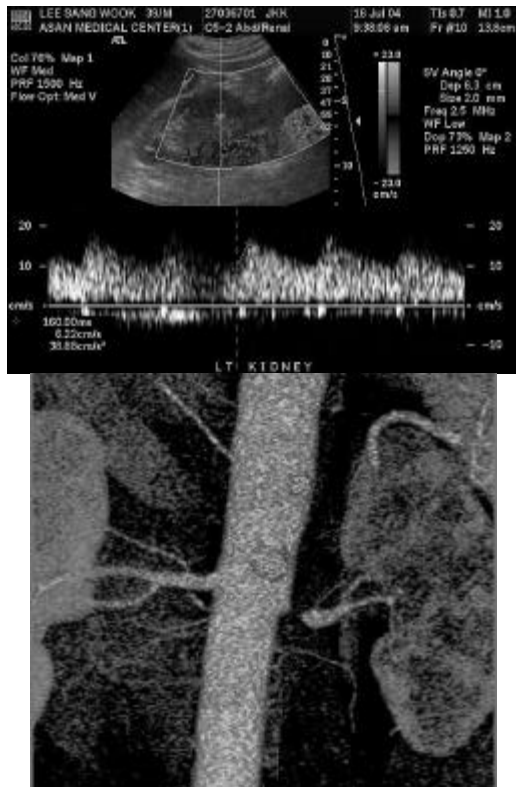


Fig.1. The figure on the left shows tardus-parvus wave-forms and delayed-dempened upstroke on Doppler US and severe stenosis at osteum of Lt.renal artery(more than 90% diameter stenosis) on 3D CT(bottom).

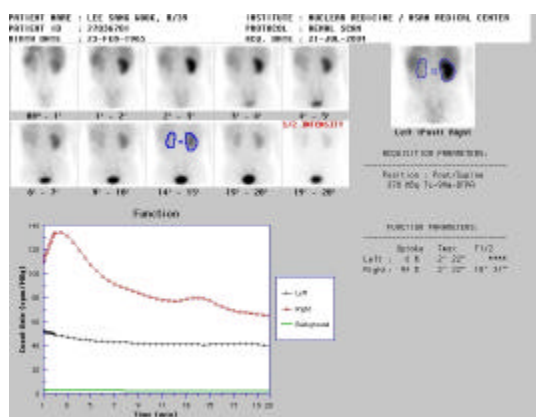


Fig.2. Kideny scan(DTPA) show severely decreased function of left kidney,measured relative function is 6%.



Fig.3. Aortogram and renal angiography demonstrate severe osteal stenosis of Lt.renal artery(more than 90% diameter stenosis).

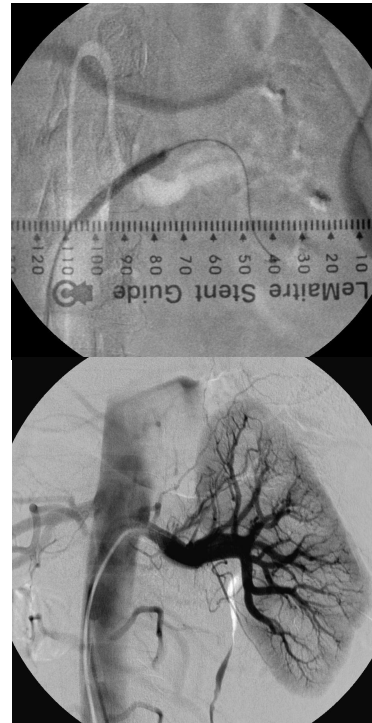


Fig.4. The figure on the left demonstrate ballooning procedure. After stent deployment, patent flow via stent is noted(right)

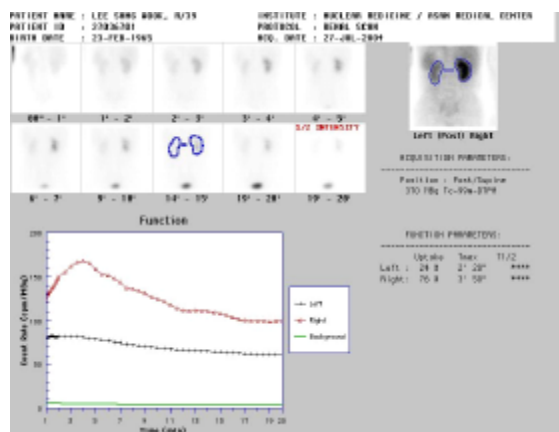


Fig.5. DTPA renal scan after stent placement show slightly improved function of left kidney, measured function is 24%.

1. John A.Kaufman. Renal arteries. In John A.Kaufman, Michael J.Lee. Vascular & Interventional Radiology : the requisites. 1st ed. Philadelphia: Mosby, 2004 : 323-349

2. Viado Perkovic, Ken R Thomson, Peter J Mitchell, et al. Treatment of renovascular disease with percutaneous stent insertion: Long-term outcomes. Australasian Radiology 2001;45:438-443

3. Tuttle KR, Chouinard RF, Webber JT et al. Treatment of atherosclerotic ostial renal artery stenosis with the intravascular stent. Am J Kidney Dis 1998;32:611-622

# Treatments of atherosclerotic stenoses of the iliac and renal arteries using stents.

Interventional procedures  
Arteries, iliac  
Renal arteries, stenosis or obstruction  
Renal arteries, transluminal angioplasty  
M/65  
TIA CABG  
claudication  
BUN/creatinin  
10/1.7 (CFA)  
(IA)  
femoro-pop-  
liteal bypass  
(LRA)  
CT:  
(CIA)  
(Fig 1).  
(EIA)  
IA stent  
LRA stent  
aorta가  
CFA US 8F sheath  
5F Cobra catheter 0.035-inch-di-  
ameter hydrophilic guide wire (Radifocus, Terumo,  
Tokyo, Japan) aorta negotiation 5F pigtail  
catheter pelvic angiography  
(Fig 2). IA가  
EIA-CFA  
3가가 IA 9mm x 61mm  
Wall stent (Boston-Scientific Natick, MA, U.S.A.)  
8mm x 80mm SMART stent (Cordis, Miami, FL, U.S.A.)  
8mmx 40mm balloon catheter  
(FOX PTA, Abott Vascular, Beringen, Switzerland)  
Stent IA 가  
(Fig 3). IA stent 8F sheath가  
CFA 8F renal guiding cathe-  
ter (RDC II, Cordis) angiog-  
raphy LRA (Fig  
4). 60%  
5F Cobra catheter Radifocus guide wire co-axial  
LRA , Guide  
wire LRA  
catheter가 . 0.035 inch hy-  
drophilic guide wire stent delivery system  
(SDS) Cobra  
catheter Simons I Catheter  
가 .  
가  
가 LRA  
2 (10cc/hr) cre-  
atinin 2.3 가  
LRA stent  
7F sheath  
Sheath 100cm 6F guiding catheter (MP  
A-1, Cordis) LRA 5F  
Cobra catheter 260cm radifocus guide wire co-ax-  
ial LRA catheter guide  
Catheter guide wire 6mm x 135cm  
SDS 6mm x 27mm balloon expandable stent  
(Express LD, Boston-Scientific)  
stent . Stent angiography

BUN/Creatinin 10/1.1

(aortaography, CTA, MRA)      renal artery가 aorta

sion      ileofemoral occlusion      ,      , in -

catheter catheter negotiation 가 ,

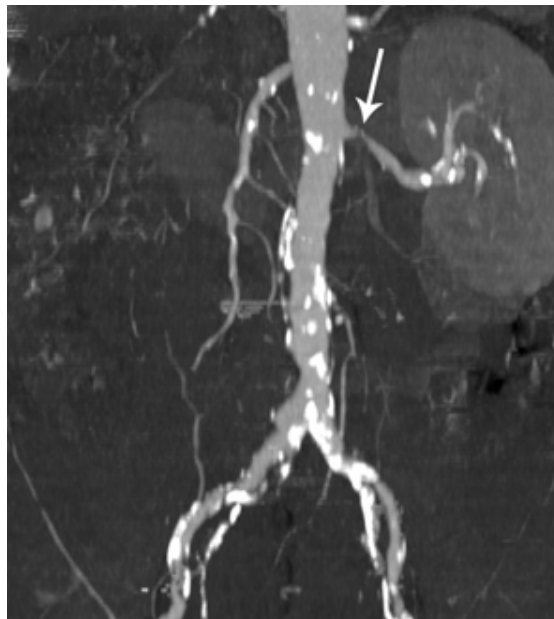
가 left brachial

fossa, mid-humerus high access

Sprayregen S. Vascular and interventional radiology.

tional radiology, the requisites. 1st ed. Philadelphia:

in diagnosis, treatment and management. Workshop



the aorta and its branches. Severe caudal angulation of the left renal artery is evident as well as a focal severe stenosis (arrow) at its proximal portion. There are multifocal iliofemoral arterial stenoses. A short segmental occlusive lesion (arrowhead) at the distal of the right external iliac artery is evident.



ment of atherosclerotic changes of aortoileofemoral arteries. There are multifocal stenoses at the right iliac artery. A severe stenosis (arrow) at the distal of the right external iliac artery is well seen.

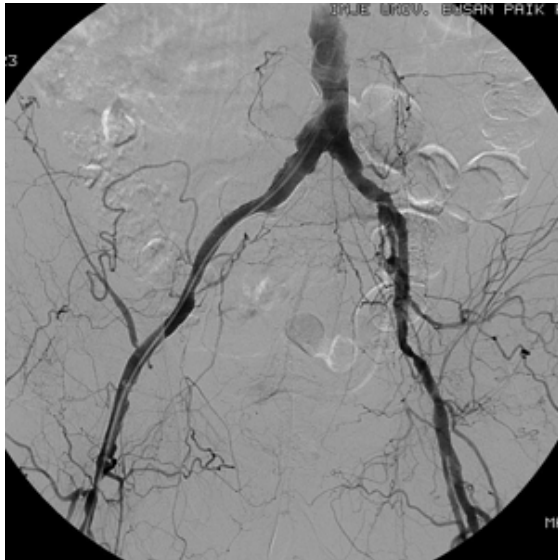


Fig. 3. After placements of two metallic stents into the right iliofemoral artery, improvement of a flow of contrast medium through the artery is evident.



Fig. 5a. A 6mm x 27mm balloon expandable stent loaded in a 135Cm long SDS was inserted astride the stenosis over a guide wire through a 6F guiding catheter



Fig. 4. Aortography via a 8F guiding catheter well demonstrates a focal stenotic lesion at the proximal of the caudally angulated left renal artery. Aortography via a 8F guiding catheter well demonstrates a focal stenotic lesion at the proximal of the caudally angulated left renal artery.

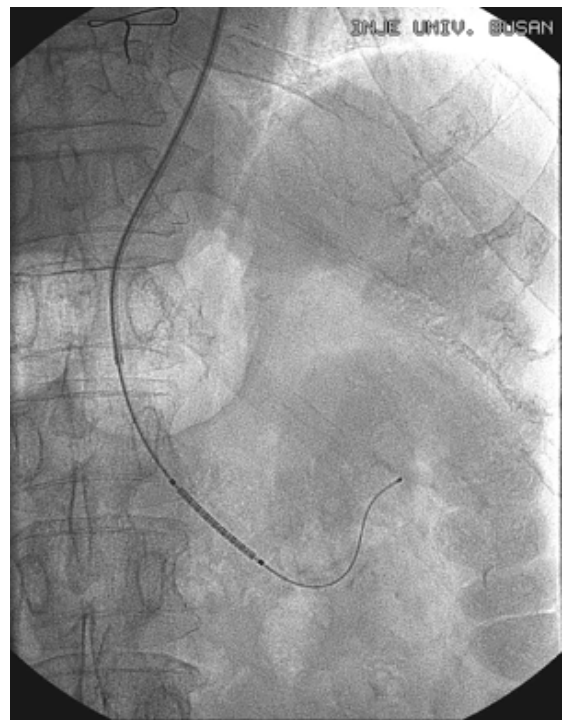


Fig. 5b. After placements of the stent, improvement of a flow of contrast medium through the left renal artery is evident.

: Biopsies, technology. Kidney, biopsy.

: 72 /

: 5 left middle cerebral artery infarction

2 serum BUN,  
creatinine 가

가 가

가 가

가

serum BUN, creatinine 가  
tracheostomy

가

가

: Renal failure of unknown origin

가 가

가 가

puncture 가

(Fig.1) 18

gauge (Transjugular Quick-Core needle biopsy set, Cook, Bloomington, Ind)

(Fig.2). 7

mesangial proliferative glomerulonephropathy

4

1. Mal F, Meyrier A, Callard P et al. Transjugular renal biopsy. Lancet 1990 Jun 23;335(8704):1512-3

2. Sam R, Chebrolu SB, Reyes CV et al. Transjugular renal biopsy in an unconscious patient maintained on mechanical ventilation. Clin Nephrol 2003 Jul;60(1):53-7

3. Abbott KC, Yuan CM, Batty DS, Lane JD, Stiles KP. Transjugular biopsy in patients with combined renal and liver disease: making every organ count. Am J Kidney Dis 2001 Jun;37(6):1304-7

4. Cluzel P, Martinez F, Bellin MF et al. Transjugular versus percutaneous renal biopsy for the diagnosis of parenchymal disease: comparison of sampling effectiveness and complications. Radiology 2000 Jun;215(3):689-93

. 1990

가

가





Fig. 1. Left renal venogram via transjugular approach shows vascular structure. Left renal venogram via transjugular approach shows vascular structure.

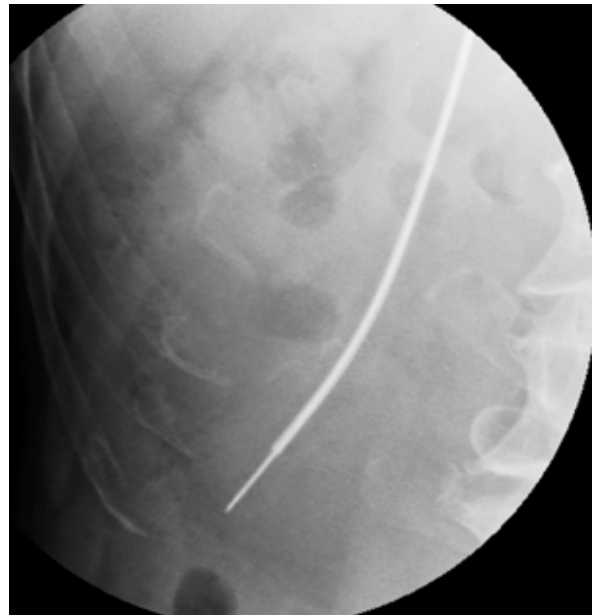


Fig. 2. After renal venogram was done, lower pole area was punctured via 18-gauge transjugular liver biopsy needle. After renal venogram was done, lower pole area was punctured via 18-gauge transjugular liver biopsy needle.

# Case 36

## Separate Stent-graft for AAA with right common iliac artery occlusion

: AAA / stent-graft / aorto-uni-iliac

: 56

: AAA with right common iliac artery occlusion

: 10 RA

가

. 3

. 20

, 가 가 가

IPF

at both lower lung field with cicatrical bronchiectasis,  
right middle lobe pneumonia, IPF

enlarged intrapulmonary lymph node가 . SMA

tortuous aorta 5cm

가 thrombosis .

Aneurysm 5cm

left common iliac artery . right

common iliac artery

multiple collaterals가 external iliac artery

collaterals reconstitution . Volume

rendering image proximal neck angle 100 ,

distal neck angle 60

7cm . Distal neck angula-

tion 2cm

5-F vascular sheath (COOK,  
Bloomington, In, USA) , 5-F pigtail

catheter (Royal Flush II, COOK, Bloomington In, USA)

stiff guidewire

(Lunderquist stiff, COOK, Bloomington, In, USA)

aorto-uni-iliac

stent-graft

stent-graft

24mm 12mm

12mm 2cm가

stent-graft 12mm 9cm

stent-graft 24mm 1cm

가 Dacron graft . Stiff guidewire

5-F vascular sheath 12-F dilator

tract stent-graft

stent-graft

가 2cm

stent-graft stent-graft 2cm 가

. stent-graft 가 30mm

large occlusion balloon catheter (Medi-Tech, Cork,  
Ireland) stent-graft

. Stent-graft

stent-graft aneurysmal sac

가 1 CT

type II endoleak

3 6 (CT) 가 collateral

vessel aneurysmal sac

aneurysmal sac . stent-graft

3 leukocytosis 38

to-uni-iliac type

. Aorto-uni-iliactype

Onyx (ethylene vinyl alcohol copolymer; Micro Therapeutics, Irvine, CA), Glue , Gianturco coil (COOK, Bloomington, In, USA)

aor -  
to - uni - iliac stent - graft  
collateral vessel  
type II endoleak 가  
Stent - graft stent - graft  
aneurysmal sac contrast filling . 1 , 3 , 6  
CT collateral vessel aneurysmal  
sac retrograde filling . Stent - graft  
, stent - graft  
가 stent - graft  
가 . Type II endo -  
leak stent - graft 가 가  
type II endo -  
leak  
EUROSTAR study type II endoleak  
aneurysmal sac 가 가  
0.52%, endoleak 0.25%  
가 Kasirajan type  
II endoleak , aneurysmal sac 가  
( 가 ) 가  
collateral coil embolization, CT - guided  
puncture, laparoscopic ligation  
Filis aneurysmal neck angulation proximal and  
distal angulation , proximal neck  
angulation  
secondary intervention 가  
proximal angulation  
neck length가 proximal angulation  
distal angulation stent - graft  
type I en -  
doleak 가 secondary intervention 가  
Stent - graft  
inflammatory reaction Hayoze  
neu -  
trophil cytokine reaction 가

1. Lee DY, Kang SG, Choi DH, et al. Percutaneous modular stent-grafts in the treatment of abdominal aortic aneurysms. J Endovasc Ther 2003;10:752 - 759.

2. Kasirajan K, Matteson B, Marck JM, Langsfeld M. Technique and results of transfemoral super-selective coil embolization of type II lumbar endoleak. J Vasc Surg 2003;38:61 - 6.

3. Filis KA, Arko FR, Rubin GD, Raman B, Fogarty TJ, Zarins CK. Aortoiliac angulation and the need for secondary procedures to secure stent graft fixation: Which angle is important? Intervent Angiol 2002;21(4):349 - 354

4. Hayoz D, Do DD, Mahler F, Triller J, Spertini F. Acute inflammatory reaction associated with endoluminal bypass grafts. J Endovasc Surg 1997;4:354 - 360.

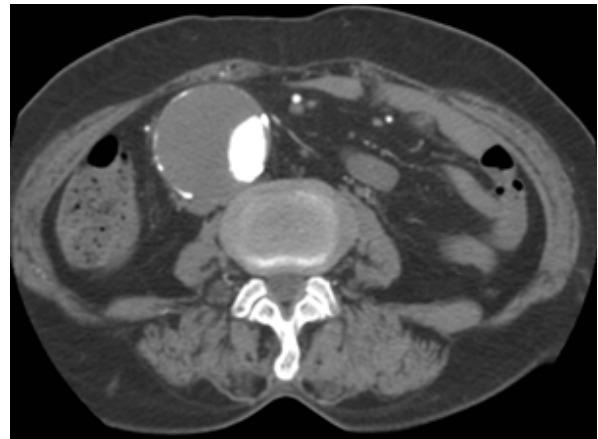


Fig. 1. Axial CT scan shows AAA with luminal thrombosis. Interventional Radiology

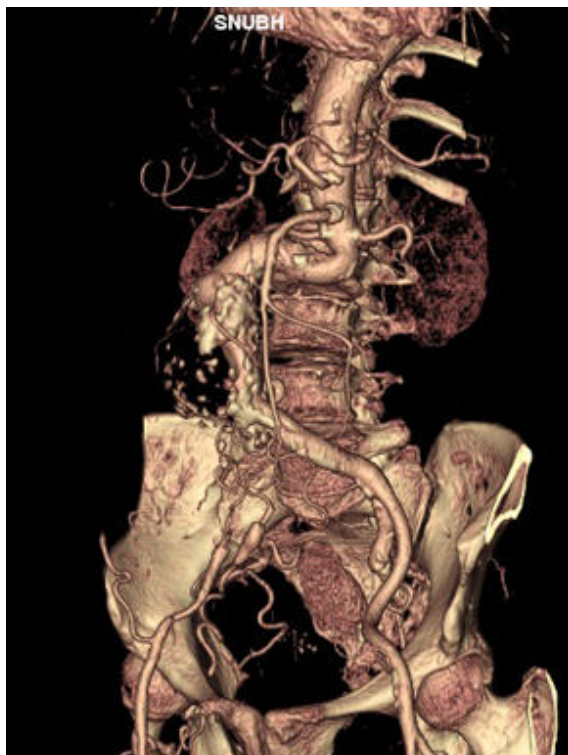


Fig. 2. Volume rendering image shows severe angulation in aneurysmal neck.

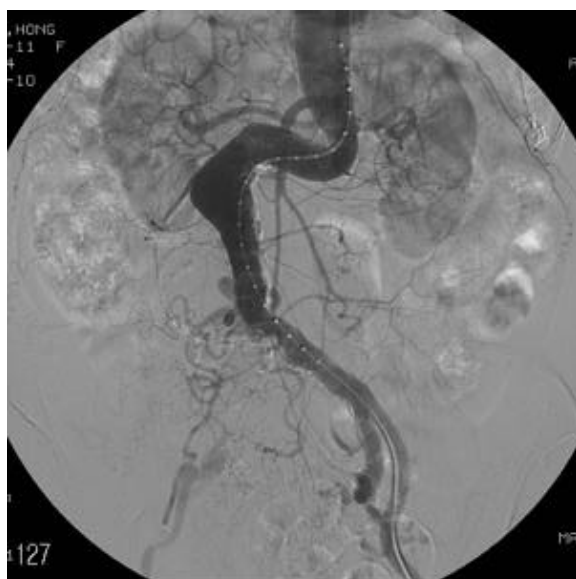


Fig. 3. DSA shows thrombosed aneurysm, and complete occlusion of right common iliac artery with multiple collateral vessels.

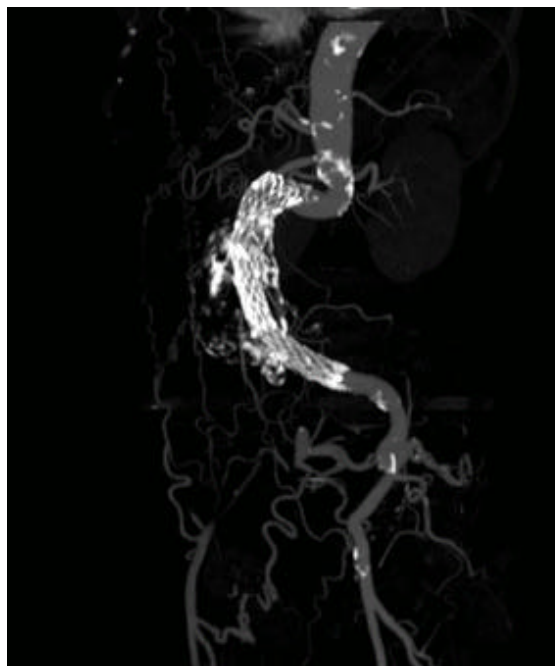


Fig. 4. MIP image obtained one week after stent-graft placement, shows aorto-uni-iliac stent-graft in abdominal aorta and left common iliac artery

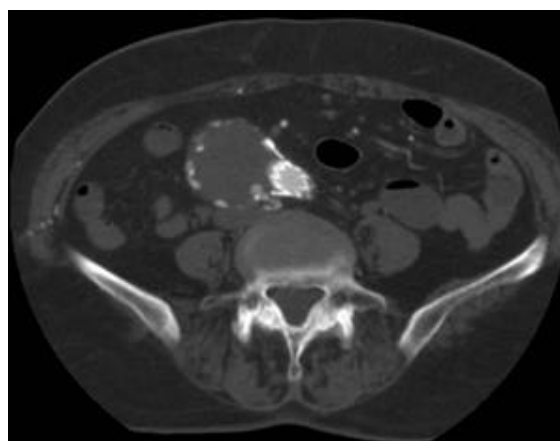


Fig. 5. Axial CT scan show retrograde filling (type II endoleak) of contrast media to aneurysmal sac through collateral vessel. Axial CT scan show retrograde filling (type II endoleak) of contrast media to aneurysmal sac through collateral vessel.

# Treatment of a arterioenteric fistula between the right external iliac artery and the sigmoid colon using a stent graft.

: arterioenteric fistula  
hemorrhage  
endovascular repair  
stent graft  
: 38  
: 3

가  
(hematochezia)

80/60  
100

CT S

(Fig 1).

CFA 8F sheath  
Cobra catheter 0.035 hydrophilic guide wire  
(Terumo, Tokyo, Japan)  
4~9mmx 48mm balloon expandable stent graft  
(peripheral stent graft, Jomed) 7mmx60mm balloon  
catheter (FOX PTA Catheter Abbott Vascular, Beringen,  
Switzerland) guide wire

balloon catheter stent graft

CIA

(Fig. 3).

가

CIA EIA  
(Fig. 4),

가 CFA sheath가

가

. 20 CT  
stent graft

stent graft stent  
graft가

가

(CFA)  
(SMA)

(IMA)  
가

IMA가 가  
가

reflux  
(EIA)

IMA

IMA

EIA S  
(Fig 2).

(CIA)  
가

stent graft

CFA 8F Balkin sheath (Cook)

CIA

CIA가

sheath

sheath가

가

stent graft stiffness

Arterioenteric fistula (0.4 - 2.4%)

fistula

가

가

arterioenteric fistula  
aortoduodenal fistula

morbidity (5 - 10%) mortality

(25 - 90%)가

stent graft

stent graft

stent

. Arterioenteric fistula  
stent

,

- 15



rv



Fig. 3b. Post-procedure angiography demonstrated complete exclusion of the fistula.

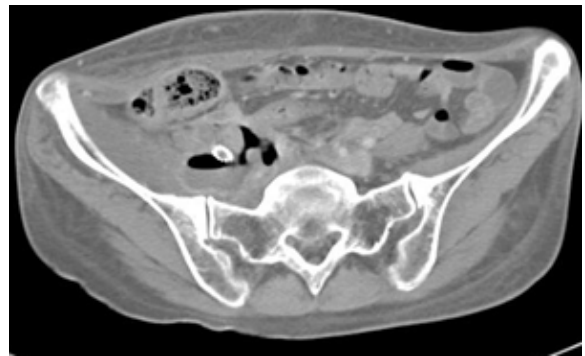


Fig. 5. Follow up CT after 20 days demonstrates the remaining collection in the pelvic cavity and the stent placed in the right iliac artery. The lumen of the stent appear to be occluded.



Fig. 4. Aortography demonstrated retarded flows through iliac arteries on both sides. No evidence of leakage of contrast through collaterals.

## Internal iliac arteriovenous fistula complicated after Lumbar-spine operation : treatment with PTFE stent-graft

Arteriovenous fistula, PTFE stent graft

51 / 7 5 1 4 4 5 4 5 가 4

artery) CT (left internal iliac (arteriovenous fistula)가

(Fig 1).

9F (introducer sheath  
Cook, Bloominton, IN, USA), 5F  
(Cook, Bloominton, IN, USA) (left common  
iliac artery)

(Fig 2).

Juan C. Parodi 가  
29 24  
83% 23 graft patency가  
PTFE

가 가 가

(Fig 4). 0.35"Amplatz (Boston scientific,  
Watertown, MA, USA)  
10 x 30mm 가  
(self-expnadable) PTFE  
(polytetrafluoroethylen stent - graft  
)  
5). 1 CT (Fig 6).

1. Lee KH, Park JH, Chung JW, et al. Vascular complications in lumbar spinal surgery: percutaneous endovascular treatment. Cardiovascular and Interventional Radiology. 200023(1):65-69

2. Juan C. parody, Claudio schonholz, Luis M. Ferreira, et al. Endovascular stent-graft treatment of traumatic arterial lesions. Annals of Vascular Surgery 1999;13:121-129



3. E. Santos, V. Peral, M. Aroca, et al. Arteriovenous fistula as a complication of lumbar disc surgery: case report *Neuroradiology* 1998;40:459-461

4. D. H. A. Mc Carter, R. D. Johnstone, G. C. McInnes, et al. Iliac arteriovenous fistula following lumbar disc surgery treated by percutaneous endoluminal stent grafting

*British Journal of Surgery* 1996;83:796-797

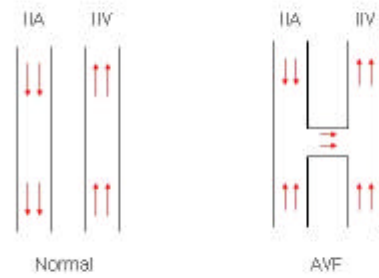


Fig 3. Diagram of blood flow at internal iliac artery, vein and AVF

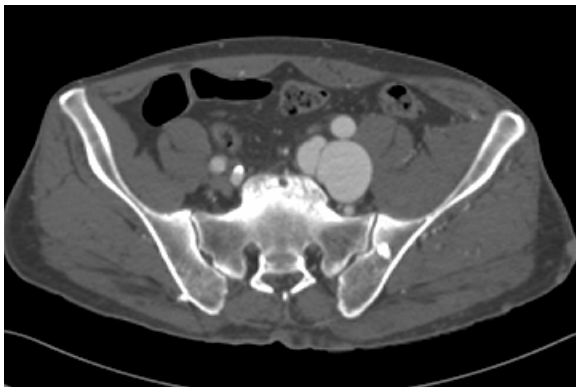


Fig. 1. Contrast enhanced CT scan shows left internal iliac arteriovenous fistula (AVF) (short arrow) and marked dilatation of Lt internal (long arrow) and external iliac vein. Dilated collateral vein is also noted in Lt subcutaneous layer.



Fig. 4. Arteriogram in left external iliac artery. Early venous drainage via AVF (arrow) from distal portion of internal iliac artery that supplied by collateral from external iliac artery.

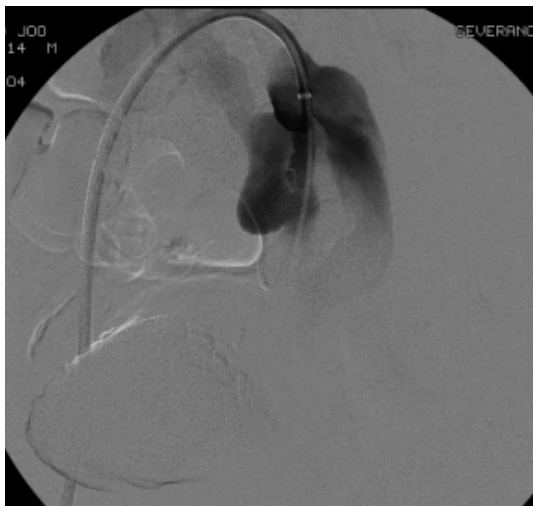


Fig. 2. Arteriogram in left common iliac artery. Left internal iliac AVF (arrow) and early venous drainage to left common iliac vein is noted.

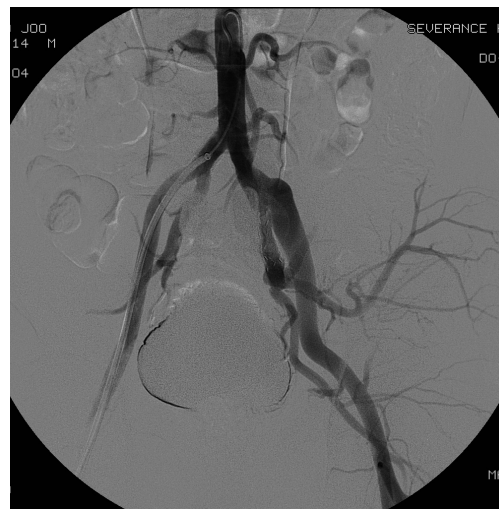


Fig. 5. Aortogram immediate after stent graft insertion. Complete exclusion of AVF and no blood flow into the internal iliac vein are shown.



Fig. 6. 1 month follow up CT after stent graft insertion. Normalization of left internal iliac vein and disappearance subcutaneous collateral vein are noted.

Stent-graft Placement for Isolated Iliac Artery Aneurysm

: Artery, graft and protheses

1.5 - 2

Aneurysm, iliac

: 85 /

:

CT

가

. 가

: Isolated iliac artery aneurysm, right.

3 cm3

5 cm

3cm

가

가

CT

5.2 cm

가

(neck) 1.2

가

cm

2 cm

(Fig. 1, Fig. 2).

2cm

3cm

가

(neck)

가

가

pig tail catheter

F sheath

12mm

, 6 cm

( 5

mm bare stent)

(S & G Biotech,

Seoul, Korea)

, endoleak

12x40mm  
(XXL ;Boston Scientific, Watertown,  
MA, USA)

(Fig. 3).

(Fig. 4)

1

CT

(Fig 5).

가

10 - 20 %

(isolated iliac ar -  
80 - 90%

tery aneurysm)

70

10

10

1. Minato N, Itoh T, Natsuaki M, Nakayama Y, Yamamoto H. Isolated iliac artery aneurysm and its management. Cardiovasc Surg 1994; 2:489-494.

2. Parsons RE, Marin ML, Veith FJ, Parsons RB, Hollier LH. Midterm results of endovascular stented grafts for the treatment of isolated iliac artery aneurysms. J Vasc Surg 1999; 30:915-921.

3. Fahrni M, Lachat MM, Wildermuth S, Pfammatter T. Endovascular therapeutic options for isolated iliac aneurysms with a working classification. Cardiovasc Intervent Radiol 2003; 26:443-447.

4. Sahgal A, Veith FJ, Lipsitz E, et al. Diameter

changes in isolated iliac artery aneurysms 1 to 6 years after endovascular graft repair. J Vasc Surg 2001; 33:289-284; discussion 294-285.

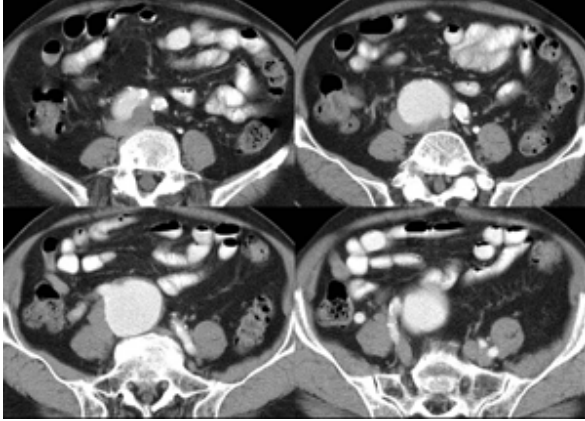


Fig. 1. Pelvic CT scan demonstrates a saccular aneurysm originated from right common iliac artery.



Fig. 2. Aortogram shows the aneurysm and its proximal neck.

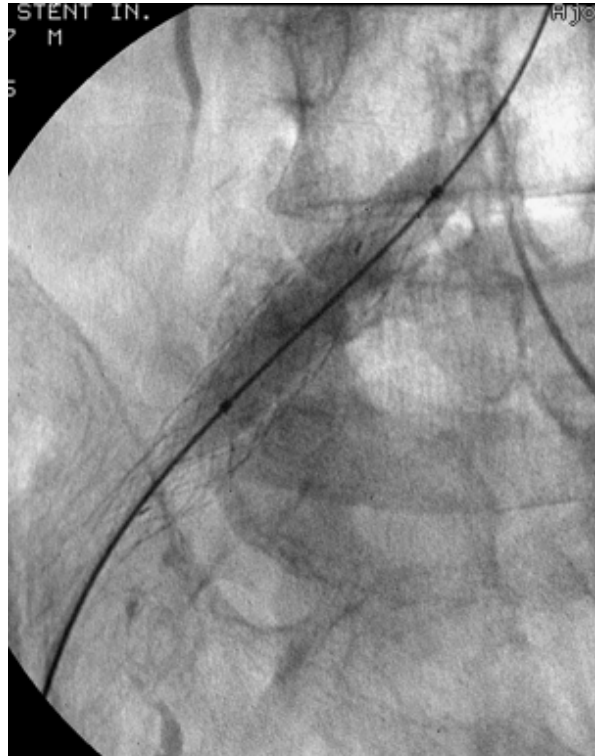


Fig. 3. Stent-graft (12x60 mm) is deployed in right common iliac artery and then angioplasty is performed with 12 mm x 4cm balloon.



Fig. 4. On follow-up angiogram after stent-graft placement, complete exclusion of the aneurysm is identified.

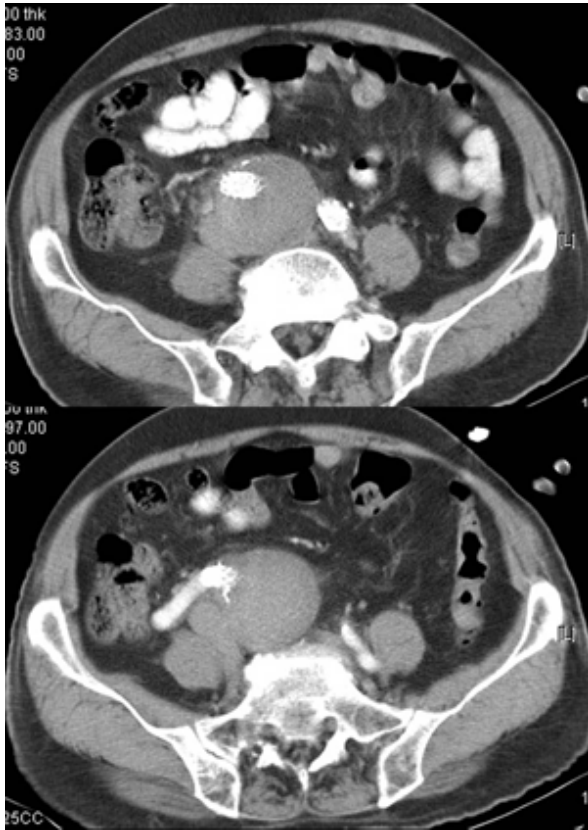


Fig. 5. Follow-up pelvic CT scan revealed complete thrombosis in the aneurysm without endoleak.

: Interventional procedure, complication

Arteries, iliac

Arteries, injuries

Stent and prosthesis

: 60

: Iatrogenic right external iliac artery rupture  
by vascular sheath

:

stent

6F, 25cm

159/87mmHg

74/52mmHg

(Fig 1),

covered stent

가

가

9F

loading TIPS covered stent (10mmx50mm, ,  
)

(Fig 2).

stent 6F

(Fig. 3).

, anterior pararenal sapce  
(Fig 4A &

B), covered stent

(Fig 4C).

가 가

1. Boontje AH. Iatrogenic arterial injuries. J Cardiovasc Surg(Torino) 1978 19:335-340.

2. Lazarides MK, Tsoupanos SS, Georgopoulos SE, Chronopoulos AV, Arvanitis DP, Doundoulakis NJ, et al. Incidence and patterns of iatrogenic arterial injuries. A decade's experience. J Cardiovasc Surg(Torino) 1998;39:281-285.

3. Cormier F, Ayoubi A, Laridon D, Melki JP, Fichelle JM, Cormier JM, et al. Endovascular treatment of iliac aneurysms with covered stents. Ann Vasc Surg 2000;14:561-566.

4. Parody JC, Schonholz C, Ferrira LM, Bergan J.

Endovascular stent-graft treatment of traumatic arterial lesions. *Ann Vasc Surg* 1999;3:121-129.

5. Martin ML, Veith FJ, Panetta TF, Cyamom T, Sanchez LA, Schwartz ML, et al. Transluminally placed endovascular stented graft repair for arterial trauma. *J Vasc Surg* 1994;20:466-473.

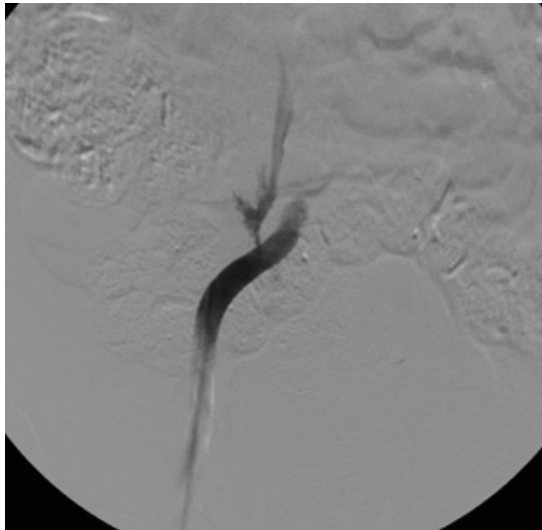


Fig. 1. Arteriogram shows contrast material leakage from the right external iliac artery.



Fig. 2. The 10x50mm covered stent is deployed along the right common and external iliac arteries.

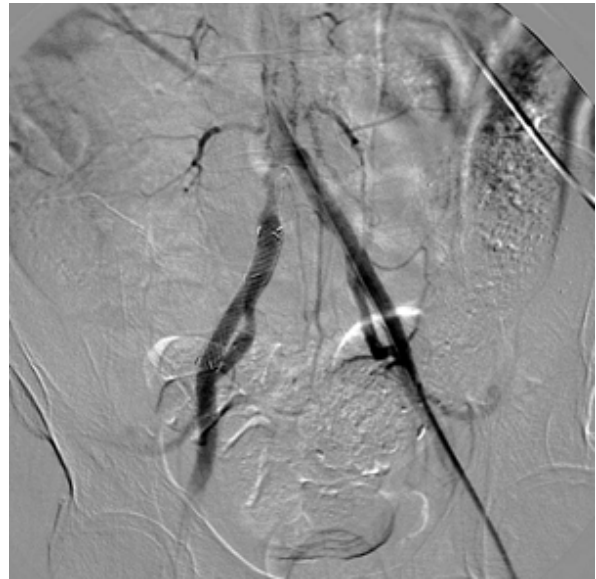


Fig. 3. Arteriogram after deployment of covered stent. No more leakage from the right common iliac artery is seen.



Fig. 4a. Contrast enhanced CT scan. A large amount of hematoma is observed in the right posterior and anterior pararenal spaces. The hematoma extends along the anterior aspect of the right psoas muscle, the abdominal aorta, and the inferior vena cava (A & B).



Fig. 4b. Contrast enhanced CT scan. A large amount of hematoma is observed in the right posterior and anterior pararenal spaces. The hematoma extends along the anterior aspect of the right psoas muscle, the abdominal aorta, and the inferior vena cava (A & B).



Fig. 4c. The covered stent is located in the right external iliac artery without leakage of contrast material.





: Veins, iliac 6mm balloon Savvy, Cordis, Miami FL)  
 Veins, obstruction 가  
 Veins, transluminal angioplasty 14mm X 9cm, 12mm X 9cm wall stent  
 Veins, iliac 14mm 12mm  
 Veins, obstruction (Fig 2).  
 Veins, transluminal angioplasty (Fig 3).

: 69 /

: May-thurner syndrome with postthrombotic 9F  
 iliac vein occlusion

: 2001 4F  
 Cobra 0.035 inch

May - Thurner syndrome

5.8F 6mm 가 0.018 inch  
 (SV - 8, Cordis, Miami, FL) 3F  
 6mm balloon Savvy, Cordis, Miami FL) 가  
 14mm X 9cm, 12mm X 9cm wall stent  
 14mm 12mm  
 (Fig 2).  
 (Fig 3).

9F

4F

Cobra 0.035 inch

May - thurner Cockett

May - Thurner syndrome

5.8F 6mm 가 0.018 inch  
 (SV - 8, Cordis, Miami, FL) 3F

May - Thurner  
 2 - 5% Venous  
 plethysmography, Duplex ultrasongram, Venogram,  
 MR venogram

1) , 2) 3)  
4)

14 - 16mm 가 12mm  
가  
2cm 가

May - thurner Cockett

May - Thurner  
2 - 5% Venous  
plethysmography, Duplex ultrasonogram, Venogram,  
MR venogram

1) , 2) 3)  
4)

14 - 16mm 가 12mm  
가  
2cm 가

1. Raju S, McAllister S, Neglen P. Recanalization  
of total occluded iliac and adjacent venous segments.  
J Vasc Surg 2002; 36:903-911

2. Endovascular surgery in the treatment of chronic  
primary and post-thrombotic iliac vein obstruction.  
Eru J Vasc Endovasc Surg 2000; 20:560 - 5

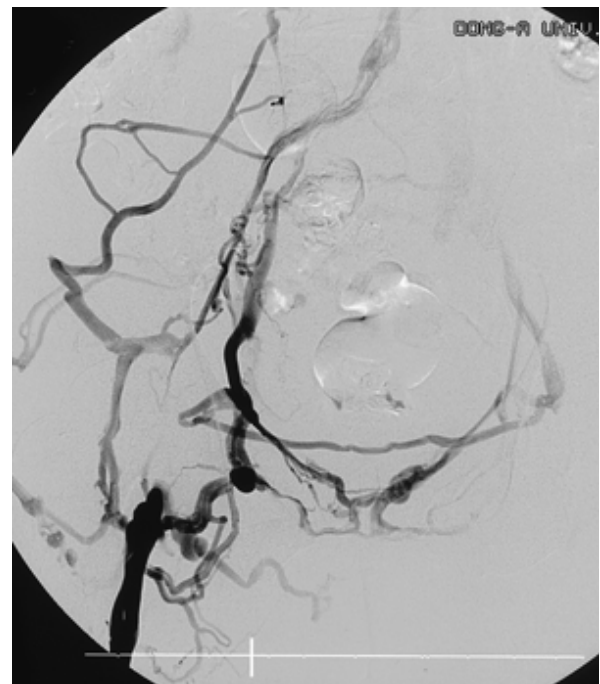


Fig. 1. Transpopliteal direct venogram show abrupt occlusion of common femoral vein and long segmental stenosis of iliac vein. Note the filling of the marked trans-collateral circulation

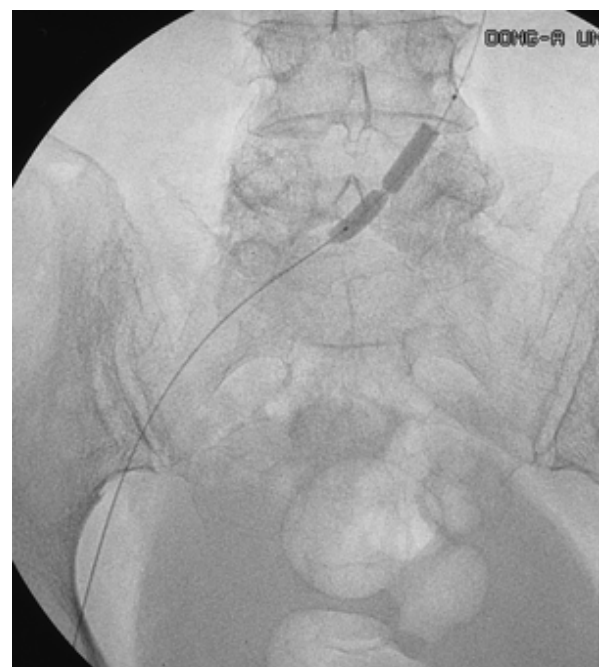


Fig. 2a. During inflation of 6mm angioplasty balloon , focal stenotic waist is seen in orifice of common iliac vein and distal common femoral vein



Fig. 2b. During inflation of 6mm angioplasty balloon , focal stenotic waist is seen in orifice of common iliac vein and distal common femoral vein

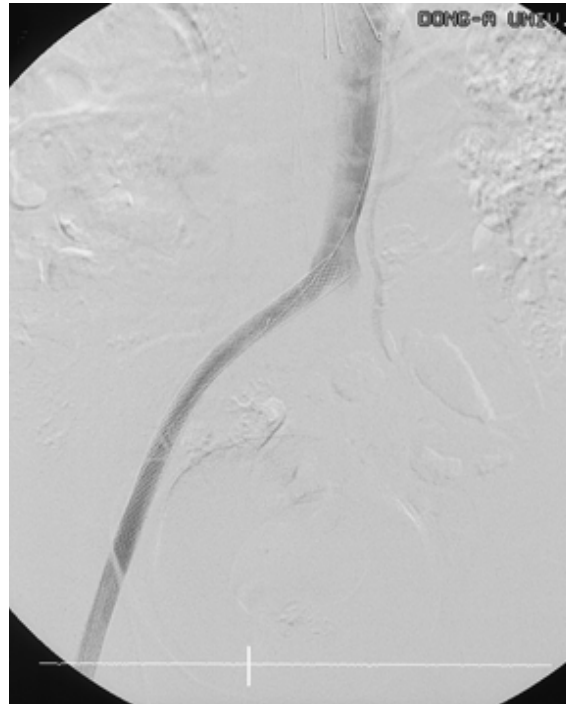


Fig. 3b. After placement of two wall stents ( 14mm X 9cm, 12mm X 9cm). direct venogram shows improved blood flow through the stent and loss of pelvic collaterals.

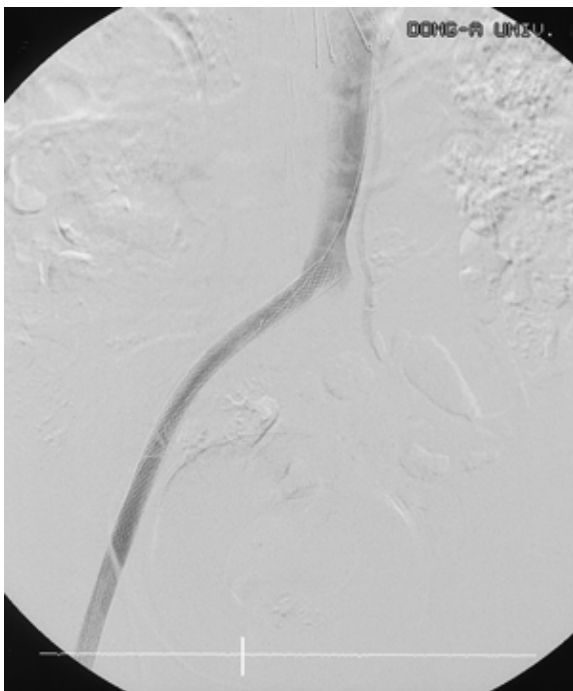


Fig. 3a. After placement of two wall stents ( 14mm X 9cm, 12mm X 9cm). direct venogram shows improved blood flow through the stent and loss of pelvic collaterals.

## Stent-graft placement for the treatment of popliteal artery pseudoaneurysm in patient with Behcet's disease

/ / / / / /

: Behcet's disease, pseudoaneurysm, stent graft, thrombin  
: 26 /  
: 10

, 30cm  
(side hole) 가 5F (infusion catheter; Cook, Bloomington, IN, USA)  
(Fig. 2 B).  
90cm 6F (introducer sheath Cook, Bloomington, IN, USA)  
5 x 37mm (balloon expandable) Jo stent-graft (JOMED, Helsinberg, Sweden) 5X40mm

가

가 1

가

(Fig.3 A).

: Pseudoaneurysm of Rt. popliteal artery in patient with Behcet disease.

(Fig.3 B).

(popliteal artery)  
8cm (aneurysm)가 (Fig. 1 A).

가  
7mm 가 (Fig. 1 B).

10~30%

15~40%

가 65%

가

가 21G 가  
(Bovine thrombin; ) 2000U

(Fig.1 C).

(Fig. 2 A). 0.018"

(dorsalis pedis artery) 8F hy -  
drolyser (Boston scientific, USA)  
, 5 x 40mm

가 가  
가 60%

(aneurysm sac)  
(extrinsic compression)

가 가

terposition)

가

(graft in -

2002;35:36 ~ 422. Park JH, John JH, Chung JW, et al. Aortic and arterial aneurysms in Behcet disease : management with stent-grafts-initial experience. Radiology 2001;220:745-7503. Perna LL, Olin JW, Goines D, et al. Ultrasound guided thrombin injection for the treatment of postcatheterization pseudoaneurysm. Circulation. 2000;102:2391-2395

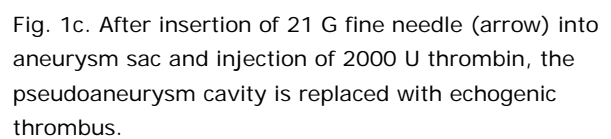




Fig. 2a. On popliteal angiography taken after the injection of 2000 U of thrombin, popliteal artery is totally occluded by extrinsic compression of thrombosed aneurysm sac. Partial contrast enhancement of aneurysm is noted.



Fig. 3a. 5 x 37 mm sized balloon expandable Jo stent-graft was deployed at aneurysm neck site.



Fig. 2b. 5F Infusion catheter with multiple side holes was inserted at popliteal artery to maintain distal blood flow of tibio-fibular artery.



Fig. 3b. After stent-graft insertion, the blood flow of the popliteal artery and tibio-fibular artery was normalized.

# Budd - Chiari : TIPS

Case **43**

## Interventional management of IVC and Budd-Chiari syndrome in a patient of obstruction of hepatic IVC

: Venae cavae,graft and prostheses, venae  
cavae,transluminal angioplasty,  
Liver, interventional procedures  
: 40 /  
:

albumin 3.8g/dl, bilirubin 0.6mg/dl  
, CT

(Fig 6).

(Child-Pugh score,  
8; albumin 3.3g/dl, PT 63%, bilirubin  
1.6mg/dl) 가 .

: IVC and Budd-Chiari syndrome of ob-  
struction of hepatic IVC

CT , 가 , 가 가  
(intrahepatic IVC) 가 (1).  
(Fig 1).  
(Fig 2).

(2)

(3). 1  
74%

(Fig 3). 5F 0.035 93%, 5  
(Terumo)  
6,10,14mm (Boston scientific)  
, 14mm  
(Boston scientific) 14mm  
(4).

가 (Fig 4).

2 TIPS , 가

8mm

8mm

(Fig 5). -

19cmH2O 8cmH2O .

1. Furui S. Percutaneous transluminal angioplasty and stent placement for obstruction of hepatic inferior vena cava. In Han MC, Park JH. Interventional radiology. Seoul : Ilchokak 1999:355-363

2. Mancuso A, Fung K, Mela M, Tibballs J, et al. TIPS for acute and chronic Budd-Chiari syndrome: a single-centre experience. J Hepatol. 2003;38:751-4.

3. Rossle M, Olschewski M, Siegerstetter V, et al. The Budd-Chiari syndrome: outcome after treatment with the transjugular intrahepatic portosystemic shunt. Surgery. 2004 Apr;135:394-403

4. Gasparini D, Del Forno M, Sponza M, et al. Transjugular intrahepatic portosystemic shunt by direct transcaval approach in patients with acute and hyperacute Budd-Chiari syndrome. Eur J Gastroenterol Hepatol. 2002;14:567-71



Fig. 1. Contrast-enhanced CT scan reveals no visible hepatic ven and decreased diameter of hepatic portion of the IVC filled with low attenuation thrombi. Note the large amounts of ascites and right pleural effusion. Contrast-enhanced CT scan reveals no visible hepatic ven and decreased diameter of hepatic portion of the IVC filled with low attenuation thrombi. Note the large amounts of ascites and right pleural effusion.



Fig. 2. Contrast-enhanced CT scan inferior to fig 1 shows extensive thrombi in the IVC and left renal vein. Contrast-enhanced CT scan inferior to fig 1 shows extensive thrombi in the IVC and left renal vein.



Fig. 3. Inferior vena cavogram shows complete occlusion of the inferior vena cava at its hepatic portion. Inferior vena cavogram shows complete occlusion of the inferior vena cava at its hepatic portion.



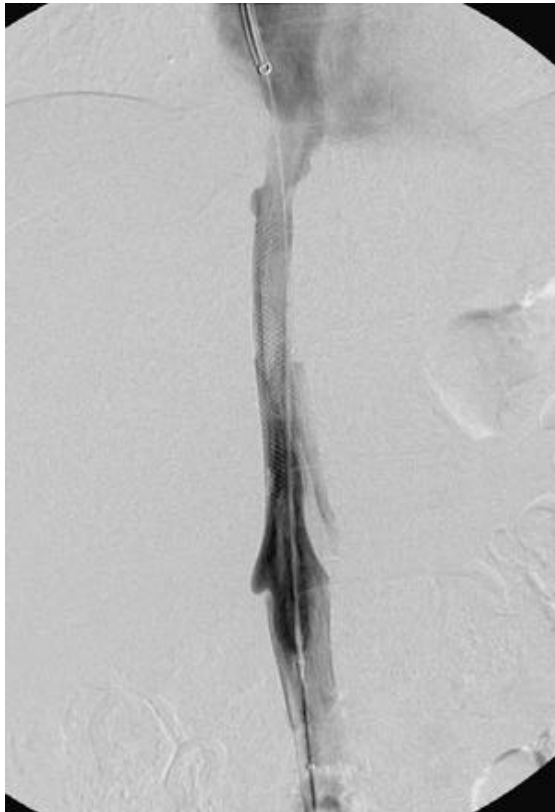


Fig. 4. Inferior vena cavogram obtained after stenting and angioplasties shows patent IVC with good blood flow into the right atrium.

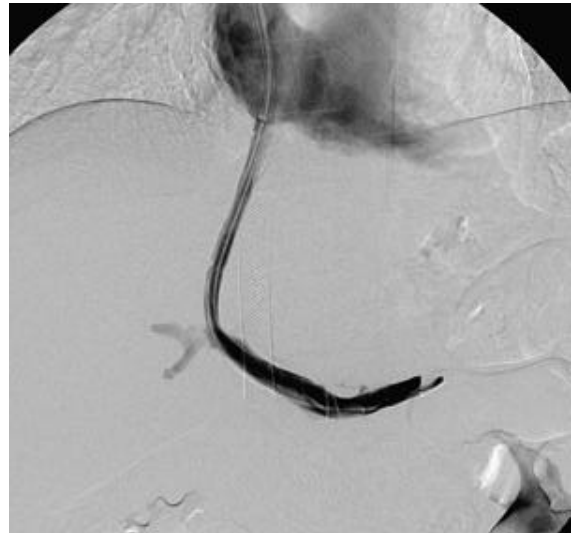


Fig. 5. Splenic portogram obtained after TIPS by trans-caval approach shows good blood flow through TIPS stent. Splenic portogram obtained after TIPS by trans-caval approach shows good blood flow through TIPS stent.



Fig. 6. Follow-up CT scan shows patency of stents in the TIPS tract and IVC. Note the interval decrease in amounts of both ascites and right pleural effusion. Follow-up CT scan shows patency of stents in the TIPS tract and IVC. Note the interval decrease in amounts of both ascites and right pleural effusion.

## Primary stent placement in membranous obstruction of inferior vena cava with Budd-Chiari syndrome

: Budd-Chiari syndrome. Venae cavae, trans-luminal angioplasty. Venae cavae, stenosis or obstruction.

: 77 /

: 2

prominent (Fig.1)  
thrombocytope-  
nia(50,000 /mm<sup>3</sup>), leukopenia(2700 /mm<sup>3</sup>)가,

CT

: Budd-Chiari syndrome due to membranous obstruction of IVC.

CT

(Fig.2).  
가  
CT

45mmHg (Fig.3).

0.038-inch 가  
(Terumo, Tokyo, Japan) pigtail catheter(Royal  
Flush;Cook, Bloomington,Ind)

16

gauge Colapinto needle(Cook, Bloomington, Ind)

(Fig.4) 10mm, 4cm balloon cathe-  
ter(Ultra-thin; Boston Scientific) 10 dilata-  
tion(fig.5)

24mm, 45mm self expandable met-

allic stent(wallstent, Meditech/Boston Scientific)  
(Fig.6). 가 8mmHg  
가 (Fig.7).

Budd-Chiari syndrome(BCS)

BCS

BCS

BCS,

membranous obstruction of inferior  
vena cava(MOVC)

1)

2)

3)

가

BCS thrombolytics medical  
treatment, transjugular intrahepatic portosystemic  
shunt(TIPS), angioplasty with stent, surgical shunt,  
liver transplantation stent in-  
section angioplasty

MOVC

가

surgery

liver transplantation  
life-threatening proce-  
dure

restenosis

shunt occlusion 가

MOVC type 1

Budd-Chiari syndrome

가 (Fig.8).

1. Baijal SS, Roy S, Phadke RV, Agrawal DK, Kumar

S, Choudhuri G. Management of idiopathic Budd-Chiari syndrome with primary stent placement: early results. J Vasc Interv Radiol 1996 7: 545-553

2. Menon KV, Shah V, Kamath PS. The Budd-Chiari syndrome. N Engl J Med. 2004 Feb 5;350(6):578-85

3. Cejna M, Peck-Radosavljevic M, Schoder M et al. Repeat interventions for maintenance of trans-jugular intrahepatic portosystemic shunt function in patients with Budd-Chiari syndrome. J Vasc Interv Radiol. 2002 Feb;13(2 Pt 1):193-9

4. Razavi MK, Hansch EC, Kee ST, Sze DY, Semba CP, Dake MD. Chronically occluded Inferior vena cavae: endovascular treatment Radiology 2000;214:133-138



Fig. 2. Focal narrowing of inferior vena cava at the intra-hepatic level suggests membranous obstruction of inferior vena cava(MOVC) and Budd-Chiari syndrome.



Fig. 1. Prominent collateral vessels are seen on abdominal wall.

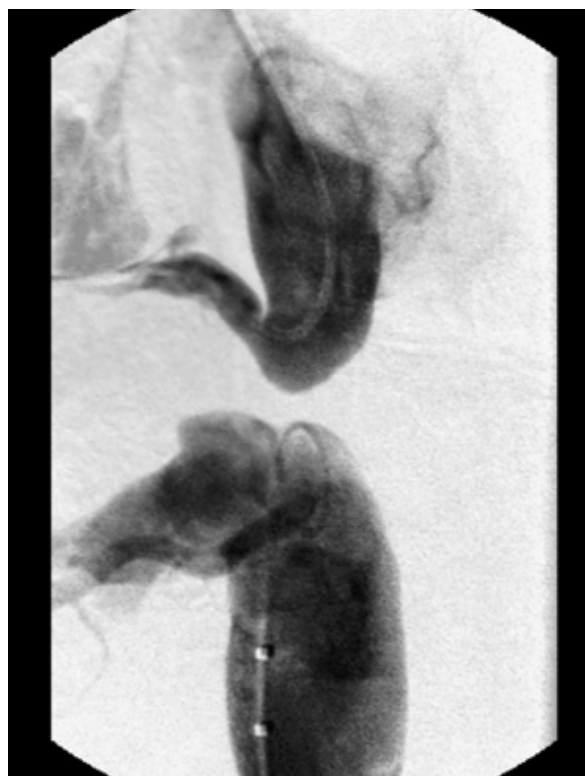


Fig. 3. Vena cavogram shows complete obstruction of inferior vena cava due to membranous obstruction.

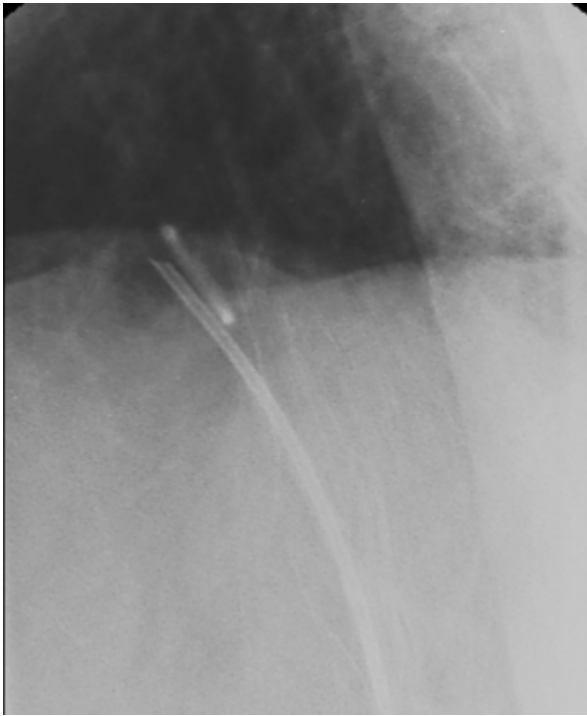


Fig. 4. The membranous portion was punctured by 16 gauge Colapinto needle(Cook, Bloomington, Ind).



Fig. 5. Dilatation of obstructive lesion by balloon catheter was tried.

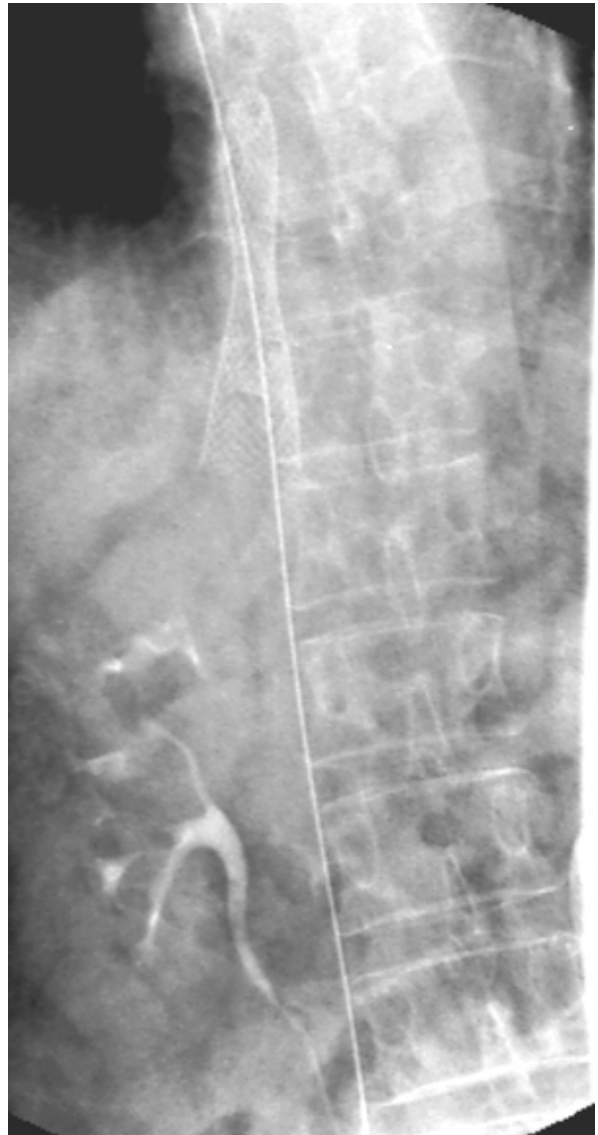


Fig. 6. Stent placement was done because balloon dilatation shows equivocal change of flow of inferior vena cava.



Fig. 7. After stent placement, improvement of flow of inferior vena cava and decreased pressure gradient was noted.



Fig.8. After 3 days later of stent placement, abdominal distension and prominent collateral vessels was decreased.

## Acute Caval Thrombosis in Patients with TrapEase IVC Filter Placements

: Inferior vena cava (Fig 2). 5F  
 Inferior vena cava, Filter Cobra (Cook, Bloomington, USA) 5F  
 Inferior vena cava, Thrombosis Mewissen infusion (Boston Scientific, MA, USA)  
 Inferior vena cava, Recanalization UK 200000 unit/30cc 30  
 : 52 / 100000 unit/1hr 12 Heparin  
 : Acute caval thrombosis related to the IVC filter 500 - 1000unit  
 : 3 9F  
 (mural thrombus)  
 7  
 5F Cobra 8mm  
 Plegmasia cerula dolense (Fig 2).  
 (Fig 3). 7 IVC  
 3  
 (Fig 4).  
 7F  
 7  
 Plegmasia cerula dolense (Fig 2). 5F Cobra  
 (Cook, Bloomington, USA) 5F  
 Mewissen infusion (Boston Scientific, MA, USA)  
 UK 200000 unit/30cc 30  
 100000 unit/1hr 12 Heparin  
 500 - 1000unit  
 9F  
 (mural thrombus)  
 (Fig. 1) 5F Cobra 8mm  
 (Fig 2).  
 (Fig 3). 7  
 IVC  
 7F  
 (Fig 4).

가 ..

3

Trapease 가

Trapease 6F (Cordis, Miami Lakes, FL) Nitinol 가 ,

. Trepease

filter 가

. Trapease

Richard Trapease

가

가 , 가 Nitinol ..

3

Trapease 가

Pulse spray ,

Glycoprotein IIb/IIIa complex , Pulse spray

가

가

Glycoprotein IIb/IIIa complex

Trapease 6F (Cordis, Miami Lakes, FL) Nitinol 가 ,

. Trepease

filter 가

. Trapease

Richard Trapease

가

가 , 가 Nitinol

Trapease 가

Pulse spray ,

Glycoprotein IIb/IIIa complex , Pulse spray

가

가

Glycoprotein IIb/IIIa complex

1. Leask RL, Johnston W, Ojha M. Hemodynamic effects of clot entrapment in the Trapease inferior vena cava filter. J vasc Interv Radiol 2004; 15:485-490

2. Vedantham S, Vesely TM, Parti N, et al. Endovascular recanalization of the thrombosed filter bearing inferior vena cava. J Vasc Interv Radiol 2003; 14:893-903

3. Poon WL, Luk SH, Yam KY, Lee ACW. Mechanical thrombectomy in inferior vena cava thrombosis after caval filter placement: A report of three cases. Cardiovasc Intervent radiol 2002; 25:440-443



Fig. 1a. Abdominal CT scan shows filling of thrombi within the Trepease IVC filter and IVC.

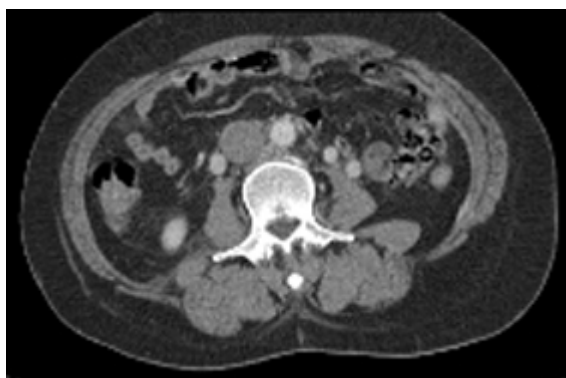


Fig. 1b. Abdominal CT scan shows filling of thrombi within the Trepease IVC filter and IVC.



Fig. 2a. Transfemoral venogram shows filling defect within the IVC and iliac vein.

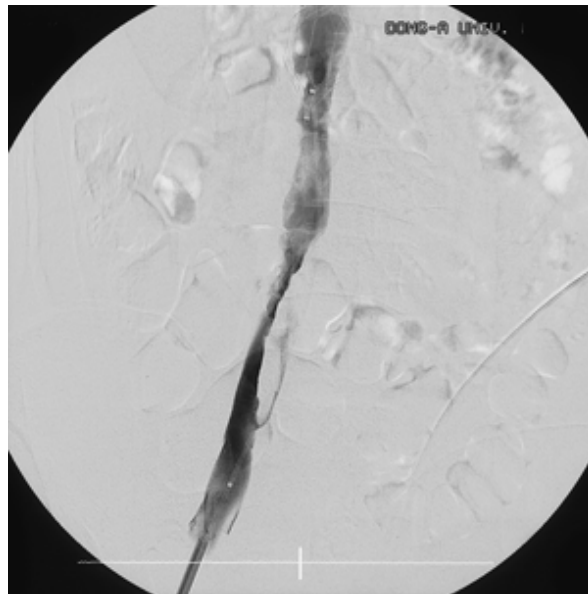


Fig. 2b. After overnight catheter directed thrombolysis and aspiration thrombectomy, venogram shows partial recanalization of IVC and mural attached thrombi.



Fig. 3a. Separation of mural thrombi from IVC wall using balloon catheter.



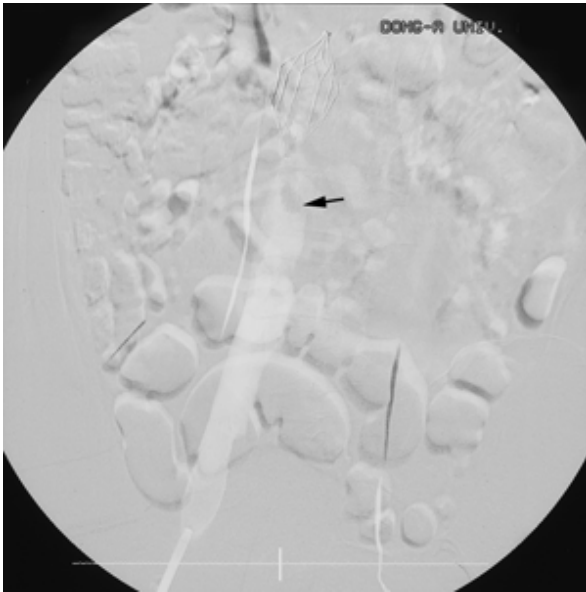


Fig. 3b. Venogram shows occlusion of IVC due to detached mural thrombi (arrow).

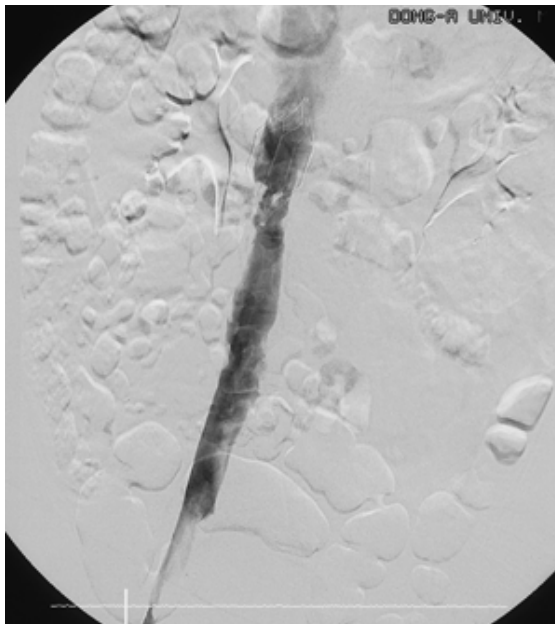


Fig. 3c. After aspiration thrombectomy, Venogram shows recanalized IVC.



Fig. 4a. After a week, follow up CT scan shows patent IVC without residual thrombosis.

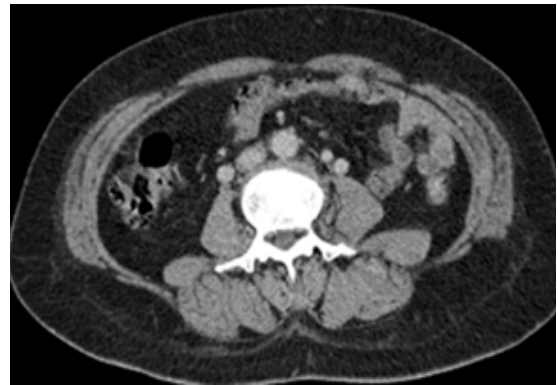


Fig. 4b. After a week, follow up CT scan shows patent IVC without residual thrombosis.

## : Primary Subclavian Vein Thrombosis: Treatment with Thrombolysis and Balloon Angioplasty

: Veins, stenosis or obstruction  
Veins, Interventional procedure  
Veins, subclavian

: 22 /

: 6

thrombosis) (effort thrombosis)

costocla-  
vicular space 가 ,  
large costoclavicular ligament or subclavius muscle,  
more anterior insertion of anterior scalene muscle, con-  
genital fibromuscular band, pectoralis minor muscle  
tendon . , ,

CT  
(Fig.1).

costoclavicular space가 . Stress posi-  
tion

(Fig 2). 5 Fr multi-side  
hole spray catheter (Angiomed, NY, USA)  
Urokinase 100,000/hour ( )  
(160 IU ), 6Fr guiding catheter (Cordis,  
FL, USA) aspiration .

57-100%

(Fig 3). 12 mm (Boston scientific,  
Watertown, MA, USA)

(Fig 4).

costoclavicular space  
(Fig 5).

가

trans-  
axillary first rib resection 가 .

Paget von  
Schroetter 가 1875 1884  
Paget-Schroetter syndrome ,  
(primary axillosubclavian vein

1. Angle N, Gelabert HA, Farooq MM, et al. safety  
and efficacy of early surgical decompression of the  
thoracic outlet for Paget Schroetter syndrome. Ann

Vasc Surg 2001; 15:37-42.

2. Hurbert SN, Rutherford RB. Subclavian-axillary vein thrombosis. In Rutherford RB. Vascular Surgery. 5th ed. Philadelphia: Saunders, 2000:1208-1221.

3. Urschel HC Jr, Razzuk MA. Paget-Schroetter syndrome: what is the best management? Ann Thoracic Surg 2000; 69: 1663-1668.

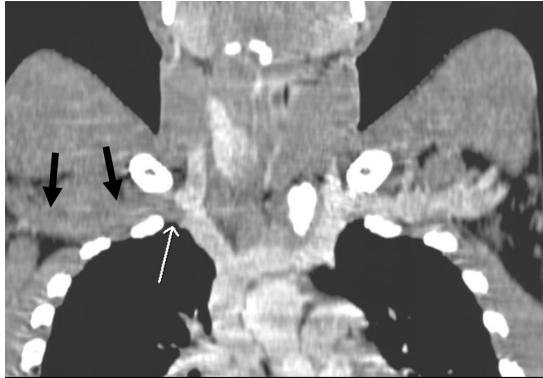


Fig. 1. Thoracic CT MPR image shows thrombotic occlusion of right subclavian vein (arrow).

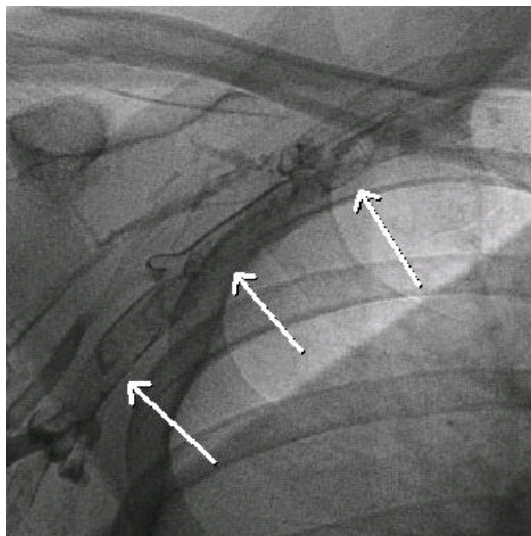


Fig. 2. After contrast injection through right brachial vein, fluoroscopic spot image shows extensive thrombosis in axillosubclavian vein (arrows).



Fig. 3. After thrombolysis using urokinase and aspiration thrombectomy, the subclavian vein was recanalized. A focal severe stenosis was noted at costoclavicular space (arrow).

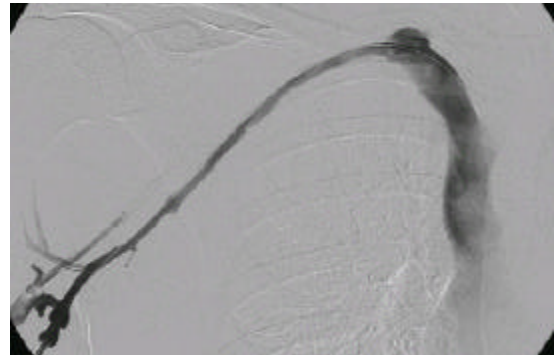


Fig. 4. After balloon angioplasty, venogram shows patent blood flow through the subclavian vein



Fig. 5. Venogram with abduction position shows a focal stenosis in costoclavicular space due to extrinsic compression (arrow).

# Case 47

## Recannalization of central venous occlusion : Treatment with Stent

: Central venous occlusion, Stent placement

: 58

:

: Total occlusion of right subclavian vein

AVF

(1 - 4).

(SVC) 가  
venous  
drainage가  
2cm 가 ( Fig 1 ) .

needle puncture  
septum  
Brockenbrough Curved Needle( Medtronic vascular,  
Santa Rosa, USA)

Brockenbrough Curved Needle 18Gauge  
Tips 16Gauge Transjugular needle(Cook  
Bloomington, USA)

(basilic vein) 5F cobra cathe-  
ter(Cook, Bloomington, USA)

가

(Brockenbrough  
Curved Needle)  
tip  
(Fig. 2).

needle  
snare technique  
through and through technique

(Fig. 3) Terrumo  
guidewire(Terumo, Tokyo, Japan) . Snare  
wire sheath

Through and through technique guidewire  
femoral vein 6mm balloon cathe-  
ter( Boston, Watertown, USA ) predilatation

12mm 43mm Wallstent(Schneider, Inc,  
Plymouth, MN, U.S.A) 12mm 4cm  
( Fig 4 ).

(Fig 5).

Basilic vein 8mm balloon 가

1. Vesely TM, Hovsepian DM, Pilgram TK, Coyne  
DW, Shenoy S. Upper extremity central venous ob-  
struction in hemodialysis patients: treatment with  
Wallstents. Radiology. 1997 Aug;204(2):343-8.

2. Kalman PG, Lindsay TF, Clarke K, Sniderman KW, Vanderburgh L. Management of upper extremity central venous obstruction using interventional radiology. *Ann Vasc Surg.* 1998 May;12(3):202-6.

3. Haage P, Vorwerk D, Piroth W, Schuermann K, Guenther RW Treatment of hemodialysis-related central venous stenosis or occlusion: results of primary Wallstent placement and follow-up in 50 patients. *Radiology.* 1999 Jul;212(1):175-80.

4. Sprouse LR 2nd, Lesar CJ, Meier GH 3rd et al. Percutaneous treatment of symptomatic central venous stenosis *J Vasc Surg.* 2004 Mar;39(3):578-82.

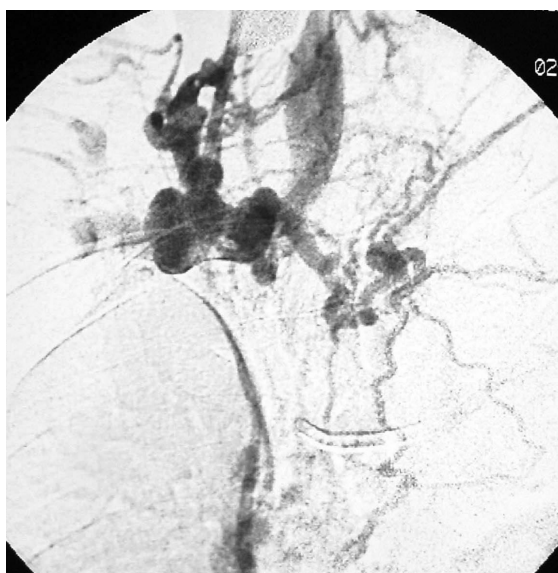


Fig. 1. Right subclavian venogram shows abrupt segmental occlusion and multiple collaterals.

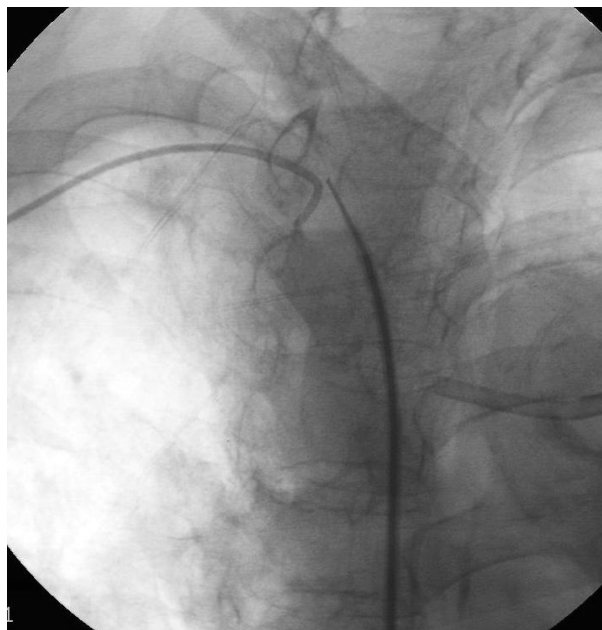


Fig. 2. Needle puncture to the right subclavian vein was performed.



Fig. 3. After puncture, venogram through needle show the right subclavian vein and jugular vein

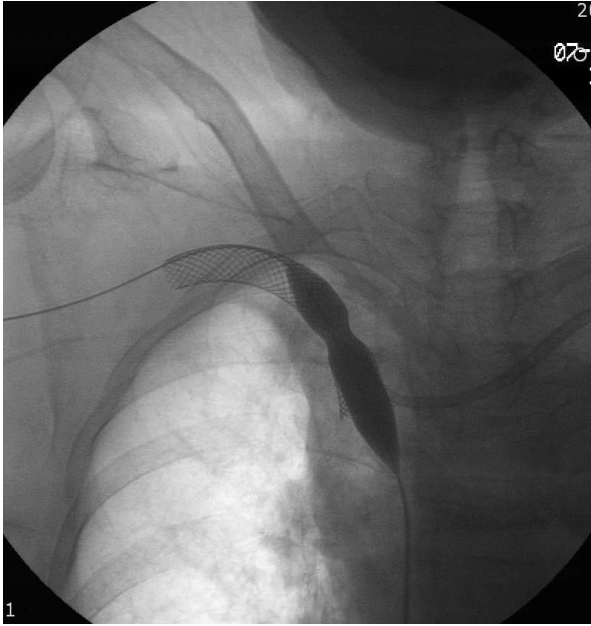


Fig. 4 . Balloon angioplasty and wallstent placement(12mm in diameter) across the occlusion was performed after predilatation with smaller balloon( 6mm in diameter)



Fig. 5 . After Stent placement, venogram shows luminal patency and blood flow is restored with resolution of collateral flow.

1.

2.

3.

4.

1)

2)

3)

4)

## Index to Imaging Literature

5)

6)

7)

8)

9)

10)

5.

## (Checklist)

1)

2)

, 3

RSNA

index Medicus

- 6 3 “ ” “et al.” , 7  
 1. 1993: 29:711-717  
 2. Palmaz JC. Richer GM. Noeldge G. et al. Intraluminal stents in atherosclerotic iliac artery stenosis preliminary report of multicenter study. Radiology 1988;168:727-731  
 3. Fraser RG. Pare JAP. Diagnosis of disease of the chest. 2nd ed. Philadelphia: Saunders. 1979:1420-1430  
 chapter  
 4. Decvere white R. Nagler H. Priapis. In Krane RJ. Siroky MB. Coldstein. Male sexual dysfunction. 1st ed. Boston: Little Brown & Co. 1983:101-111

3) (Figure)

- (5x7 )  
 가  
 - text

300DPI PACS  
 jpg, tif E-mail Bmp, disk

5x7 (13X18cm)

가

2

. ( : Fig.1A, Fig. 1B).

4)

5)

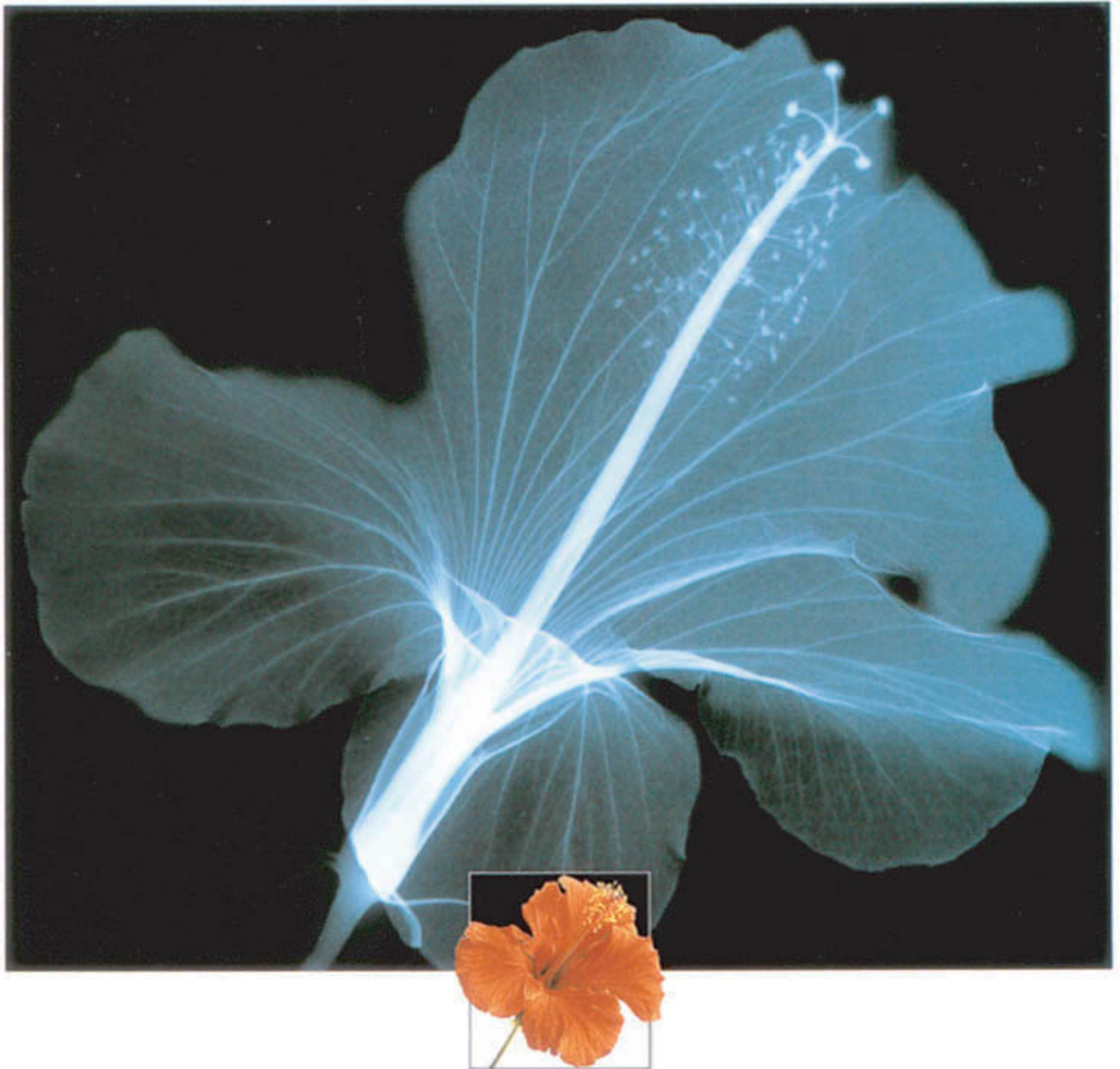




:  
:  
:  
:  
: , , , ,  
: S & G Biotech(PDF),  
: 2004 10 12

---





E d u c a t i o n   i n   d i a g n o s t i c   i m a g i n g

*"Supported by Grant from the BRACCO International Award 2004"*



[www.bracco.com](http://www.bracco.com)